

POLITECNICO DI MILANO

First School of Engineering (Ing.I – CIV)

Master of Civil Engineering for Risk Mitigation



**STUDY OF THE IMPACTS OF CLIMATE  
CHANGE ON THE WATER LEVEL RISE OF  
THE DES-PRAIRIES RIVER**

Referent: Prof. Francesco Ballio (Politecnico di Milano)

Project done in  
POLYTECHNIQUE DE MONTREAL  
Referent: Prof. MusandjiFuamba

POLYTECHNIQUE  
MONTREAL

LE GÉNIE  
EN PREMIÈRE CLASSE



Master Thesis in Civil Engineering of:

Elsa SORMAIN

Matr.nb. 767736

Academic Year 2011-2012

POLITECNICO DI MILANO

Scuola di Ingegneria Civile, Ambientale e Territoriale

Corso di Studi: Civil Engineering for Risk Mitigation



# **STUDY OF THE IMPACTS OF CLIMATE CHANGE ON THE WATER LEVEL RISE OF THE DES-PRAIRIES RIVER**

Relatore: Prof. Francesco Ballio (Politecnico di Milano)

Progetto effettuato alla  
POLYTECHNIQUE DE MONTREAL

Relatore: Prof. Musandji Fuamba

**POLYTECHNIQUE  
MONTREAL**

LE GÉNIE  
EN PREMIÈRE CLASSE



Tesi di Laurea Specialistica in Ingegneria Civile di:

Elsa SORMAIN

Matr. n. 767736

Anno Accademico 2011-2012

# Abstract

---

This project studies the impacts of climate change on the water level rise of the Des-Prairies River (Montreal, Quebec, Canada), i.e. the expected increase in water surface elevation due to a future precipitation event.

However, the aim is not to produce exact results about future level in the Des-Prairies River that could be used directly by the municipalities to make urbanization plans or to take adaptive measures. Indeed there are a lot of uncertainties involved in the different steps of such a process, and it was not possible with limited time, data and resources to provide so precise results.

The main objective was rather to provide municipalities and public services managers involved in such a matter with a methodology to follow, different numerical methods that can be used, type of results that can be expected, and kind of uncertainties related to this approach. That is why a critical and comparative view on the different available methods and results has been adopted at each step, in order to give the more complete information, and to develop a full comprehensive approach of the effects of climate change on a river system, from the definition of climate change scenarios to the delimitation of an eventual flooding zone. So that the municipalities managers and experts would have information and tools in hands if they want to go forwards and sponsor a deep study to take eventual adaptive measures.

The percentage of augmentation of precipitation intensity for 2041-2070 period taken from Mailhot et al (2007), applied to a 24h rainfall event of 50 years return period, permitted to determine the future precipitation data. The utilization of the Hec-GeoHMS software to make the rainfall-runoff transformation gave the future flow hydrograph, which was input into Hec-GeoRAS and River2D software – calibrated with known water elevations and flows. The results of the hydrodynamic simulations showed that some flooded zones were expected in the upper reach of the Des-Prairies River as well as near the outlet, but that the bridges would not get submerged or swept away. Finally, recommendations of use for 1D and 2D models were done according to the quality of the terrain data available, the complexity and the extent of the area under investigation, the flow regime, the existence of hydraulic structure and the type of results desired.

## Key Words

---

Climate change scenarios – climate model – downscaling methods – storm hyetograph – future precipitations – digital elevation model – terrain data processing – rainfall-runoff transformation– one-dimensional simulation – two-dimensional simulation – flooding zone – water surface elevation.

Hec-HMS – Hec-RAS – River2D – ArcGIS.

# Acknowledgments

---

With the achievement of this paper comes the end of my student years. They took me to very different cities, countries and continents, and from each of them I learned valuable academic and life lessons. I will have of them imperishable memories. This would not have been possible without the support of many persons that I would like to thank a lot.

I would like to express my deep regards to Professor Francesco Ballio, of Politecnico di Milano, who followed me through my project of making a thesis in a foreign university, who accepted to be my referent despite the distance, and who let me the independence needed to complete this project successfully.

I express my sincere thanks to Professor Musandji Fuamba, of Polytechnique Montreal, who accepted me in this project, trusted me from the beginning, and who took time nearly every week to assess the progress of my work and to answer my numerous questions, despite his very busy timetable. I hope that I met all his expectations and that he had as much pleasure to work together as I had.

I give a special thanks to Mr. Jean Bélanger, professor of topology at Polytechnique Montreal, for its help and for the time he spent on the field and processing the data for my project.

I take the opportunity to thank the international mobility team of the Centrale Marseille School of Engineering, which made possible this incredible adventure of two years which is now ending.

I gratefully acknowledge all the members of the administrative staff of the Lecco Campus and of the studek 8 in Milan, for their help through the maze of officialdom.

I also would like to thank all the professors I had in my student years, who taught me very diverse but always valuable lessons

Finally, I would like to express my gratitude to my family and my friends, in France, in Italy and in Canada, for their ever support and their love.



# Table of Contents

---

<b>Abstract</b> .....	<b>i</b>
<b>Key Words</b> .....	<b>i</b>
<b>Acknowledgments</b> .....	<b>ii</b>
<b>Introduction</b> .....	<b>1</b>
<b>Chapter 1 – Climate change and impacts prediction</b> .....	<b>3</b>
1.1. Climate change scenarios .....	3
1.1.1. Incremental scenarios .....	3
1.1.2. Analogue scenarios.....	4
1.1.2.1. Spatial analogues .....	4
1.1.2.2. Temporal analogues.....	4
1.1.3. SRES scenarios.....	4
1.1.3.1. Context .....	4
1.1.3.2. SRES scenarios.....	5
1.2. Climate models.....	6
1.2.1. Simple models .....	6
1.2.2. Global ClimateModels.....	7
1.2.2.1. General Circulation Models .....	7
1.2.2.2. Coupled circulation models .....	7
1.2.2.3. Climate projections.....	8
1.3. Downscaling methods .....	9
1.3.1. High resolution AGCM experiments.....	9
1.3.2. Statistical downscaling .....	9
1.3.2.1. Transfer functions.....	10
1.3.2.2. Weather typing .....	10
1.3.2.3. Weather generators.....	11
1.3.3. Dynamical downscaling: Regional Climate Models .....	11
1.3.3.1. Principle.....	11
1.3.3.2. The Canadian Model .....	11
1.4. Comparison between different tools predicting climate projections, recommendations and limitations.....	12
1.4.1. Comparison and recommendations .....	12
1.4.2. Limitations of this approach for the present study .....	14

<b>Chapter 2 – Presentation of the basin of the Des-Prairies River</b> .....	15
2.1. Des-Prairies River and Ottawa Basin .....	15
2.1.1. Des-Prairies River .....	15
2.1.2. Ottawa Basin .....	15
2.2. Area of study .....	16
2.2.1. Basin of the Du-Nord River .....	16
2.2.2. Basin of the Milles-Iles River.....	18
<b>Chapter 3 – Hydrological considerations</b> .....	19
3.1. Rainfall hyetograph .....	19
3.1.1. IDF Curve .....	19
3.1.2. Design Hyetograph.....	19
3.1.2.1. Constant and triangular hyetographs .....	20
3.1.2.2. Desbordes hyetograph .....	20
3.1.2.3. Chicago and Sifalda hyetograph.....	21
3.1.2.4. SCS hyetograph.....	21
3.1.2.5. Comparison of the methods and recommendations.....	22
3.1.3. Application to the Du-Nord Basin.....	23
3.1.3.1. IDF curves .....	23
3.1.3.2. Current Chicago hyetograph.....	23
3.1.3.3. Future Chicago hyetograph .....	24
3.2. Rainfall-runoff transformation with Hec-GeoHMS .....	26
3.2.1. Presentation of Hec-HMS and Hec-GeoHMS.....	26
3.2.1.1. Hec-HMS.....	26
3.2.1.2. Hec-GeoHMS .....	26
3.2.2. Preparation of the data in ArcGIS with Hec-GeoHMS .....	26
3.2.2.1. Terrain Preprocessing .....	27
3.2.2.2. Basin Processing.....	28
3.2.2.3. Basin characteristics .....	28
3.2.2.4. Hydrologic parameter estimation .....	28
3.2.2.5. Export for Hec-HMS .....	29
3.2.3. Preparation of the Hec-HMS models .....	29
3.2.3.1. Choice of a method and of its parameters for every step of the transformation.....	29
3.2.3.1.1. Loss method .....	30
3.2.3.1.2. Transformation method .....	30
3.2.3.1.3. Base-flow method.....	32

3.2.3.1.4.	Routing method .....	32
3.2.3.2.	Meteorological model.....	33
3.2.4.	Calibration of the model.....	34
3.2.4.1.	Data for the calibration.....	34
3.2.4.2.	Optimization runs .....	34
3.2.4.3.	Results .....	35
3.2.5.	Validation of the model.....	36
3.2.5.1.	Data for validation.....	36
3.2.5.2.	Results .....	36
3.2.6.	Simulation of the future 24h rainfall event.....	37
3.2.6.1.	Simulation .....	37
3.2.6.2.	Results .....	37
3.3.	Hydrographs for the 1D and 2D hydraulic software .....	38
3.3.1.	Consideration of the Ottawa River and of the Lake of Two Mountains.....	38
3.3.2.	Consideration of the Mille-Ile Basin .....	39
3.3.3.	Hydrographs for the simulation software .....	40
	<b>Chapter 4 – Determination of hydrodynamic conditions .....</b>	<b>42</b>
4.1.	1D and 2D modeling .....	42
4.1.1.	Introduction to 1D and 2D modeling.....	42
4.1.2.	Main differences between 1D and 2D models.....	42
4.1.3.	Comparison of different software.....	43
4.1.4.	Choice of the software.....	43
4.2.	Preparation of the raw terrain data .....	45
4.2.1.	Available terrain data .....	45
4.2.2.	Correction of the DEM.....	45
4.2.2.1.	Field study .....	46
4.2.2.2.	Bathymetric points.....	46
4.2.3.	Combination of the data .....	47
4.3.	1D Simulation with Hec-GeoRAS .....	48
4.3.1.	Presentation of Hec-RAS and Hec-GeoRAS.....	48
4.3.1.1.	Hec-RAS .....	48
4.3.1.2.	Hec-GeoRAS.....	48
4.3.2.	Preparation of the geometry file in ArcGIS.....	49
4.3.2.1.	Creation of a TIN.....	49
4.3.2.2.	Creation of the river, bank and flowpath layers .....	49
4.3.2.3.	Creation of the cross sections .....	49

4.3.2.4.	Creation of the bridges and inline structures .....	50
4.3.2.5.	Assignment of the roughness coefficient.....	51
4.3.2.6.	Export to Hec-RAS.....	51
4.3.3.	Simulation in Hec-RAS .....	52
4.3.3.1.	Correction of the geometry, bridges and inline structures.....	52
4.3.3.2.	Calibration and Validation of the model .....	53
4.3.3.3.	Input of the boundary and initial conditions for unsteady flow simulation.....	55
4.3.4.	Results .....	55
4.3.4.1.	In Hec-RAS .....	55
4.3.4.2.	Export in ArcGIS.....	58
4.3.4.3.	Simulation without the inline structure .....	60
4.4.	2D Simulation with River2D.....	61
4.4.1.	Presentation of River2D .....	61
4.4.2.	Preparation of the data in Arc-GIS .....	62
4.4.3.	Simulation with River-2D .....	62
4.4.3.1.	Bed topology with R2D-Bed .....	62
4.4.3.2.	Mesh generation with R2D-Mesh .....	63
4.4.3.3.	Calibration and validation of the model .....	64
4.4.3.4.	Hydrodynamic simulation with River2D .....	65
4.4.4.	Results .....	66
<b>Chapter 5 – Results Processing .....</b>		<b>70</b>
5.1.	Results discussion.....	70
5.1.1.	Comparison between 1D and 2D results .....	70
5.1.2.	Results Uncertainties.....	72
5.1.3.	Conclusion on 1D and 2D models.....	73
5.2.	Impacts of climate change on theDes-Prairies River.....	75
5.2.1.	Expected consequences on the Des-Prairies River.....	75
5.2.1.1.	Bridges.....	75
5.2.1.2.	Floodplain.....	76
5.2.2.	Adaptive measures.....	76
5.2.2.1.	Protective measures .....	76
5.2.2.2.	Preventive measures .....	77
<b>Conclusion and recommendations .....</b>		<b>78</b>
<b>Bibliography .....</b>		<b>80</b>
<b>Appendix .....</b>		<b>84</b>

# List of Figures

---

Figure 1: projection of SRES emissions for 21st century[IPPC, 2001] .....	6
Figure 2: development of Global Climate Models[IPPC, 2001] .....	7
Figure 3: prediction of global temperature change from different coupled GCM for three SRES scenarios [IPPC, 2007] .....	8
Figure 4: scheme of downscaling procedure with transfer function (left) and weather typing (right)[CCIS, 2012] .....	10
Figure 5: temperature (top) and precipitation (bottom) predictions, averaged from 17 simulations of the CRCM [Ouranos, 2010] .....	12
Figure 6: Lake of Two Mountains and Des-Prairies River[Robitaille, 1999] .....	15
Figure 7: Basin of Ottawa River [Wikipedia, 2012] .....	16
Figure 8: Basin of Du-NordRiver [Abrinord, 2008].....	17
Figure 9: Basin of Mille-Ile River[Cobamil, 2011].....	18
Figure 10: constant and triangular (left) and Desbordes(right) hyetographs [Adaptated from Sanfilippo& Paoletti, 2011 & Bertrand-Krajewski, 2006a] .....	20
Figure 11: Chicago (left) and Sifalda (right) hyetograph [Th��berge, 1996 andSanfilippo&Paoletti, 2011].....	21
Figure 12: SCS rainfall distributions [Ven Te Chow et al, 1988] .....	21
Figure 13: IDF curves at the Ste-Agathe station [Environment Canada,2012].....	23
Figure 14: Current Chicago hyetograph in St-Jerome and Ste-Agathe. ....	24
Figure 15: Ratio of MOAM estimates (control/future climate) with 90% confidence intervals (vertical bars) [Mailhot et al, 2007].....	25
Figure 16: Du Nord terrain file prepared in ArcGIS (left) and basin with Hec-HMS representation (right).....	29
Figure 17: characteristics of an UH (left) and principle of superposition of UH (right) [VICAIRE, 2012].....	31
Figure 18: Observed and simulatedflow at St-Andre after calibration by Hec-HMS .....	35
Figure 19: Observed and simulated flow at St-Andre with Hec-HMS(validation) .....	37
Figure 20: Simulated Hydrograph by Hec-HMS at the outlet of the Du-Nord Basin for a future 24h rainfall event.....	38
Figure 21: repartition of the water of the Lake of Two Mountains [adapted from CEHQ, 2005] .....	39
Figure 22: Hydrographs of the Des-Prairies River and of its tributaries for the simulation software... ..	40
Figure 23: principle of RTK method [resourcesupplyllc.com, 2012] .....	46
Figure 24: extract of the ArcGIS project with the data from all sources to form the raw terrain data.. ..	47
Figure 25: extract of the attribute table of the XSCutLines layer.....	50
Figure 26: attribute table of the bridges layer .....	50
Figure 27: TIN model and geometry layers of the Des-Prairie River .....	52
Figure 28: representation of the LachapelleBridge and of the Des-Prairies dam in Hec-RAS .....	53
Figure 29: initialand maximum water surface profile for the simulation of the future 24h rainfall event in Hec-RAS .....	56
Figure 30: Initial and maximum water elevation simulated by Hec-RAS at Bizard Island Bridge .....	57
Figure 31: stage and flow hydrographs simulated by Hec-RAS just after Bisson Bridge .....	57
Figure 32: Representation in ArcGIS of the water depth of the maximum WS profile of the Des-Prairies River simulated in Hec-RAS .....	59

Figure 33: Representation in ArcGIS of the velocity distribution of the maximum WS profile of the Des-Prairies River simulated in Hec-RAS .....	59
Figure 34: initial and maximum water surface profile for the simulation of the future 24h rainfall event in Hec-RAS without the inline structure .....	60
Figure 35: Bed elevation of the Des-Prairies River after triangulation in R2D-Bed.....	63
Figure 36: zoom on a small portion of the topographic mesh of the Des-Prairies River. ....	63
Figure 37: zoom on the hydrodynamic mesh of the Des-Prairies River around Bigras Island in R2D-Mesh.....	64
Figure 38: maximum water surface elevation of the Des-Prairies River simulated with River2D. ....	67
Figure 39: water depth at peak time in the Des-Prairies River simulated by River2D.....	67
Figure 40: velocity distribution and vectors at peak time in the Des-Prairies River simulated by River2D. ....	67
Figure 41: Representation of the maximum water extent simulated by River2D and of the river banks in ArcGIS. ....	68
Figure 42: maximum water extent simulated by Hec-RAS and River2D .....	71
Figure 43: Comparison of cross-section's elevation and simulated water level between Hec-RAS and River2D at the beginning of the middle reach (section 40678.27).....	72

# List of Tables

---

Table 1: summary of the strengths and weaknesses of the different methods to obtain prediction of future climate [Adapted from IPCC, 2001] .....	13
Table 2: Characteristics of the sub-basins of Mille-Ile River.....	18
Table3: comparison of the different methods to get a design hyetograph.....	22
Table4: IDF parameters of two stations in the Du-Nord basin [adapted from EC, 2012].....	24
Table 5: percentage of increase for precipitation in 2041-2070 compared to 1961-1991[adapted from Mailhot et al, 2007] .....	24
Table6: Comparison between observed and simulated flow after calibration in Hec-HMS .....	35
Table7: Parameters calibrated by Hec-HMS and their values.....	36
Table8: baseflow and peak flow of the hydrographs of the Des-Prairies River and its tributaries .....	40
Table9: statistics on the flow rates at the Cheval Blanc Rapids in the Des-Prairies Rivers (data from 1923 to 2010).....	41
Table10: comparison table of different 1D and 2D hydraulic software .....	44
Table 11: values of Manning's coefficient in floodplains.....	51
Table 12: comparison between known water surface elevations and simulated ones by Hec-RAS after calibration.....	54
Table13: water rising at several cross-sections according to simulation in Hec-RAS .....	56
Table14: comparison of maximum water levels simulated by Hec-RAS with historical measured data at two stations of the Des-Prairies River.....	58
Table 15: water rising at several cross-sections according to simulation in Hec-RAS without the inline structure, and comparison with the simulation with the inline structure.....	61
Table 16: comparison between known water surface elevations and simulated ones by River-2D after calibration.....	64
Table 17: water rising at several cross-sections according to simulation in River2D.....	68
Table 18: comparison between maximum water levels simulated by River2D and historic ones at two stations of the Des-Prairies River.....	69
Table19: Comparison between water surface elevations simulated with Hec-RAS and River2D. ....	71
Table 20: Maximum water surface elevation simulated by Hec-RAS with increased hydrographs of 10 and 20% .....	73
Table 21: Fitting of 1D and 2D models to different criteria of simulation.....	75

# List of Appendix

---

**Appendix 1:** Table of value and graphs of the IDF curves for the Ste-Agathe and St-Jerome meteorological stations (*EC, 2012*).

**Appendix 2:** Table of value and graphs of the current and future Chicago hyetographs and histograms for the Ste-Agathe and St-Jerome meteorological stations

**Appendix 3:** Parameters of the models for the rainfall-runoff transformation in Hec-HMS

**Appendix 4:** Parameters of the meteorological model of Hec-HMS.

**Appendix 5:** Table of value and graphs of the hydrographs at the exit of the Du-Nord Basin and at the entrance of the Des-Prairies River and of its tributaries

**Appendix 6:** Historical measured data at the CEHQ flow station of the Carillon Dam.

**Appendix 7:** Land-Use file used for the input of the roughness coefficient in ArcGIS

**Appendix 8:** Representation of the Des-Prairies River geometry in Hec-RAS

**Appendix 9:** Extract of the construction plans used to input the bridges' geometry in Hec-RAS.



# Introduction

---

## **Problem Context**

Climate change is now unequivocal. Even if the causes are still in debate, scientists from all over the world agree to say that observations of climate trends in the last years highlight a global warming of the planet. According to the Intergovernmental Panel on Climate Change (*IPPC, 2007*), there is “a very high confidence that the net effect of human activities since 1750 has been one of warming”. Indeed, human activities result in greenhouse gases emissions – carbon dioxide, methane, nitrous oxide and halocarbons. And “most of the observed increase in global average temperatures since the mid-20<sup>th</sup> century is very likely due to the observed increase in anthropogenic GHG concentrations. It is likely that there has been significant anthropogenic warming over the past 50 years averaged over each continent (except Antarctica)”.

However in every case, we are currently facing an important change in climate, which does not seem – or is expected – to fade. The measured consequences at this time – which have an increasing tendency –include a warming of the surface temperature, especially in the region in northern latitudes, a rising of the sea levels, a decrease of snow and ice extent, a change in rainfall pattern – increase in some part, decrease in already dry regions, and more tropical cyclones and other extreme events – storms, draughts, etc.

In Southern Quebec, place of the River under consideration in this project, it is expected an increase of 2.5 to 3.8°C in winter and 1.9 to 3.0°C in summer in 2050. An increase of precipitations from 8.6 to 18.1% is also forecasted in winter. Moreover, an increase in the frequency, intensity and/or duration of the rainfall events is anticipated (*Ouranos, 2010*).

With more frequent and intense rainfall events awaited, the problem of inundations is naturally raised, with all its consequences: flooded zones, damages on infrastructures and ecosystems, endangerment of people life's and goods, economics repercussions, etc. In order to reduce those possible adverse impacts, it is important for the population and for the decision makers to be aware of the danger, of its possible damages and of the measures that could be undertaken, at local scale. Indeed, preparedness is a crucial point in risk management.

## **Literature Review**

Climate change is a topic of current interest, as it can be seen with the many recent international meetings and conferences on the subject. There are several climate models developed by different scientific groups in order to highlight tendencies of change in past climatic data and to predict future climate, adapted to diverse regions of the globe. And efforts are made to evaluate the adverse consequences described previously at global scale, to look for solutions to avoid them and to diffuse the knowledge to the public – taking into consideration the high uncertainties related to the predictions. Moreover, hydrologic and hydraulic simulations of basins and river systems are well known and developed for years, with several software created for this purpose.

However practical complete studies at very local scales, linking those different elements, are rare. That is why there is the need to study the subject, at targeted scale, in order to be prepared for those changes. To have knowledge about what could happen in a given region, at basin or river scale, it is essential for the local authorities in order to take eventual preventive and adaptive measures to reduce the risk for the population and the infrastructures.

## **Objectives**

The goal of this project is to study the impacts of climate change on the water level rise of the Des-Prairies River, and to give a methodology to do so with several methods explained and compared for each step. More specifically, the purposes are first to make an overview of the different existing tools for future climate prediction and to make a choice of a model to use for the determination of the future precipitations in the zone of study. In second place, the project aims to present different models to make the rainfall-runoff transformation and to choose one of them and to apply it to the area under consideration. And finally, it intends to compare different software to make the hydrodynamic simulation, to apply some of them to the Des-Prairies River, to present and compare the results and to draw constructive conclusions and recommendations from them about the consequences on the Des-Prairies River as well as the use of 1D and 2D models.

## **Adopted methodology**

First of all some background about climate change will be provided, in order to give an overview of the different scenarios, models and downscaling methods that exist at that time. Then the emphasis will be put on the Des-Prairies River and its watershed, the Ottawa Basin – then restricted to the Du-Nord and Mille-Iles Basins. Different methods to draw a storm hyetograph will be presented, and the rainfall-runoff transformation done for the area of study described. After that, the one- and two-dimensional simulations carried out for the Des-Prairies River will be explained, with some theoretical considerations, and the results analyzed. Finally, the results obtained with 1D and 2D models will be compared, in order to draw conclusions on the impacts of climate change on the Des-Prairies River and on the use of 1D and 2D models for such simulations.

# Chapter 1 – Climate change and impacts prediction

Climate change can be defined as a difference of mean climate or of its variability lasting for a long period of time with respect to a reference period – usually at least 30 years, corresponding to a statistically significant trend. This can be due to both natural and human causes.

It is worldly recognized now (*IPPC, 2007*) that we are facing climate change – even if the causes and magnitude of it are still debated – and one of the challenges of this century will be to deal with the consequences. Therefore, to get prepared and to avoid severe effects, it is of first importance to study the possible impacts of climate change. For that, it is necessary to start with the development of climate change scenarios.

## 1.1. Climate change scenarios

A climate scenario is “a plausible representation of future climate that has been constructed for explicit use in investigating the potential impacts of anthropogenic climate change” (*IPPC, 2001*). It is obtained by combining, in a climate model, a climate change scenario – which represents the expected changes in climate variables – with the description of the current climate (baseline climate).

The development of climate change scenario is a necessary step – the first one and maybe the most important – of any vulnerability, impacts and adaptation assessment study, especially as far as extreme events are concerned. They are defined as input of the climate models, which generate a prediction of future climate. And the more precisely are the scenarios developed, the more accurate will be the results for impacts assessment. But currently, we still have to deal with a lot of uncertainties in the field of scenario development. That is why the elaboration of climate scenarios is currently one of the major challenges of the scientific community in this discipline.

Different kinds of scenarios have been developed since the mid-1970s; the three main types are described below (*Canadian Climate Impacts Scenarios [CCIS], 2012; EC, 2004; IPCC, 2001*).

### 1.1.1. Incremental scenarios

The incremental scenarios – also called synthetic or arbitrary scenarios – are the easiest scenarios one can develop and apply, and so the first one ever implemented. In those scenarios, one climatic parameter – mean temperature, precipitation amount, etc. – is changed incrementally, perturbed from its historical records. This can provide quickly information on a wide range of possible changes, by allowing the test of a lot of different parameters, to generate different future climate. And it is applicable in any area of study. But with this method it can be difficult to develop credible, realistic scenarios, which could really happen. Indeed the true future climate is very likely to be very complicated, involving a change of all the variables, totally unpredictable by changing the variables “manually”. So incremental scenarios are particularly well suited for a sensitivity analysis, or the determination of threshold values, before applying another more credible method of scenario development for impact analysis.

## 1.1.2. Analogue scenarios

Analogue scenarios are based on recorded climate regimes, at a different place or in a different time, that may resemble the future climate in a specific region of interest. There are two types of analogue scenarios: the spatial analogues and the temporal analogues.

### 1.1.2.1. Spatial analogues

A region that currently has a climate that can be expected in the future in the studied area – in another location – is identified, and its climate is used as climate scenario for the area under investigation. But if this method is quite simple, and insures the creation of a physically credible scenario, it has to be dealt with carefully. Indeed, there can be a lack of correspondence between some important features of the study region and its spatial analogue – like day-length, vegetation or soil type, etc. However, this method can be used to determine how systems respond to an expected climate.

### 1.1.2.2. Temporal analogues

Those scenarios use climatic information from the past, at the same location, to construct future scenarios. That information can come from geological records – and we speak of paleoclimatic analogues – or from instrumental records, more recent – and we speak of instrumental analogues.

Paleoclimatic analogues: Reconstructions of past climate from geological evidences – fossil flora and fauna, sediment deposits, tree rings, etc. – give information about past temperature and precipitation regimes. The found episodes of global-scale warmth are then used as climate change scenarios. But there are large uncertainties in the determination of so distant past climate. Moreover, the causes of those past events of warmth are very likely not to be the same than the current ones, so the consequences may be different too.

Instrumental analogues: Past periods of global-scale warmth are identified from instrumental records – less distant past than for paleoclimatic analogues of course – and used as climate change scenarios. Since this warmth episode has been recorded, it insures a physically plausible climate change scenario, and a quite precise one. However the magnitude of this episode is usually small and they do not represent the full range of possible climate change scenarios.

## 1.1.3. SRES scenarios

### 1.1.3.1. Context

The greenhouse gases and the aerosols are very likely the most important cause of the climate change, reducing the efficiency with which the earth's surface radiates to space, and so causing the warming of the lower atmosphere and surface. And the emissions of those agents are increasing, due to human activity, leading to an increase of their atmospheric concentration.

That is why the Intergovernmental Panel on Climate Change (IPCC) has developed the first release scenarios in 1992 – called IS92 scenarios. In 1996, due to advances in science and to a better understanding of the driving forces under those emissions – demographic and socio-economic development, technological change –, it has been necessary to renew them.

Therefore, the IPCC constructed new emission scenarios, which include improved emission baseline and updated information about the driving forces. Moreover, they examine different possibilities, hypothesis about the future tendency and rate of emission of the forcing agents. However, they do not consider any climate initiative. Those scenarios are explained in their Special Report on Emission Scenarios (SRES), and so called SRES scenarios.

### **1.1.3.2. SRES scenarios**

Four different narrative stories – A1, A2, A3 and A4 – were constructed, corresponding to four different hypothesis about the future demographic, social, economic, and technological development. However, no probability, no likelihood has been attached to any of those families.

The A1 family represents a world of very rapid economic growth with the diminution of the regional differences and the apparition of new and efficient technologies, with a population that peaks in mid-century and then declines. This storyline is subdivided into 3 categories, illustrating different choices of future technological change as far as energy source is concerned:

- A1FI: intensive utilization of fossil energy sources
- A1T: utilization of non-fossil energy sources
- A1B: balance across all the sources (no heavy dependency on one particular source of energy)

The A2 family describes a very heterogeneous world with continuously increasing population, and slow and fragmented economic development and technological change.

The B1 family assumes a convergent world with the same pattern of demographic development than in A1 – rapid growth until mid-century then decrease – but with rapid change in economic structures toward a service and information economy, with clean and efficient technologies. The focus is on global solutions of sustainability.

The B2 family represents a world with continuously increasing population but at a lower rate than in A2, with intermediate economic development and less technological change than in A1 and B1. It insists on local and regional levels.

They lead to very different results in term of future greenhouse gases emissions for the 21<sup>st</sup> century. For example, the expected CO<sub>2</sub> atmospheric concentration in 2100 varies from 540 to 970 ppm (90% to 250% above the concentration of 280 ppm in 1750) according to the chosen family. The projections of the different families for several gases are shown in Figure 1.

Those storylines are defined as input for climate models, especially the Global Circulation Models (GCM), which will develop different scenarios for each family. In total, 40 scenarios were developed in this way by the IPCC (*IPPC, 2001*).

## The global climate of the 21st century

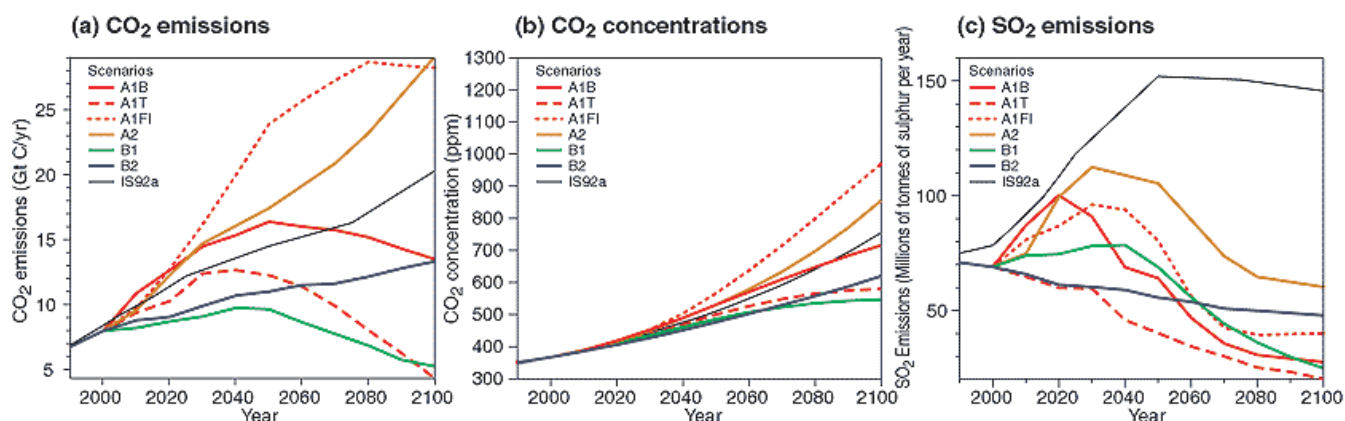


Figure 1: Projection of SRES emissions for 21st century [IPPC, 2001]

## 1.2. Climate models

A climate model is “a numerical representation of the climate system based on the physical, chemical and biological properties of its components, their interactions and feedback processes, and accounting for all or some of its known properties” (IPPC, 2001). Therefore, it can determine the impact of anthropogenic perturbation on the climate system through a mathematical formulation of all involved key processes.

A climate model can be of varying complexity, depending on its number of dimensions, represented processes, and all made simplifications. Different types of models are presented in this section.

### 1.2.1. Simple models

The simplest climate models, and the first one developed, are the one doing the greatest number of simplifications. They are based on the basic comprehension of the energy balance of the Earth system, and can provide a broad quantitative estimate of some globally averaged variables. Some models reduce their complexity to two, one or even zero dimensions, and are very easy and quick to use. However, they allow looking at the sensitivity of the climate to only one process among the wide range of parameters. They can be used within larger assessment model, to analyze the impact of a particular decision.

Climate models of higher complexity have then being created, and are still under development: the Earth system Models of Intermediate Complexity (EMIC). They described most of the process involved, however in a much parameterized form. They can make long-term simulations and sensitivity analysis, but they cannot assess regional climate change.

## 1.2.2. Global Climate Models

### 1.2.2.1. General Circulation Models

Developed from the mid 1970's, the General Circulation Models (GCM) simulates separately the important processes governing the future evolution of the climate. The first ones to be created were the models representing the atmosphere circulation (AGCM) and the ocean circulation (OGCM). Then, it has been possible to model also the cryosphere, the land surface, the carbon cycle, etc.

The GCM are based on discretized mathematical equations solved using a three-dimensional grid over the globe. Their resolution is limited by the computing capacity, and is usually around 300 km horizontally, and 1 km vertically. As far as time scale is concerned, the results of GCM can usually be annual, seasonal or monthly, sometimes daily for some variables. They take as input the SRES scenarios developed in the previous section, and give as outputs the future evolution of the temperature, the precipitation, the humidity rate, etc.

### 1.2.2.2. Coupled circulation models

The coupled circulation models integrate many processes; they not only consider one circulation pattern, but they also take into consideration their mutual interaction. The first one to be developed, in the mid 1980's, was the Atmosphere-Ocean General Circulation Model (AOGCM). For that matter, all the coupled circulation models are often called in that way, even if they now combine even more processes (IPPC, 2001). Figure 2 illustrates the development of the global and coupled climate models.

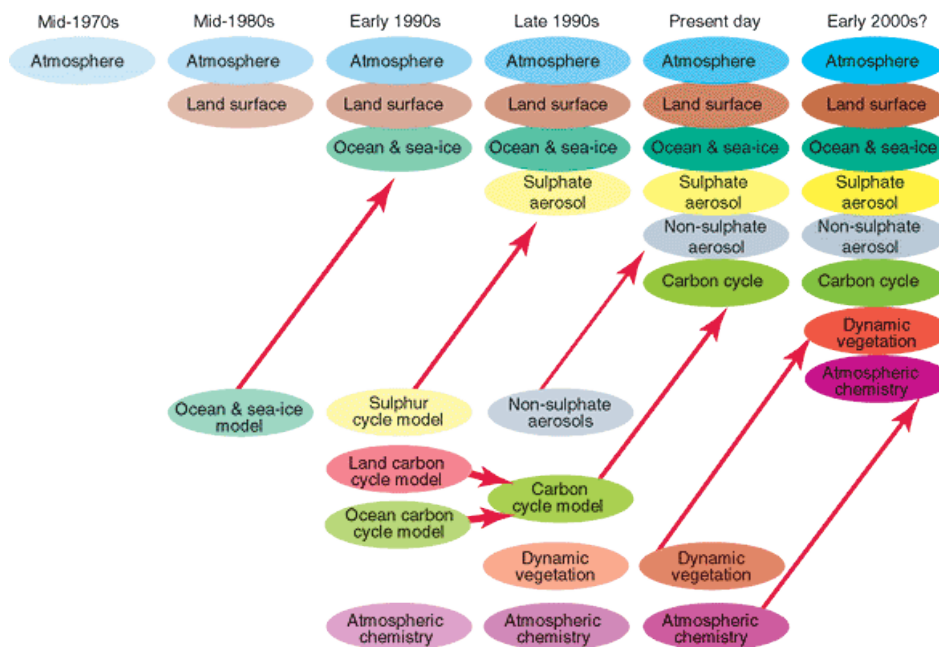


Figure 2: Development of Global Climate Models [IPPC, 2001]

Those comprehensive models are more precise, more complete than the simpler ones, but they are very complex and need large computer resources.

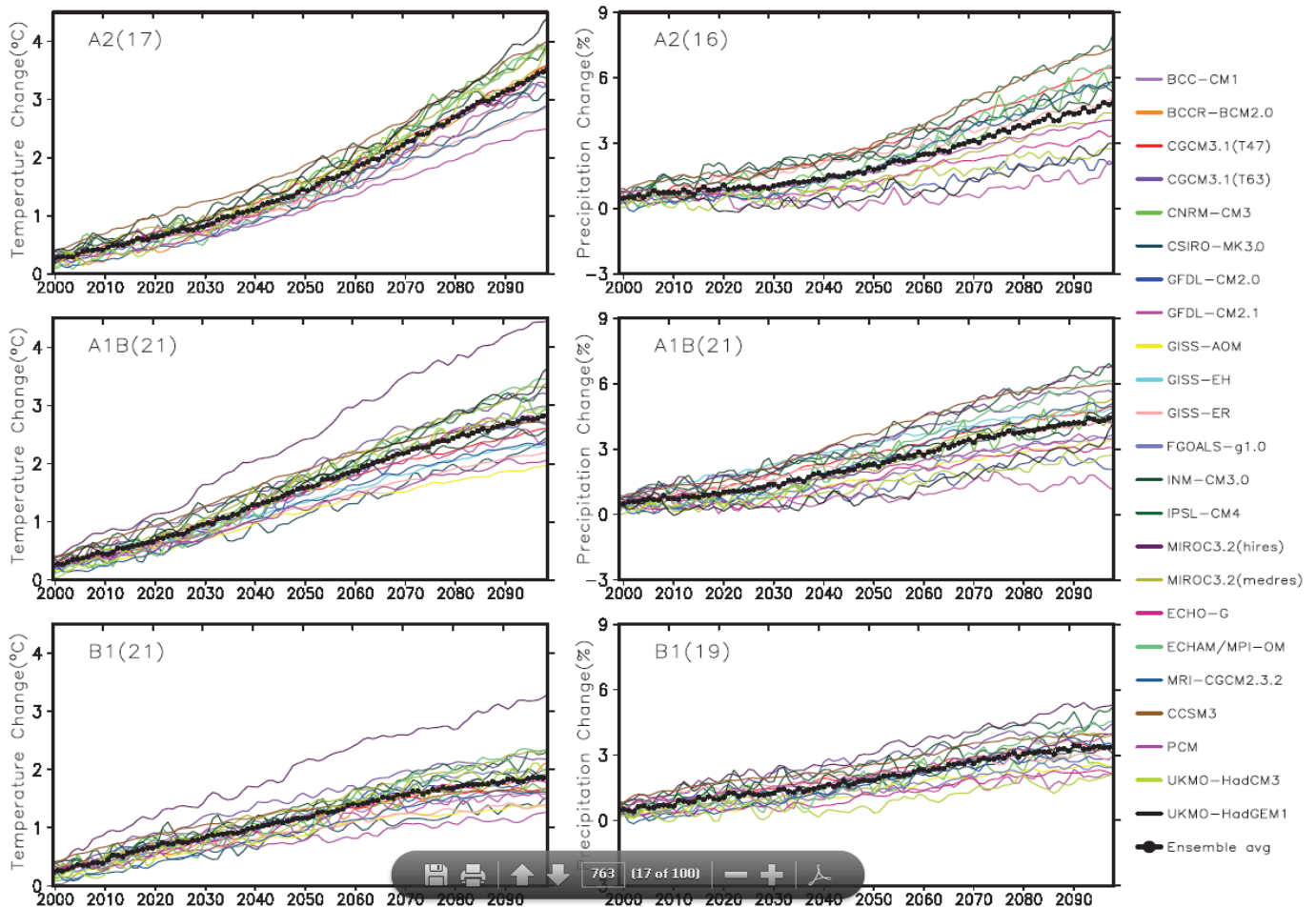
Different models have been developed within the scientific community, by several research centers. The most popular are certainly the HadCM3, developed by the UK Hadley Center for Climate



Prediction and Research (MetOffice, 2012), the ECHAM5 by the German Max-Plank Institute for Meteorology (MPI, 2003) and the CGCM4 built by the Canadian Centre for Climate Modeling and Analysis (CCCma, 2012).

### 1.2.2.3. Climate projections

Climate projections done with different coupled global circulation models present a wide range of results, as it is shown in the graph below.



*Figure 3: Prediction of global temperature change from different coupled GCM for three SRES scenarios [IPPC, 2007]*

However, there have been a lot of climate projections done these last years, with different models and different scenarios. Therefore, despite of the high variability of climate projections, it is now possible to draw a trend, a mean response for each input SRES scenario.

For example, the global averaged temperature response using the A2 forcing for the 2080-2099 period is  $+3.13^{\circ}\text{C}$  compared to the reference years (1980-1999), and the average precipitation response is an increase of around 4 %.



## 1.3. Downscaling methods

The main issue with the Coupled global climate models is that their results have a coarse horizontal resolution – around 300km – which is not enough for impact studies, where more regional or even local precision is required. Moreover the regional specificities of the climate are not taken into consideration by the GCM, like the effect of mountains on local climate, or the effects of the Great Lakes system in Canadian local climate. That is why different spatial downscaling techniques have been developed, and are still under development, to derive more detailed regional climate information from the results of GCMs – especially temperature and precipitation data – and are exposed in this section (EC, 2004; CCIS, 2012; Gachon, 2005; IPCC, 2001; Mearns et al., 2003; Wilby et al., 2004).

### 1.3.1. High resolution AGCM experiments

The AOGCMs have a coarse resolution of 300 km, but the simple AGCMs can have a finer resolution of 50 km. The idea of this downscaling method is to use AOGCMs to make a global simulation, and then to use the AGCMs to reinterpret the atmospheric response at a finer scale, for a certain period of interest, having as input the same forcing scenario as the AOGCMs, and its responses for that period: ocean response, ice distribution, etc. – all except the atmospheric response.

This approach is based on the hypothesis that the large scale circulation patterns in the AOGCM and in the AGCM are similar. If this hypothesis is not validated, the results of the two models would not be consistent. This method catches the atmospheric response at regional level quite well. However, one of its weaknesses is that the AGCM considers feedback effects only from the regional zone in which it is run. However in reality they come from a wider geographical zone. Moreover, it uses the same formulation than the AOGCM for which it has been optimized, so there can be some accuracy problems at a finer scale. Finally, this method is very computationally demanding, which limits the resolution to 50 km, and also restricts the number of simulations.

A wise utilization of this method is done if the method appears as an intermediate step between the raw output of GCMs and a dynamical or statistical downscaling method.

### 1.3.2. Statistical downscaling

Statistical downscaling regroups various methods based on the principle that regional climate is conditioned by two factors: the large-scale climate and the local physiographic features – topography, ground utilization, and land/sea distribution. Therefore, statistical relationships are built empirically between variables of the large-scale current climate – predictors – given as result of a GCM, and observed variables of the local climate – predictand. Future predictors – results of the projection of a GCM – are then input in the model to find the future regional climate.

This technique is not demanding computationally and easy to apply to different GCMs. Moreover, it can give very local result, at a basin or station scale, which is very useful for impact studies.

However, it is based on the hypothesis that those statistical relationships – found with current climate data – will remain the same in the future. One can immediately see that this is precisely the main weakness of those methods, in a context of climate change.

Another drawback is that statistical downscaling requires a lot of observed data, and a very precise calibration with observed data. Besides, theoretically the method is valid only within the range of the

calibration data, which can be a problem in the context of climate change. Finally, the user has to be very careful in the choice of the predictors. Indeed, not all climate variables are suited to be predictors: it has to be strongly correlated and sensible with the predictand, to have enough records, and to be modeled accurately by GCMs. And the choice of the predictor impacts a lot on the results of the downscaling.

The three main categories of statistical downscaling, – transfer function, weather typing and weather generators – are explained below.

### 1.3.2.1. Transfer functions

They are statistical downscaling methods with a direct quantitative relationship between the predictors and the predictand.

There is different kind of transfer functions, the most common and easiest ones being derived from linear regression techniques, like the multiple regressions models, the canonical correlation analysis or the singular value decomposition. Other transfer functions are also based on piecewise linear or non-linear interpolations, like the artificial neural network.

The procedure of this method is represented in Figure 4.

### 1.3.2.2. Weather typing

The principle of the methods based on weather typing is similar to the one of the transfer function methods, but weather types – i.e. atmospheric circulation patterns, like cyclonic or anti-cyclonic conditions – are used as predictors instead of large-scale climate variables. So the statistical relationship is calculated between weather classes rather than climate variables. This method of course requires the preliminary step of weather typing.

Its procedure is illustrated in Figure 4.

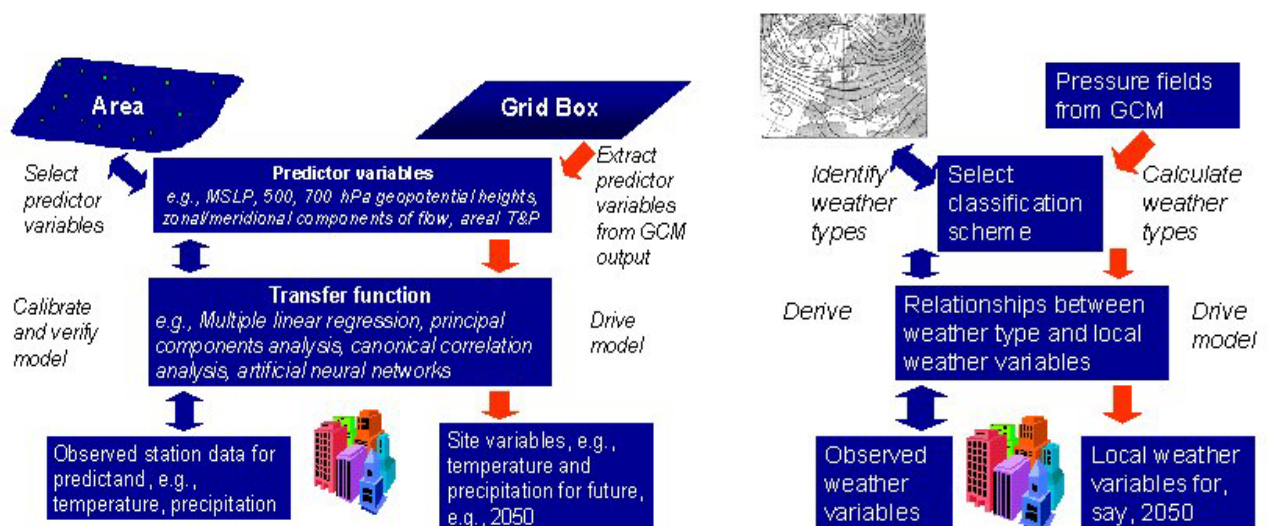


Figure 4: Scheme of downscaling procedure with transfer function (left) and weather typing (right)[CCIS, 2012]

### **1.3.2.3. Weather generators**

They are statistical models of observed weather data, and are generally on daily or even sub-daily time-scale, thus providing temporal downscaling in addition to the spatial one, which can be particularly interesting in impact studies.

They are usually stochastic, based on the representation of precipitation occurrence with Markov processes for wet- / dry- day's alternation, and on the reconstruction of the rainfall intensity.

They produce local artificial daily series of weather data – maximum and minimum temperature, solar radiation, wind speed, precipitation, etc. – based on the statistical characteristics of local observed weather and the results of GCMs.

However, they require a lot of observed data. And they represent better events with high frequency, so they are not well suited to represent extreme events.

Some non-parametric weather generators also exist, based on sorting algorithm.

## **1.3.3. Dynamical downscaling: Regional Climate Models**

### **1.3.3.1. Principle**

The dynamical downscaling is the use of Regional Climate Models (RCM) to improve the spatial resolution of the climate predictions.

The principle is to imbricate a limited area model (LAM) of high resolution into a global model. The GCM drives the simulation, while the regional model provides a better representation of local topography and of some local climate processes. The initial conditions and the time-dependent lateral boundary conditions of the RCM are taken from the outputs of the GCM.

Developed recently, this method is now widely used, and gives physically based long-term prediction at high spatial resolution, usually around 30-50 kilometers.

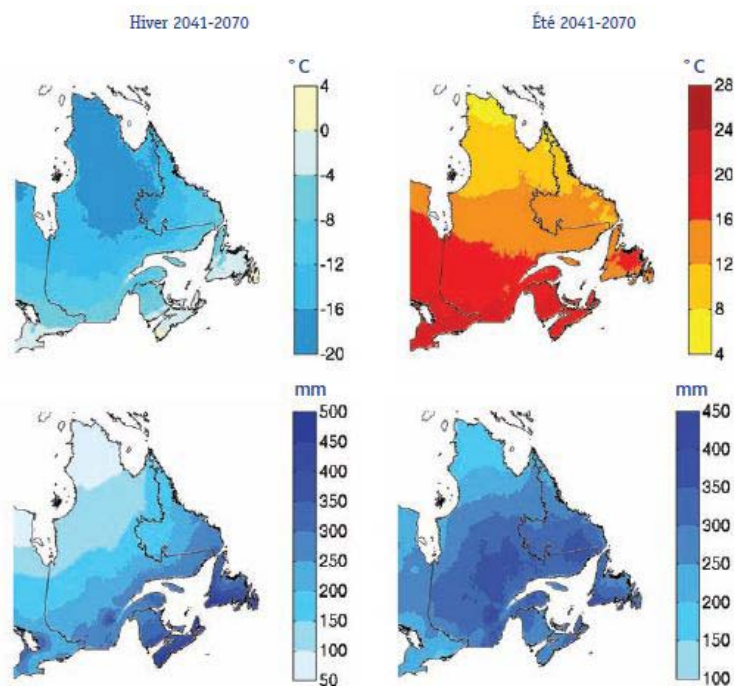
However, this is for the moment only a one-way process: there is no feed-back from the RCM simulation to the driving GCM. Moreover, it is very demanding computationally, which limits the number of simulations.

### **1.3.3.2. The Canadian Model**

Different models have been created all around the world, for different areas.

In Canada, a regional model was developed and is regularly upgraded from 1990, by the Canadian Center for Climate Modeling and Analysis (CCCma). The Canadian Regional Climate Model (CRCM), now at its fourth generation, is based on the Canadian GCM (CGCM4). It has a resolution of 45 km horizontally, and 29 levels vertically from the surface to around 30km.

Figure 5 is an example of result from the CRCM, showing the temperature and precipitation predictions for 2041-2070 period.



*Figure 5: Temperature (top) and precipitation (bottom) predictions, averaged from 17 simulations of the CRCM [Ouranos, 2010]*

## **1.4. Comparison between different tools predicting climate projections, recommendations and limitations.**

### **1.4.1. Comparison and recommendations**

In this section, a list – non exhaustive – of the main tools available to obtain predictions of future climate is, from the building of simple incremental scenarios to the refinement of predictions of GCM with downscaling methods. As shown, each method of each step has advantages and drawbacks, leads to different resolutions, and can be combined with others to improve its results.

The main point to remember is that there is no absolute best method, the combination to use should be chosen case by case, according to the area of study, the data available, the resolution needed – so the purpose of the study, the time and money that can be spent on this purpose, and the number of simulations desired. Moreover, the user must be well aware of the limitations – weaknesses –and the uncertainties linked to each method or group of methods, and very careful in the choice of the parameters. If possible, the combination chosen should be tested on prediction of past climate in the same area of study, to validate it.

Table 1 summarizes the strengths and weaknesses of all the tools presented in this section to obtain predictions of future climate, and the recommendations of utilization.

*Table 1: Summary of the strengths and weaknesses of the different methods to obtain prediction of future climate [Adapted from IPCC, 2001]*

<b>Scenarios / Tools</b>	<b>Strengths</b>	<b>Weaknesses</b>	<b>Recommendation of use</b>
<b>Incremental Scenario</b>	<ul style="list-style-type: none"> <li>- Very easy and quick to design and apply</li> <li>- Can make a lot of simulations on different parameters</li> <li>- Applicable everywhere</li> </ul>	<ul style="list-style-type: none"> <li>- Not realistic scenarios</li> </ul>	<ul style="list-style-type: none"> <li>- Sensitivity analysis</li> <li>- Determination of threshold value</li> </ul>
<b>Analogue Scenarios:</b>			
Spatial Analogue	<ul style="list-style-type: none"> <li>- Simple</li> <li>- Physically credible scenarios</li> </ul>	<ul style="list-style-type: none"> <li>- Lack of correspondence between the area of study and its spatial analogue</li> </ul>	<ul style="list-style-type: none"> <li>- Determination of a system's response to an expected climate</li> </ul>
Temporal Analogue	<ul style="list-style-type: none"> <li>- Physically credible scenarios</li> </ul>	<ul style="list-style-type: none"> <li>- Magnitude of change underestimated</li> <li>- Does not represent the full range of possible future scenarios</li> </ul>	<ul style="list-style-type: none"> <li>- Assessment of past sensitivity and adaptation to climate change</li> <li>- Assessment of a system's vulnerability to abrupt climate change</li> </ul>
<b>Climate Models based on SRES scenarios:</b>			
Simple models	<ul style="list-style-type: none"> <li>- Give a quick estimate of averaged global variables</li> </ul>	<ul style="list-style-type: none"> <li>- Only broad estimation</li> </ul>	<ul style="list-style-type: none"> <li>- Analysis of the impact of a particular decision</li> <li>- Sensitivity analysis</li> </ul>
AOGCM	<ul style="list-style-type: none"> <li>- physically based models</li> <li>- Integrate many processes</li> <li>- SRES scenarios very complete</li> </ul>	<ul style="list-style-type: none"> <li>- Computationally demanding</li> <li>- Different models give wide range of results</li> <li>- Poor spatial resolution</li> </ul>	<ul style="list-style-type: none"> <li>- Large scale response to anthropogenic forcing</li> <li>- Starting point for downscaling methods</li> </ul>
High resolution AGCM experiments	<ul style="list-style-type: none"> <li>- Physically base</li> <li>- Good spatial resolution (50km)</li> </ul>	<ul style="list-style-type: none"> <li>- Some accuracy problems at local scale</li> <li>- Computationally very demanding</li> </ul>	<ul style="list-style-type: none"> <li>- To obtain information at high spatial resolution on global scale</li> </ul>
Statistical downscaling:			
- Transfer function & weather typing	<ul style="list-style-type: none"> <li>- Not demanding computationally</li> <li>- Provide high spatial resolution results</li> </ul>	<ul style="list-style-type: none"> <li>- Assumes that the empirical relationship will not change with time</li> <li>- Require a lot of data an precise calibration</li> </ul>	<ul style="list-style-type: none"> <li>- Provide high spatial resolution results at local or station scale</li> </ul>
- Weather generator	<ul style="list-style-type: none"> <li>- Provide high spatial and temporal (sub-daily) resolution</li> </ul>	<ul style="list-style-type: none"> <li>- Require a lot of observed data</li> <li>- Not well suited for extreme events</li> </ul>	<ul style="list-style-type: none"> <li>- Generate artificial time-series of climate variables</li> <li>- Impact studies</li> </ul>
Dynamical downscaling	<ul style="list-style-type: none"> <li>- Good spatial resolution</li> <li>- Good temporal resolution</li> <li>- Good representation of extreme events</li> </ul>	<ul style="list-style-type: none"> <li>- Very demanding computationally</li> <li>- Only one-way process</li> </ul>	<ul style="list-style-type: none"> <li>- Provide high spatial and temporal resolution results</li> </ul>

### 1.4.2. Limitations of this approach for the present study

As explained in this section, a lot of tools exist to obtain predictions of future climate, with a very high variability of results, and the method to use must be chosen according to the characteristics of the study. The objective of the present report is to study the impacts of climate change on the hydraulic structures of a local river – the Des-Prairies River. This will be done by determining the appropriate hydrograph at the entrance of the river, as required input data for the hydrodynamic simulation software, which will give the response of the river in term of water level rise. To do so, one of the required data is the predicted future precipitation in the basin of the Des-Prairies River for a long period of time, on a sub-daily basis in order to obtain the future Intensity-Duration-Frequency (IDF) curves, and the temporal distribution of precipitation for an event of 24h with a return period of 50 years.

Among all methods described before, predictions of future precipitation from the Canadian GCM (CGCM3) downscaled with weather generators could be interesting, since it provides results with high spatial and temporal resolution. However, this method would require a lot of observed precipitation data, not easy to obtain, and is not well suited for the prevision of extreme events, which is what we are interested in. The use of dynamical downscaling of the results of CGCM3 using the Canadian RCM (CRCM3) was also foreseen. However, the required results – sub-daily precipitations – are not public. And even if it was possible to obtain them, they would require some more processing, which is time-consuming, especially to make all the required validation steps.

Besides, as mentioned previously, there are a lot of uncertainties in all those methods. That is why a very careful calibration of the models – which is very demanding in observed data – and a long validation process of the results are needed. Nevertheless, there is still a very high variability of the results.

Moreover, some scientists have already studied this issue of constructing future IDF curves. In particular a team of researchers already looked at the trends in Southern Quebec – where the case study of this report is located – built future IDF curves, and made comparison with the actual ones, making all the validation steps of their model and of their results (Mailhot et al., 2007)

From all listed reasons – high variability of the results, lack of data, limit of time – it has been decided that this complete approach was not worthy for this study. Therefore the required future precipitation data are taken based on Mailhot et al. (2007): “*Assessment of future change in intensity-duration-frequency (IDF) curves for Southern Quebec using the Canadian Regional Climate Model (CRCM)*”. Details of this study, its results and the data that have been used in this report will be explained in Chapter 3.



# Chapter 2 – Presentation of the basin of the Des-Prairies River

## 2.1. Des-Prairies River and Ottawa Basin

### 2.1.1. Des-Prairies River

The Des-Prairies River is located in Canada, in Québec’s Province. Its water comes from the Ottawa River, through the Lake of Two Mountains where it originates, and from which it receives approximately 40% of the water. It flows into the Saint-Lawrence River around 50 km after, separating the north of the Island of Montreal from the Island of Laval (Jesus Island). It has two tributaries: just after the Bizard Island, it is joined by another small reach of the Lake of Two Mountains; and no long before it flows into the Saint-Lawrence River, it is joined by the Mille-Ile River, which also originates in the Lake of Two Mountains.

The Des-Prairies River is crossed by twelve bridges: five highway bridges, five mototway bridges and two railway bridges. There are also one run-of-river power station – the power station of the Des-Prairies River – and two dams near: the earth dam of the Visitation Island and the Simon-Sicard concrete dam. Numerous rapids can also be found in this river.

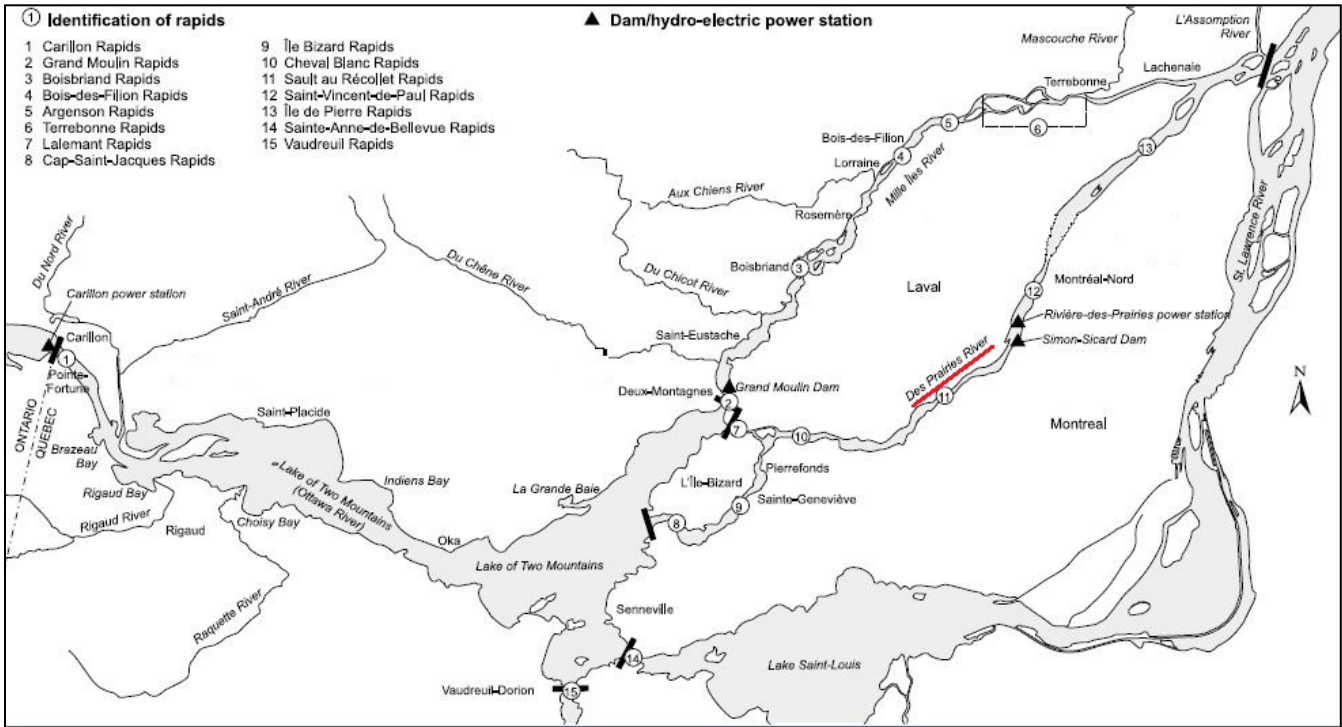


Figure 6: Lake of Two Mountains and Des-Prairies River [Robitaille, 1999]

### 2.1.2. Ottawa Basin

The catchment area of the Des-Prairies River is the Ottawa River basin, the biggest basin in east Canada with a territory of 146 000 km<sup>2</sup> – part in Québec and part in Ontario. Its main river, Ottawa River, is 1271 km long, and flows from the Lake Timiskaming, at the exit of the Vérendrye Reserve, to the Lake Saint-Louis. This hydrographic network includes nineteen sub-basins of more than 2000 km<sup>2</sup>.



Figure 7: Basin of Ottawa River [Wikipedia, 2012]

## 2.2. Area of study

The purpose of this study is to make a rainfall-runoff transformation, from the future rainfall, in order to get the expected future hydrograph at the entrance of the Des-Prairies River, and the hydrograph of its tributaries, in case of extreme rainfall events. However, it is very complex to make a hydrological study of a catchment as big as the Ottawa basin. Indeed, the characteristics – soil properties and utilization, slope, etc. – are not homogeneous at all, neither the rainfall – intensity, duration, etc. Moreover, we are mainly interested in the rainfall events and their consequences in the surroundings of Montreal, not 700 km away. Therefore, it has been decided to restrict the area of study to two sub-basins: the basin of the North River and the Basin of the Milles-Iles River.

### 2.2.1. Basin of the Du-Nord River

The Du-Nord River originates in the Lake of Black Mountain and flows for 141 km through the cities of Sainte-Agathe-des-Monts, Sainte-Adèle, Saint-Jerome, and Lachute. It flows into the Ottawa River just after the Carillon power station, at the entrance of the Lake of Two Mountains. Its mean slope is 3.1 meter per kilometer, corresponding to a difference in altitude of more than 430 meters between the source and the outlet.

The Du-Nord River drains a basin of 2200 km<sup>2</sup>. It is occupied mainly by forests (73%) and agriculture (13%), whereas the urban area represents around 7% of the basin, and the water 6%. The soil is mainly composed of gleysols in the Saint-Lawrence low lands (in the south part) and podzols in the Laurentien Plateau (in the north part).



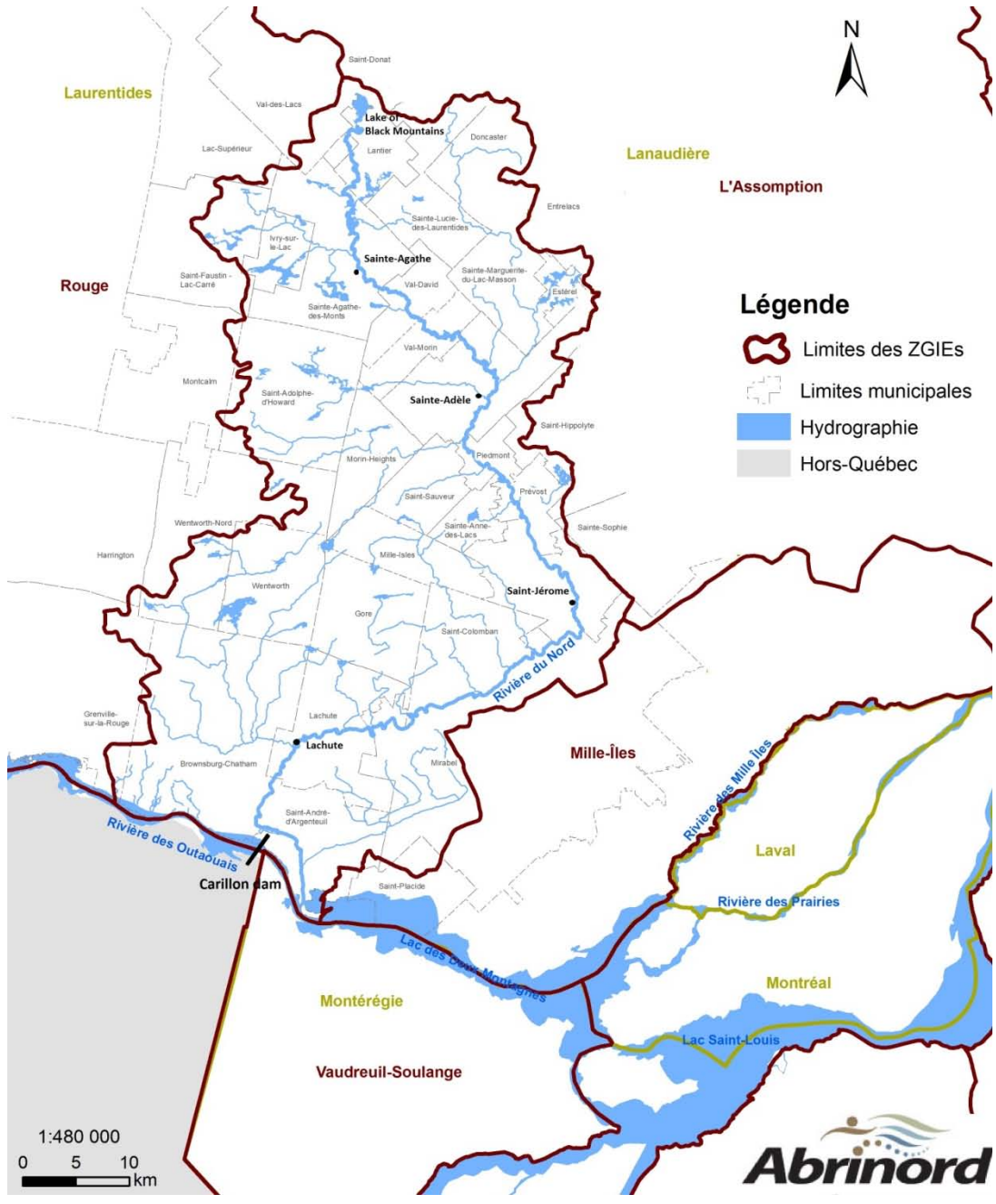


Figure 8: Basin of Du-Nord River [Abrinord, 2008]

## 2.2.2. Basin of the Milles-Iles River

The Mille-Ile River originates in the Lake of Two Mountains, from which it receives approximately 10% of the water, and flows for 42 km on the north of Jesus Island (city of Laval). It flows into the Des-Prairies River just before it joins the Saint-Lawrence River.

The Mille-Ile River drains has basin of 1053 km<sup>2</sup>, very flat, in which four main rivers define four sub-basins: the Du Chêne, Du Chicot, Aux Chiens and Mascouche Rivers. The characteristics of those sub-basins are reported in Table 2.

Table 2: Characteristics of the sub-basins of Mille-Ile River

	River		Area [km <sup>2</sup> ]	Basin			Type of soil
	Length [km]	Mean slope [%]		Ground occupation [%]			
				Agricultural	Forest	Urbanized	
Du Chene River	29	0.17	212	64	24	12	Clays, clay loams, sandy loams
Du Chicot River	18	0.23	77	63	25	12	
Aux Chiens River	15	0.19	79	20	30	50	
Masouche River	58	0.11	411	56	30	14	

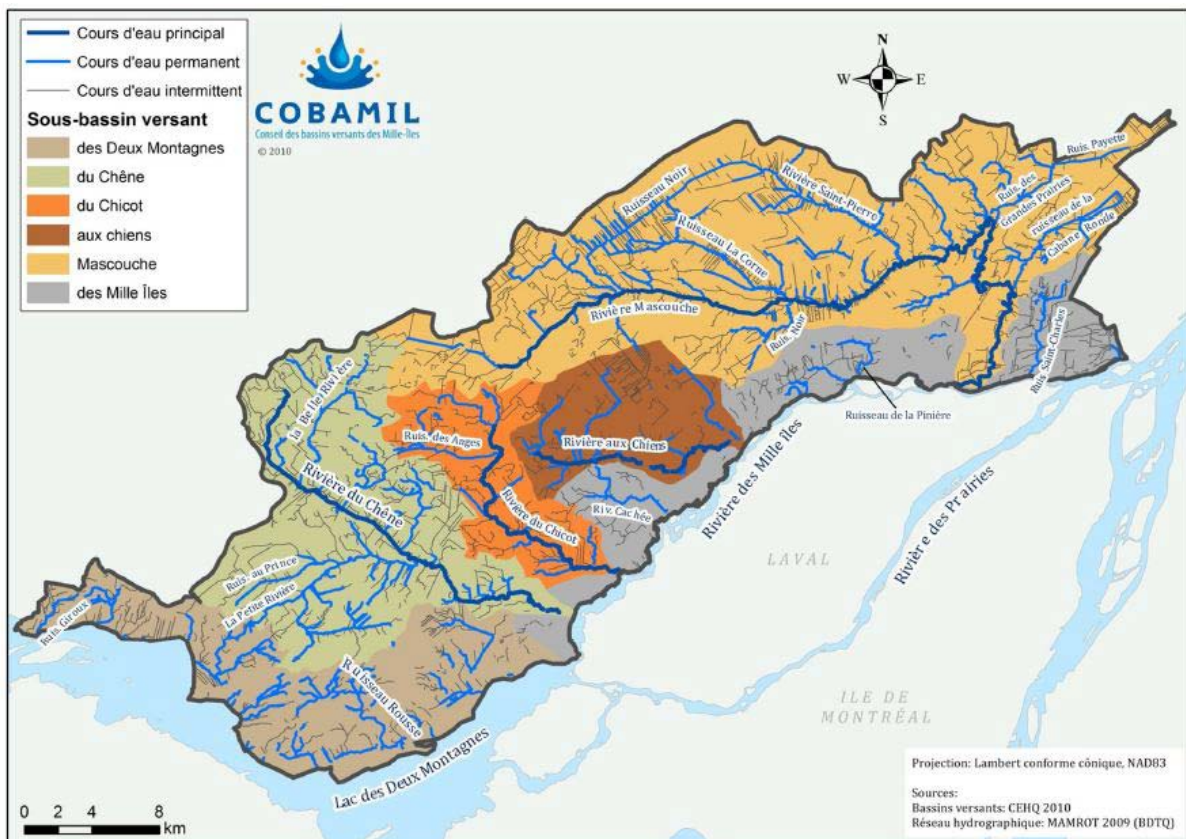


Figure 9: Basin of Mille-Ile River [Cobamil, 2011]

## Chapter 3 – Hydrological considerations

The purpose of this part is to make a rainfall-runoff transformation, for future precipitation in the basins of the Du-Nord River and of the Mille-Ile River, in order to obtain the hydrograph at the entrance of the Des-Prairies River, and the hydrograph of its tributaries. Those hydrographs will then be input in the simulation software, to model the response of the river in term of level rise.

First of all, some background about IDF curves and hyetograph will be given. Then, different methods to get the rainfall hyetograph will be explained and compared. Finally, the rainfall-runoff transformation, done with the Hec-HMS software, will be described, and the results given.

### 3.1. Rainfall hyetograph

#### 3.1.1. IDF Curve

An Intensity-Duration-Frequency (IDF) curve is a graphical representation of average rainfall intensity versus storm duration, at a given place. Usually, several curves are plotted, corresponding to several return periods (*Osman Akan, 1993, Sanfilippo&Paoletti, 2011*).

They are drawn by making a frequency analysis of rainfall events. First, the annual maximum rainfall depths for events of given durations are extracted. The series thus obtained are analyzed to be fit to a certain statistical distribution – usually the Gumbel distribution, also called distribution of generalized extreme values of type I. The frequencies of exceedence for various rainfall depths are then determined, and the depths are divided by the duration of the storm to obtain the intensity.

The mathematical expression of the intensity, for a given return period, can be expressed with two (Eq.1) or three (Eq.2) parameters:

$$\bar{i} = a * \theta^{n-1} \quad (1) \quad \text{or} \quad \bar{i} = \frac{a}{(b + \theta)^c} \quad (2)$$

where  $\theta$  is the storm duration, and  $a, b, c, n$  are local parameters to be calibrated for each return period – for example using least square analysis.

From the IDF curve, one can derive the hyetograph, using different methods explained in the following.

#### 3.1.2. Design Hyetograph

The rainfall design hyetograph, representation of the temporal distribution of the rain during a rainfall event in a given place for a given return period, can be derived from the IDF curves. Different techniques are exposed in this paragraph (*Osman Akan, 1993; Sanfilippo&Paoletti, 2011; Bertrand-Krajewski, 2006a; MDDEP, 2011*).

### 3.1.2.1. Constant and triangular hyetographs

The constant hyetograph – or rectangular hyetograph – is drawn from the IDF curve for a given return period by drawing a horizontal line at the height corresponding to the given storm duration. It therefore assumes a constant distribution of rainfall all along the storm event. This is obviously the easiest hyetograph to draw, but it does not represent truly the event. However, it can be useful in case we are interested in the peak value of runoff to evacuate and not to the temporal distribution of the rainfall event.

The triangular hyetograph is a little bit more sophisticated. It distributes the same volume of rainfall in a triangular shape. The three parameters are the total rainfall depth, the duration of the storm and the time of the peak – usually around 1/3 of the duration of the event.

### 3.1.2.2. Desbordes hyetograph

The Desbordes hyetograph – or double triangular hyetograph – is an improvement of the triangular hyetograph, developed in 1974 with the aim of minimizing the sensitivity of the hydrographs on the lag time, and particularly well suited to small urban catchments. It is based on the principle that rainfall events usually have a short period of intensive rainfall within the total event, which is more uniformly distributed.

This design hyetograph is therefore defined by five parameters that can be chosen by the user, or directly derived from the ISF curves by some formulas:

- The total duration of the rainfall event:  $t_3$
- The duration of the intense period:  $t_1$
- The position of the beginning of the intense period:  $t_2$
- The rainfall intensity reached at the beginning of the intense period:  $i_1$
- The maximum rainfall intensity reached during the intense period:  $i_2$

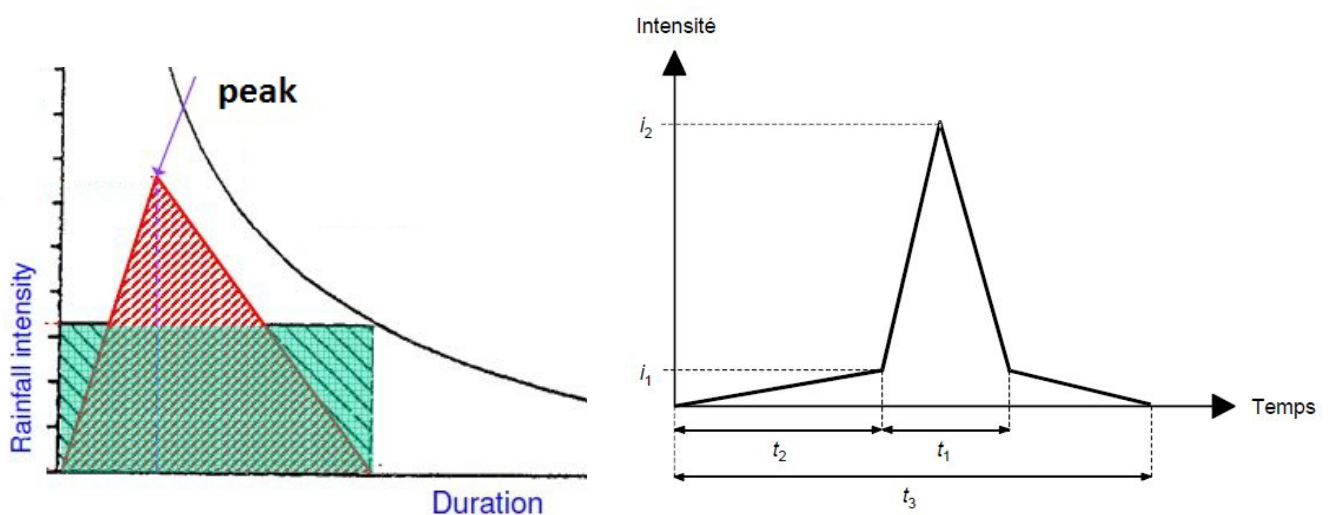


Figure 10: Constant and triangular (left) and Desbordes(right) hyetographs [Adaptated from Sanfilippo & Paoletti, 2011 & Bertrand-Krajewski, 2006a]

### 3.1.2.3. Chicago and Sifalda hyetograph

The Chicago hyetograph was developed in 1957 by Keifer and Chu, originally designed especially for storm sewer design in the region of Chicago.

It is based on the direct transformation of the average intensity-duration relationship with three parameters that we have seen previously (Eq.2).

The instantaneous intensities of the design storm are then calculated (Eq.3), with the definitions of Figure 11. The parameter  $r$  – giving the time of the peak – thus describes the asymmetry of the hyetograph, and depends on the place of study.

$$i = a \left[ \frac{(1 - c) \left( \frac{t_p - t}{r} \right) + b}{\left( \frac{t_p - t}{r} + b \right)^{c+1}} \right] \text{ for } t \leq t_p \text{ and } i = a \left[ \frac{(1 - c) \left( \frac{t_b}{1 - r} \right) + b}{\left( \frac{1 - t_p}{1 - r} + b \right)^{c+1}} \right] \text{ for } t \geq t_p \quad (3)$$

The Sifalda hyetograph is a kind of simplified Chicago hyetograph, where the parameters are the storm duration and the total rainfall depth.

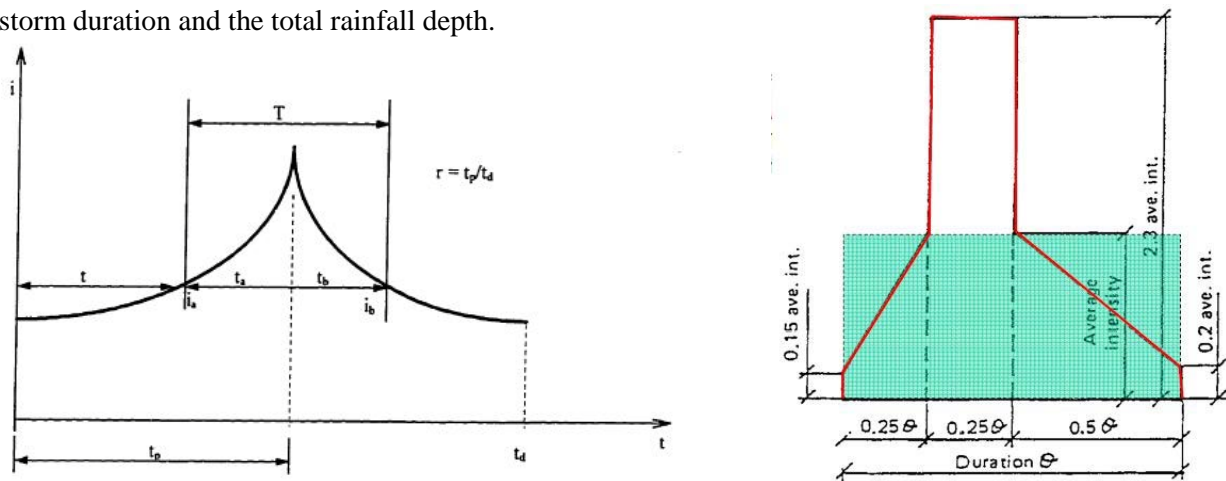


Figure 11: Chicago (left) and Sifalda (right) hyetograph [Théberge, 1996 and Sanfilippo & Paoletti, 2011]

### 3.1.2.4. SCS hyetograph

The U.S. Soil Conservation Service (SCS) decided to divide the U.S territory into four categories of rainfall pattern, and so developed four types of rainfall distributions, in a dimensionless form  $(P/P_{tot})$ , for rainfall events of 6 and 24 hours. Those distributions are represented in Figure 12.

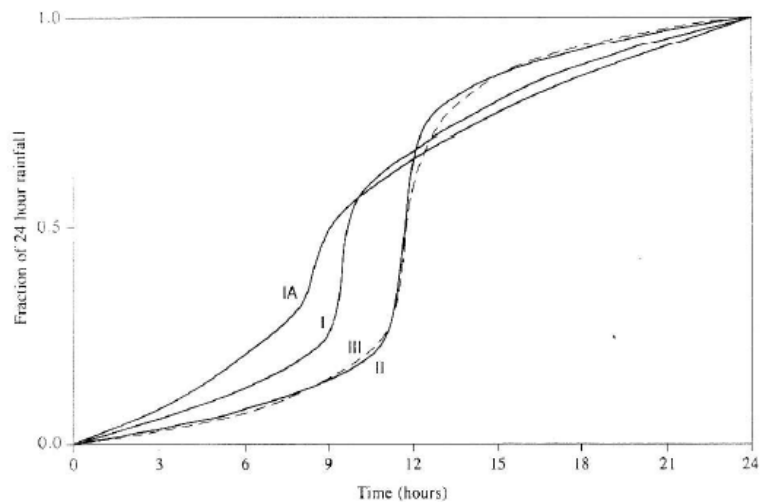


Figure 12: SCS rainfall distributions [Ven Te Chow et al, 1988]



### 3.1.2.5. Comparison of the methods and recommendations

In this section several methods have been listed to derive the rainfall hyetograph from the IDF curves. This was not the complete list of all the methods ever developed, however the most famous and used methods were described.

As always, it is important to point out that there is no absolute best method. It depends on the characteristics of the basin – size, urban or rural, on the data we have, on the soil type and utilization, and on the purpose of the study. More than everything else, the user must be well aware of the strengths and weaknesses of the method he chooses, and of its limitation. Moreover, particular attention must be taken in the choice of the parameters of the model, which could impact a lot on the result. Finally, before any simulation, the model should be tested with a rainfall event for which both rain and runoff measurements are available, to validate the choice of parameters.

Table 3 summarizes the strengths and weaknesses of all the tools presented in this section to get a design hyetograph.

*Table3: Comparison of the different methods to get a design hyetograph*

Method		Strengths	Weaknesses	Recommendation of use
<b>Design Hyetograph</b>	Constant	- Simple	- Not representative of a true rainfall event	- Determination of peak discharge value
	Triangular	- Simple - Represents the rainfall event with a peak, of position adjustable	- Still very basic representation	- Quick overview of hyetograph pattern
	Desbordes	- Suits well the small urban catchment - Customable (parameters to choose)	- Not for big catchment	- In small urban catchment
	Chicago	- Widely used - Well defined - Fit large basins	- Parameters to adjust locally - Need full IDF curves - Overestimate the peak	- Sewer design - Large basins when IDF curves available
	Sifalda	- Same global pattern as Chicago - Less parameters, easier to estimate	- Less precise than Chicago	- Large basins, when no IDF curves are available
	SCS	- Rainfall distributions well defined	- Area of use defined only in the US - Only for 6 and 24h rainfall events - Only for relatively small basins ( $T_c < 10h$ )	- For small basins - With the associated rainfall-runoff model - When the IDF curves are not available

For this project, it has been decided to use the Chicago hyetograph. Indeed, the basin under study is large – around 1200 km<sup>2</sup> – and IDF curves were available, with local parameters, as it will be explained in the following. Moreover, those methods are often used in Canada, so there are a lot of publications that could be taken as guidelines.

### 3.1.3. Application to the Du-Nord Basin

#### 3.1.3.1. IDF curves

The IDF curves for more than 100 stations in the province of Québec are published by Environment Canada, with the corresponding table of recorded annual maximums, the interpolated a, b and c parameters, and some statistics about those data. For the Du-Nord basin, IDF curves were available in Ste-Agathe and in St-Jérôme meteorological stations, drawn from precipitation data until the 1990's. An example of IDF curves at the Ste-Agathe station is presented in Figure 13. The full tables of value of the two stations and their corresponding graphs are available in Appendix 1.

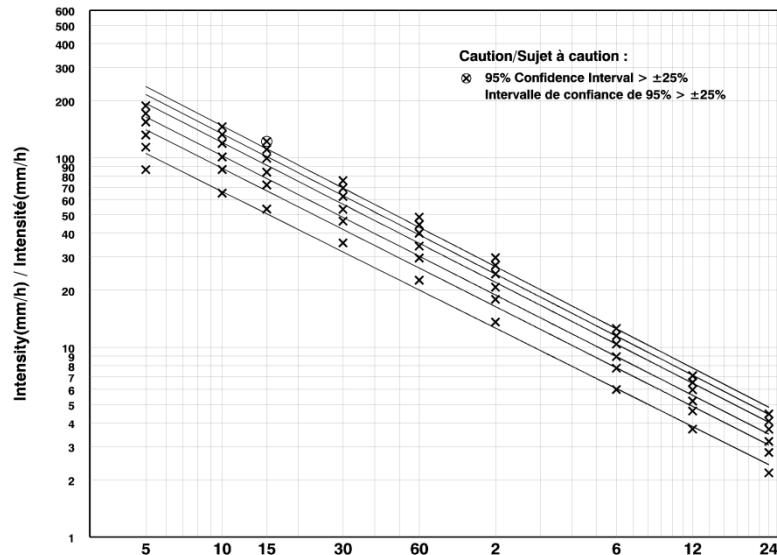


Figure 13: IDF curves at the Ste-Agathe station [Environment Canada,2012]

#### 3.1.3.2. Current Chicago hyetograph

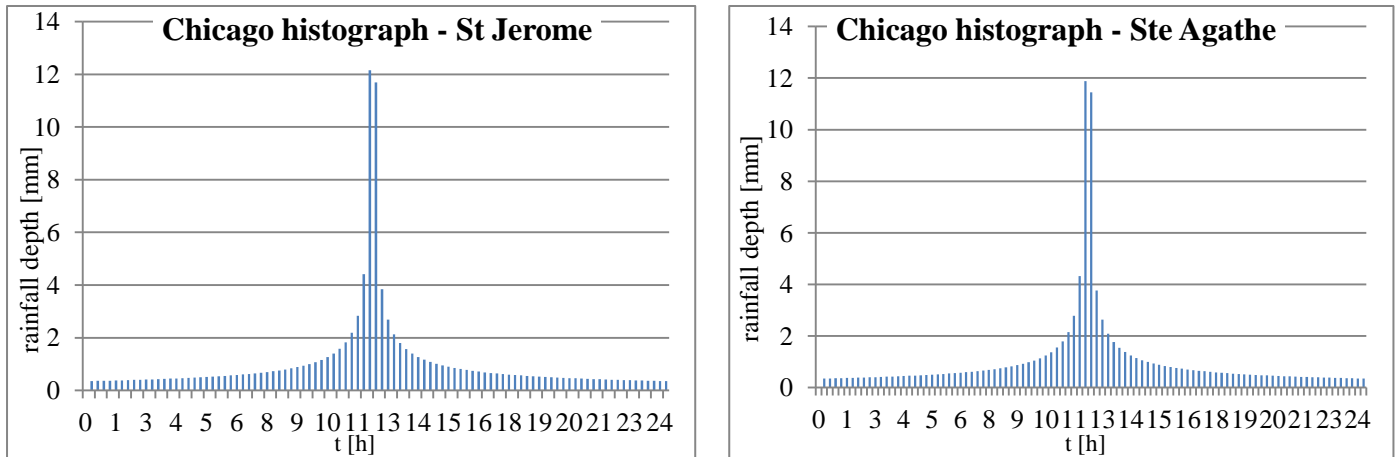
The formula given previously has been applied to calculate the Chicago hyetograph at the St-Agathe and at the St-Jerome stations. Their respective a, b and c parameters given with the IDF curves of Environment Canada have been chosen for an event of return period of 50 years and of duration of 24 hours. The  $r$  coefficient has been taken from Daynou and Fuamba (2008), who developed a Chicago hyetograph in the Montreal area, and found this value, originally for Ontario, well suited.

The time step advised in literature is around 10-15mn. Since most of the recorded data of rainfall and flows available are given with a time step of 15mn, it has been decided to take it also for the Chicago hyetograph, in order to facilitate the calibration of the model and the comparison of the results.

All those variables are shown in Table 4, and the resulting Chicago hyetograph are displayed in Figure 14. The corresponding tables of value are available in Appendix 2.

**Table4: IDF parameters of two stations in the Du-Nord basin [adapted from EC, 2012]**

Ste-Agathe					St-Jerome				
T	a	b	c	r	T	a	b	c	r
[years]	[mm/h]	[h]			[years]	[mm/h]	[h]		
2	20.1	0	0.667	0.488	2	18.7	0	0.67	0.488
5	26.2	0	0.676	0.488	5	25.6	0	0.684	0.488
10	30.3	0	0.68	0.488	10	30.1	0	0.689	0.488
25	35.4	0	0.684	0.488	25	35.9	0	0.694	0.488
50	39.2	0	0.686	0.488	50	40.1	0	0.687	0.488
100	43	0	0.688	0.488	100	44.3	0	0.7	0.488



**Figure 14: Current Chicago hyetograph in St-Jerome and Ste-Agathe.**

### 3.1.3.3. Future Chicago hyetograph

As it has been said before, the determination of future hyetograph has been done based on the study of Mailhot et al. (2007). They made a climate projection for the 2041-2070 period with the CRCM driven by the CGCM2, considering the SRES-A2 scenario. They calibrated and validated their model with annual May-to-October maximum rainfall depths (MOAM series) from 51 meteorological stations in Southern-Quebec for the 1961-1990 period.

Their conclusion was that the intensity of future rainfall event in Southern Quebec, for a given intensity, will increase in 2041-2070, of 1.5 to 20.6 % compared to 1961-1990 period. The magnitude of this increase is more important for the events of short duration and short return period.

Table 5 summarizes those percentages of increase.

**Table 5: Percentage of increase for precipitation in 2041-2070 compared to 1961-1991 [adapted from Mailhot et al, 2007]**

return period [years]	duration [h]			
	2	6	12	24
2	20.6	13.9	11	10.6
5	18.1	14.5	10	8.8
10	15.8	13.1	8.2	6.9
25	13	10.1	5.1	3.9
50	11.2	7.3	2.5	1.5



For the rainfall event considered in this project – duration of 24 hours with a return period of 50 years - an increase of 1.5% of the rainfall depth is expected. The Chicago hyetograph previously found has then been increased of this percentage.

The tables and the graphs of those future Chicago hyetographs and histograms are available in Appendix 2.

Of course, there are high uncertainties associated with such future climate prediction, and it is very difficult to estimate them properly at the current state of knowledge on that field. However, in order to give an idea of their magnitude, the ninety percent confidence intervals of the ratio between estimates in control and future climates have been calculated for the different return period and durations of the study (Mailhot et al, 2007), and are reported in Figure 15.

It can be seen that the 90% confidence interval is quiet large, especially for large return periods. This can be explained by the fact that the analysis was done on short data series – only 30 years. It could be reduced by using larger samples. Moreover, differences between control and future precipitations are really important – at 90% confidence level – for 2h-events with return period up to 25 years and for 6h-event with return period up to 10 years, while for 12h- and 24h- event the difference is significant only with 2- and 5- years return period.

However, the predicted future value is systematically higher than the control one – ratio smaller than one – which confirms the trend of more heavy rainfalls expected in Southern Quebec in the future.

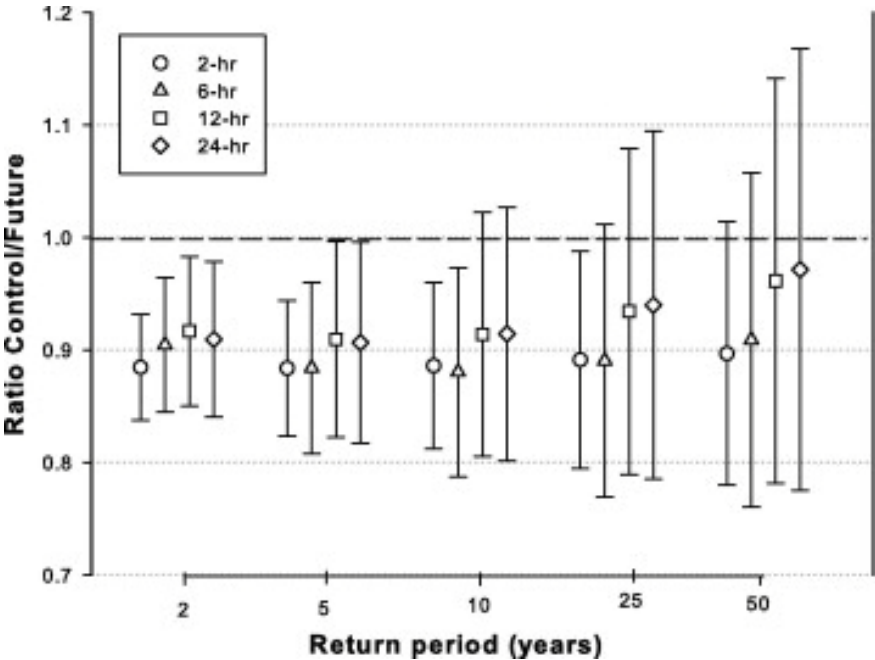


Figure 15: Ratio of MOAM estimates (control/future climate) with 90% confidence intervals (vertical bars) [Mailhot et al, 2007]

## 3.2. Rainfall-runoff transformation with Hec-GeoHMS

A rainfall-runoff model transforms the rain that is falling down into surface runoff. However, some part of the rainfall does not produce surface runoff, due to several processes such as interception – rainfall captured by vegetation or buildings, surface depression storage, evaporation, transpiration or infiltration. Moreover, a base flow must also be defined, since the rainfall-runoff transformation only calculates the direct hydrograph deriving from a storm. Finally, some routing aspects can be necessary, in complex basins. For this project the Hec-HMS software, which comprises all those aspects in several models, has been used. The methodology and the results are detailed in this section.

### 3.2.1. Presentation of Hec-HMS and Hec-GeoHMS

#### 3.2.1.1. Hec-HMS

Hec-HMS – for Hydrologic Engineering Centers Hydrologic Modeling System –software has been developed by the Hydrologic Engineering Centers of the U.S. Army Corps of Engineers (USACE) around 1970, and still is the most used hydrological model in the USA (*USACE, 2000& USACE, 2010a*). It is designed to simulate the rainfall-runoff transformation in dendritic watershed systems, and is applicable in a wide range of basins, from small urban watershed to large agricultural ones.

It comprises a data manager, a calculator and a graphical interface. It includes six components:

- The basin model for the watershed physical description, with several methods available.
- The meteorological model, for the meteorological data analysis
- The simulator, controlled by control specifications, to make the rainfall-runoff transformation.
- The optimization trials, to estimate the parameters, with several methods available.
- The analysis tool, to provide more information about the simulations.
- A GIS connection, as it will be explained in the next paragraph.

#### 3.2.1.2. Hec-GeoHMS

Hec-GeoHMS is an extension for the ArcGIS software which allows the user to visualize the watershed under study and to prepare the data for an analysis with Hec-HMS: sub-basins and streams delimitation and characteristics, preparation of the input for the hydrological models (*USACE, 2010b*). The aim is to prepare in ArcGIS most of the input required by Hec-HMS, and to export them in a basin file that can then be read by Hec-HMS. This is particularly useful for complex studied systems, where the manual determination of the characteristics of the sub-basins can be very complicated, whereas it is easily done in ArcGIS with this geospatial hydrological tool.

### 3.2.2. Preparation of the data in ArcGIS with Hec-GeoHMS

The first step of a work with Hec-GeoHMS is to input into ArcGIS a raw digital terrain model, in order to extract from it the drainage network of the basin under study. This is the terrain preprocessing. The second step is the basin processing, to modify the delimitation of the sub-basins if necessary. The basins characteristics are then calculated in a third step, and the hydrological parameters can be estimated in a fourth one. The last step is then to export the data into Hec-HMS, where the simulation will be run.

### 3.2.2.1. Terrain Preprocessing

For the studied zone – the Du-Nord Basin– a Digital Elevation data Model (DEM) was available freely on the Geobase website. Geobase is a Web platform created by a common initiative of the federal, provincial and regional governments, overseen by the Canadian Council on Geomatics. It provides free geospatial data for the Canadian territory, such as maps of administrative boundaries, road network, geodetic network, land cover and digital elevation data. All those data can be visualized online, or downloaded for use in Geographic Information System (GIS) software (*GeoBase, 2012*).

The Canadian Digital Elevation Data (CDED) is available at scales 1:250000 and 1:50000. The Canadian territory is divided into several files, each of them covering half of a National Topographic System (NTS) map sheet – so there are a western and an eastern file for each NTS tile. Depending on the location chosen, the resolution of the grid ranges from 0.75 to 3 arc seconds for the 1:50000 scale and from 3 to 12 arc seconds for the 1:250000 scale. The reference coordinate system used is the North American Datum 1983 (NAD83) and the orthometric elevations are expressed in meters relative to the mean sea level.

For this project, ten DEM have been downloaded, namely the NTS 031H13\_west, 031H12\_west, 031I04\_west, 031J01\_east, 031J01\_west, 031G16\_east, 031G16\_west, 031G09\_east, 031G09\_west, 031G10\_east, and 031G15\_east. All those DEM have been combined into a unique DEM file, then cut to the shape of the Du-Nord Basin, and finally projected into NAD\_1983\_UTM\_Zone\_18, to form the raw terrain file for the study. This raw terrain file has then been processed by several Hec-GeoHMS tools in order to extract the drainage network.

First of all, if an informatics file of the river network system is available, it is possible to use the DEM reconditioning tool of ArcGIS, in order to ensure that the river will be correctly recognized in the future steps. For this project, the river network of the Du-Nord Basin has been found on Geobase. The National Hydro Network (NHN) provided on this website, achieved in 2004, collects all the best data of the federal, provincial and local governments about the hydrographic features such as rivers, canals, lakes, reservoirs, dams, islands, waterfalls, etc. The river layer of this file has been extracted, and used to make the DEM reconditioning.

After that, several steps are needed to extract the drainage network form this reconditioned DEM, each of them creating a grid or feature file that has to be checked to ensure that every step is going well(*USACE,2010b*):

- *Fill sinks*, to fill the depressions and pits of the DEM to allow water to flow across the landscape, like it happens during a storm event
- *Flow direction*, to define the direction of the steepest descent in each cell, from the classical eight directions of the compass.
- *Flow accumulation*, to determine the number of upstream cells draining to a given cell.
- *Stream definition*, to associate each cell having a flow accumulation bigger than a certain threshold with the stream network.
- *Stream segmentation*, to divide the stream grid previously found into segments, connecting junctions, drainage divides and outlets.
- *Catchment grid delineation*, to define a sub-basin for every stream segment.
- *Catchment polygon processing*, to transform the catchment grid defined in the last step into a polygon feature class.
- *Drainage line processing*, to create a line feature class stream layer.
- *Watershed aggregation*, to aggregate the upstream basins at each stream confluence. This is only done for computational reasons, and has no physical meaning.

Once all those steps are done, the terrain processing is finished, which means that the terrain is ready to be used by the specific tools of Hec-GeoHMS to extract the information required by Hec-HMS. An HMS project can therefore be created in a new layer of the ArcGIS project, requiring only the definition of the control point at the outlet, representing the downstream boundary of the Hec-HMS project. The result of this terrain preprocessing is shown in Figure 15.

### **3.2.2.2. Basin Processing**

Once an HMS project has been created in ArcGIS, the user has the possibility to modify a bit the sub-basins delimitation, by using the basin processing tool.

For this project, like it is usually the case, a lot of sub-basins have been created in the previous step, since one basin is created at each confluence, even for the very small rivers. The *Basin Merge* and *River Merge* tools have therefore been used in order to reduce the number of sub-basins from 80 to 14. In this way, the sub-basin delimitation is very similar to the official description of the sub-basins of the Du-Nord River available in the report of the authority of the basin, and the calculations can be efficient, i.e. both accurate and not time-consuming.

### **3.2.2.3. Basin characteristics**

In order to prepare a basin file to export to Hec-HMS, it is necessary to calculate some characteristics of the sub-basins and of the streams. Hec-GeoHMS has all the tools required, listed below, each step populating the associated field in the attribute table of the layers.

- *River Length*, to compute the length of all the routing reaches of the model
- *River Slope*, to calculate the slope of all the rivers, from the elevations of the DEM.
- *Basin Slope*, to evaluate the average basin slope from the DEM.
- *Longest Flow Path*, to determine in a new layer the longest flow path, its length and its slope, for every sub-basin.
- *Basin Centroid*, to identify the centroid of each sub-basin. The centroid can be placed manually, or computed by one of the three methods available: center of gravity, middle of the longest flow path or point of 50% area of contribution. For this project, the latter has been chosen, since it gave the more reasonable result.
- *Centroid Elevation*, to assign an elevation to each centroid point from the DEM.
- *Centroidal Flow path*, to compute in a new layer the centroidal flow path by projecting the centroid onto the longest flow path

### **3.2.2.4. Hydrologic parameter estimation**

Hec-GeoHMS is capable to derive all the hydrologic parameters of the methods used by Hec-HMS to calculate the hydrological losses or to make the rainfall-runoff transformation, for all the sub-basins, from computer grid of basic parameters, like the percent impervious, the CN coefficient, the initial abstraction, the canopy distribution, etc. Since most of those data were not available for this project, it has been decided that the required parameters would be computed manually, and input directly into Hec-HMS.

### 3.2.2.5. Export for Hec-HMS

Once all those steps have been completed, it is possible to export all those data into a basin file that will be read by Hec-HMS. Before exporting, it is however possible to visualize the project as it will be displayed in Hec-HMS. This representation is shown in Figure 16.

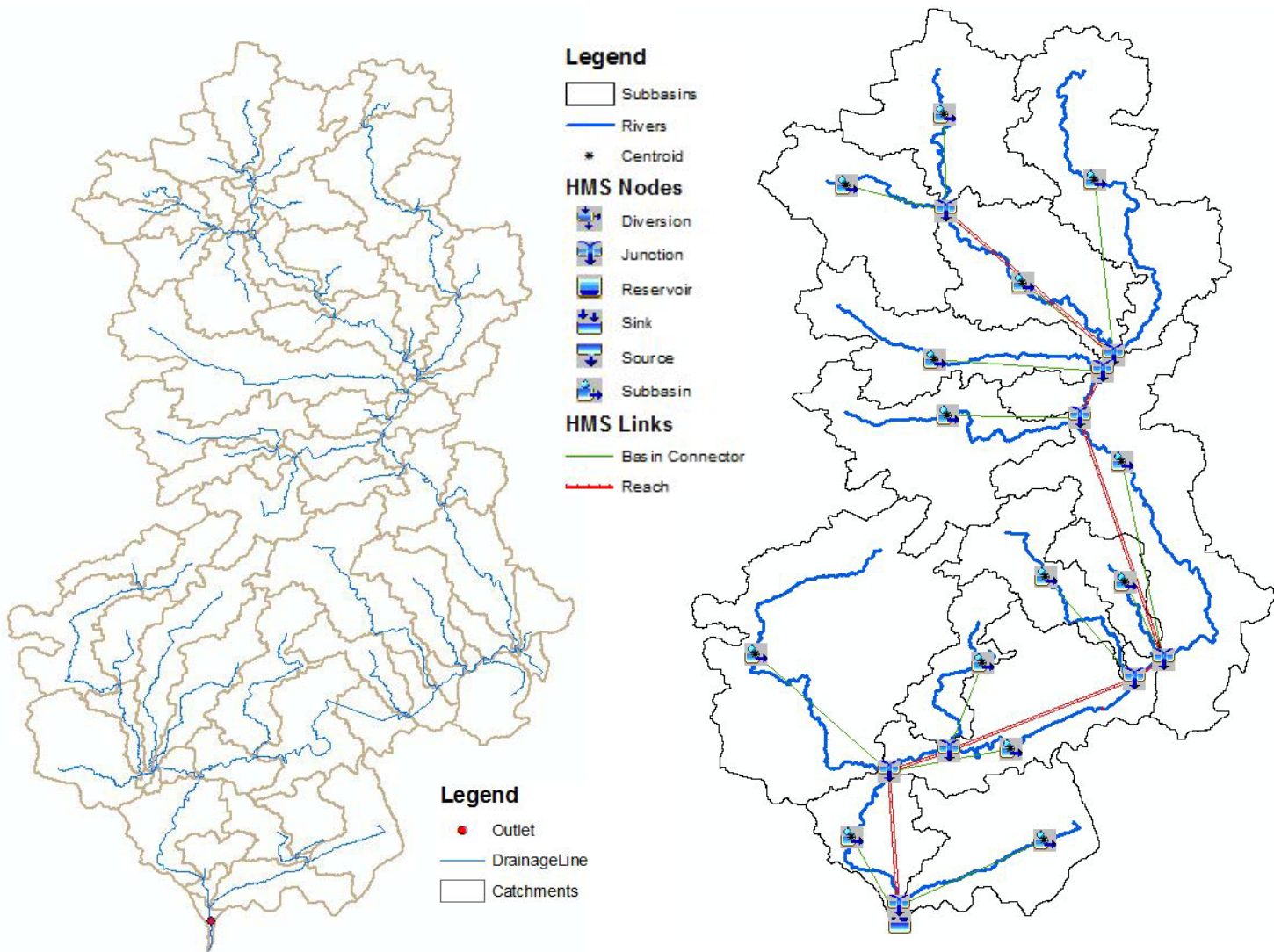


Figure 16: Du Nord terrain file prepared in ArcGIS (left) and basin with Hec-HMS representation (right)

## 3.2.3. Preparation of the Hec-HMS models

### 3.2.3.1. Choice of a method and of its parameters for every step of the transformation

As it has been said before, Hec-HMS recognizes the basin file exported by ArcGIS, so that the subbasins, their area and the links between them are automatically input. However, there is still the need to choose a method for each step of the rainfall-runoff transformation, and to input the related parameters. All those steps are described in the following. Tables summarizing the calculations performed to evaluate the parameters are available in Appendix 3.

### 3.2.3.1.1. Loss method

As it was mentioned previously, all the rain falling during a storm event does not participate to the direct runoff. Indeed, some part is intercepted by the vegetation, some goes into depression storage, and other part suffers evaporation, transpiration or infiltration. Hec-HMS proposes several methods to estimate those hydrological losses, like the initial and constant model, the deficit and constant model, the SCS Curve Number model or the Green and Ampt model.

For this project, the deficit and constant model was the most appropriate. Indeed, since the calibration and the validation will be done on a long period of five years – the reasons will be explained in the corresponding paragraph – it was not possible to use the SCS method. Moreover, the Green and Ampt model was too much data demanding (*Hingray et al., 2009; Osman Akan, 2000; USACE, 2000*). The deficit and constant method is similar to the initial and constant one, considering that the maximum potential rate of precipitation loss is constant, when the accumulated precipitation is bigger than the initial loss parameter. However it is more precise since it considers that the initial loss can “recover” after a long dry period.

For this project, the constant loss rate has been chosen equal to 5 mm/h according to the recommendation given in the Hec-HMS utilization manual for this type of soil. This was the initial guess, this parameters has then been optimized during the calibration process. The imperviousness – ratio of the impervious surface over the total surface of each basin – has been taken equal to the percentage of urbanized area in the basin. The initial deficit – i.e. the amount of water needed to saturate the soil – and the maximal deficit – i.e. the maximum storage capacity of the soil – have been approximated as being respectively the initial abstraction and the potential maximum retention of the SCS method, for which formulas based on physical characteristic on the basin are available (Eq.4). The CN coefficients of each basin have been evaluated thanks to land use information on the GeoBase website.

$$\begin{cases} S = 254 * \left(\frac{100}{CN} - 1\right) \\ I_a = 0.2 * S \end{cases} \quad (4)$$

### 3.2.3.1.2. Transformation method

In Hec-HMS, the direct runoff hydrograph of each sub-basin can be obtained by several methods. One of them is the kinematic wave mode, considering the basin as a very wide open channel, with precipitation as inflow. The shallow water equations for unsteady flow are then solved to find the resulting hydrograph. This method requires inputting many elements to describe the basin in term of a channel, and was therefore not fitted for the basin under study, very large. For such a large basin, one of the methods of Unit Hydrograph is more appropriate.

This semi-empirical Unit Hydrograph approach, first developed in 1932 by Sherman but then reviewed by other scientists, allows the direct estimation of the runoff hydrograph from the net rainfall hyetograph, through a linear and time invariant transfer function. It is based on the hypothesis that the basin can be considered as a linear non variant system – i.e. that the rainfall has a uniform spatial distribution on the basin and that the response of the basin is linear and time invariant (*Hingray et al, 2009; Hwang &Houghtalen, 1996; VenTe Chow et al., 1988*).

The Unitary Hydrograph of a basin for a rainfall event of duration  $\tau$  is the hydrograph resulting from a unitary rain of constant intensity in the basin during a time  $\tau$ . Its main characteristics, described in Figure 17, are the peak time ( $t_p$ ), the decreasing time ( $t_d$ ), the concentration time ( $t_c$ ) and the base time ( $t_b = t_p + t_d = \tau + t_c$ ).

Under the previous hypothesis, knowing the unitary hydrograph of a basin, one can derive its response hydrograph to a full rainfall event with the principle of superposition – or convolution procedure. It consists of discretization of the rain into  $n$  events of the same duration  $\tau$  and of diverse constant intensity, and superposing the  $n$  partial unitary hydrographs thus obtained (convolution process), as shown in Figure 17.

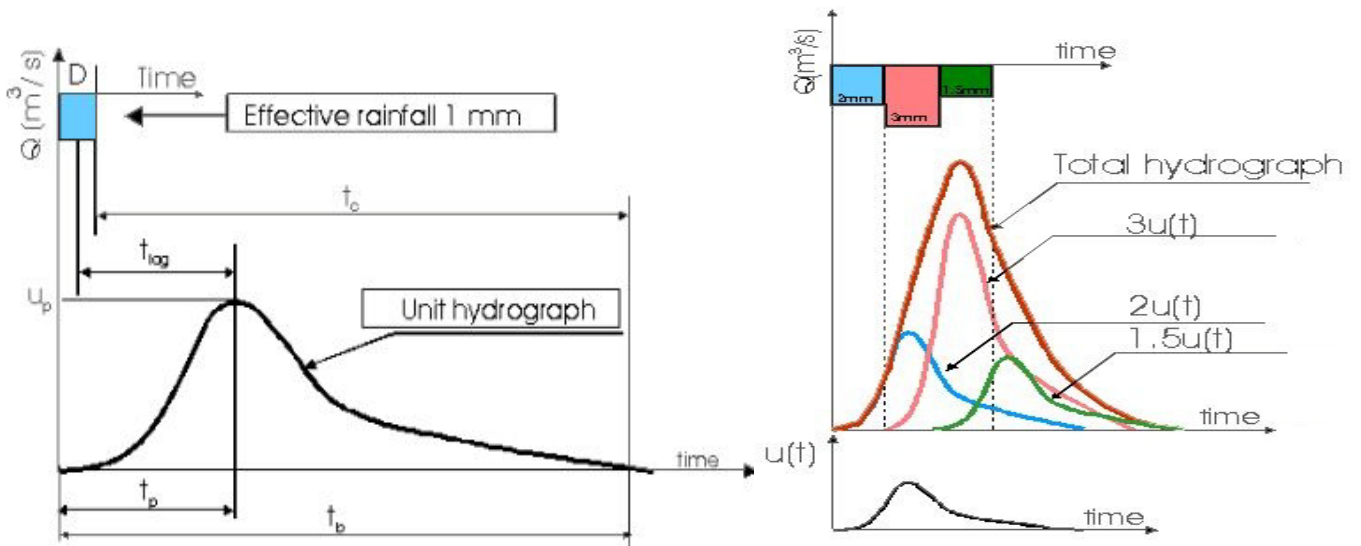


Figure 17: Characteristics of an UH (left) and principle of superposition of UH (right) [VICAIRES, 2012]

Hec-HMS proposes three models for the Unitary Hydrograph approach: the Clark unit hydrograph, the SCS unit hydrograph and the Snyder unit hydrograph. The SCS UH should be used only in small basins – basins of concentration time (calculated with the SCS formula) smaller than 10 hours– and the Snyder UH could be used, but the parameters are not easy to estimate. Therefore the Clark UH method has been chosen.

The Clark UH represents explicitly the two processes involved in the rainfall-runoff transformation, namely the translation of the flow through the basin and the attenuation due to short-term storage effects. Indeed it combines the linear reservoir theory – represented by the storage coefficient – and the linear channel mode - represented by the time of concentration.

Numerous formulas to calculate the time of concentration of a basin exist in the literature, and too often the conditions of utilization are not defined properly. For this project, the formula of Watt & Chow has been used (Eq.5), because it has been developed for medium to large basins in USA and in Canada (Ancil *et al.*, 2005). For the storage coefficient, there is no formula; it has to be found by calibrating the model. An arbitrary initial guess of 10h has been input.

$$\begin{cases} t_l = 0.00326 * L^{0.79} * S^{-0.395} \\ T_l = 0.6 * T_c \end{cases} \quad (5)$$



### 3.2.3.1.3. Base-flow method

Once the direct runoff hydrograph has been calculated, it must be added with a base-flow hydrograph, since we are dealing with perennial rivers. Hec-HMS proposes the recession method, the linear reservoir method, the non-linear Boussinesq method and the constant monthly method.

The Boussinesq method and the linear reservoir method require a lot of data – conductivity, porosity, number of reservoirs, etc. And since the calibration and the validation will be done on a long period (5 years), the most appropriate method was the constant monthly, in which a value of base-flow is defined for each sub-basin for each month (USACE, 2000).

To determine this base flow, historical minimum flow monthly values have been taken in the CEHQ website. They were available for five sub-basins of the Du-Nord watershed. The base-flows of the other sub-basins have been calculated by hydraulic transfer (Eq.6, Anctil et al., 2005). For each basin where a transfer was necessary, the corresponding reference basin has been chosen among the five available as the one with the closest hydrological properties – land use, CN – and such that the area ratio laid within the acceptable range of 0.5 to 2.

$$Q_2 = Q_1 * \left(\frac{A_2}{A_1}\right)^b \quad (6)$$

where  $Q$  is the flow and  $A$  the area of the basin, the index  $1$  and  $2$  referring respectively to the gauged and non-gauged basin. The exponent  $b$  was chosen equal to the typical value of 0.8.

### 3.2.3.1.4. Routing method

To simulate the channel flow – i.e. to compute an hydrograph downstream of a reach from the upstream one – Hec-HMS can use several methods, all of them solving the continuity and momentum equations with a finite difference method, with various approximations.

The lag model only accounts for the translation of the upstream hydrograph, with no attenuation effect, and therefore its use should be limited to short reaches with predictable travel time. The Muskingum model can consider both effects – translation and attenuation – according to the value given to its parameters, among which at least one of them needs to be calibrated. The Muskingum-Cunge model is similar to the previous one, but also requires geometric data about the reach. The modified Puls method requires a storage-outflow relationship, which is hard to define, and the kinematic wave requires a lot of geometric information about the channel (USACE, 2000).

For this project, the lag time method has been chosen, since it was possible to calculate the later with the Watt & Chow formula. This parameter has then been refined by calibration for the longest reaches.



### 3.2.3.2. Meteorological model

Once the basin model has been completed, the meteorological model must be defined. For that purpose, some rainfall data must be entered, in the form of a time-series table, and associated with some sub-basins.

For this project, the rain from two gauge stations – in Ste-Agathe and in St-Jerome – has been used, for calibration and validation. The sub-basins in the upper part have been associated with the Ste-Agathe rain gauge, whereas the sub-basins in the lower part have been directed by the St-Jerome gauge.

Then, some specific parameters of the project must be specified. For example for this project, since the calibration and validation will be done on a long time-scale, and in a region with large variation of temperature between summer and winter, evapotranspiration and snowmelt could not be neglected, so they had to be parameterized.

Evapotranspiration has been evaluated with the monthly average method, based on the Thornthwaite formula (Eq.7):

$$ETP = 1.6 * \left(\frac{10t}{I}\right)^a \text{ With } \begin{cases} a = \frac{1.6}{100} * I + 0.5 \\ I = \sum i \\ i = \left(\frac{t}{5}\right)^{1.514} \end{cases} \quad (7)$$

where  $t$  is the mean temperature of the month considered, taken equal to zero when negative. The information about the mean monthly temperature for the Du-Nord Basin was found in the website of Environment Canada. The results of those calculations are given in Appendix 4.

For the snowmelt model, with temperature index method, it was necessary to define a temperature gauge, with time-series of daily or hourly temperatures. It has been chosen the two same stations of St-Jerome and Ste-Agathe, plus the station of Lachute, for which such data were available. Each sub-basin was then associated with one of the two temperature gauges and some specific data were entered. The value of those coefficients have been taken according to information of Environment Canada, with the indication of the Hec-HMS user's manual and from other studies done in Quebec.

- The PX temperature, which delimitates precipitation falling as rain or snow.
- The base temperature. Its difference with the air temperature defines the temperature index used to calculate the snowmelt.
- The wet meltrate, rate at which the snowpack melts when it is raining on it.
- The rain rate limit, which delimitates the dry and wet period.
- The ATI meltrate coefficient, used in dry period.
- The ATI meltrate function, specified in a table, defining melt rates according to temperature.
- The cold limit, to account for the rapid changes in temperature during strong precipitations.
- The ATI cold content coefficient, used to update the ATI cold content from one time step to the next one.
- The water capacity, maximum amount (in percentage) of melted water that the snowpack can hold before liquid water starts running on the surface.
- The groundmelt, amount of water that is melting per day due to the heat of the soil.

For each sub-basin, the lapse rate has then been specified, and a unique elevation band has been defined, with its mean elevation and its initial state. All the details about the meteorological model are given in Appendix 4.

## 3.2.4. Calibration of the model

### 3.2.4.1. Data for calibration

Some parameters of the basin model previously described have been precisely calculated with valid formula. But others – like the Clark storage coefficient – are not known, some were set to classical values but not specially adjusted to this study, and some were calculated with formulas with large uncertainties. That is why a calibration of the model is needed, to adjust precisely the coefficients, in order to ensure that the model is capable of predicting correctly the resulting flow hydrograph.

For that purpose, records of precipitation, temperature and flow must be available, for the same period, in order to be able to compare the predicted hydrograph with the true recorded one for a certain sequence of events.

For that project, the above data have been taken from the website of Environment Canada and of the CEHQ. Matching data – precipitation in Ste-Agathe and St-Jerome and flow in the Du-Nord River in St-Andre, near the outlet – have been found for the period of 1974-1978, in a daily basis. Moreover, daily temperature data were also available in Lachute meteorological station. Therefore, those time-series data have been entered into the model.

Since there was some missing data at the beginning of the year 1974 for the St-Jerome station, and also some at the end of the year 1978 for St-Andre station, the calibration has been done from August 1<sup>st</sup> 1974 to October 1<sup>st</sup> 1978. There is only one basin and a very small portion of the river downstream the calibration point – junction J1087 – so the model can be considered valid if the calibration is correct.

It would have been better to make the calibration on a shorter period, like one month, with hourly or even sub-hourly data, since the rainfall episode that was then simulated was a 24h event with precipitation data every 15 minutes. However, such data were not available for the DU Nord Basin. Therefore, the calibration has been done with the available data.

### 3.2.4.2. Optimization runs

The principle of the calibration is to run a series of optimization trials, each time providing the program with the list of the parameters to be tested. The program will run the trial, trying to change the chosen parameters in order to improve the result, i.e. to reduce the error. This error is estimated by the objective function, which measures the goodness-of-fit between the recorded hydrograph and the estimated one. The user can then choose to keep the new values of the parameters or to change them, possibly to add or delete some parameters, and to run a new trial in order to improve the results even more. Some statistics about the error are available at the end of each trial, in order to help the user to decide which parameters are worth to be varied, and whether the results are acceptable or not.

For this project, several objective functions have been tested:

- The peak-weighted Root Mean Square (RMS) error function, which calculates the squared differences and weights them according to their magnitude
- The sum of absolute residuals function, which gives the same weight to all errors
- The sum of squared residuals function, which gives more importance to large errors rather than to small ones
- The percent error in peak function, which focuses only on the peak value
- The percent error in volume function, which optimizes only the total outflow volume

The best result was obtained with the peak-weighted RMS error function.

The parameters calibrated were the Clark storage coefficient, the concentration time and the constant rate of infiltration of each sub-basin, and the routing lag time of the four longest reaches. Other parameters were also tested, but their modification didn't change or didn't improve the result. The tolerance has been gradually decreased in order to progressively refine the results.

### 3.2.4.3. Results

Several optimization runs have been done. The final results are presented in Figure 18 and in Table 6. It can be noticed on the graph that the global pattern of the hydrograph is correctly reproduced, with peaks and flat parts corresponding to the observed ones, and simulated baseflows with the good magnitude. Moreover, the peak value is estimated correctly, with an error of only 2.15%. Besides, this error tends to overestimate the peak, which is always safer than the contrary. As far as the total outflow volume is concerned, there is a quite significant underestimation – of 23.8% – that could not be corrected. This value could be improved with the percent error in volume objective function, but then the peak value was completely wrong, and the pattern was not caught at all. This solution was therefore not considered.

It is also worth to highlight the fact that the data used for this calibration may have been not totally accurate. Errors in those data of course lead to discrepancies in the results. Moreover, the modeled basin is very complex, with many sub-basins and reaches, which increases the number of parameters and makes the calibration more difficult.

Table 7 shows the parameters that have been changed by the calibration process, and their values.

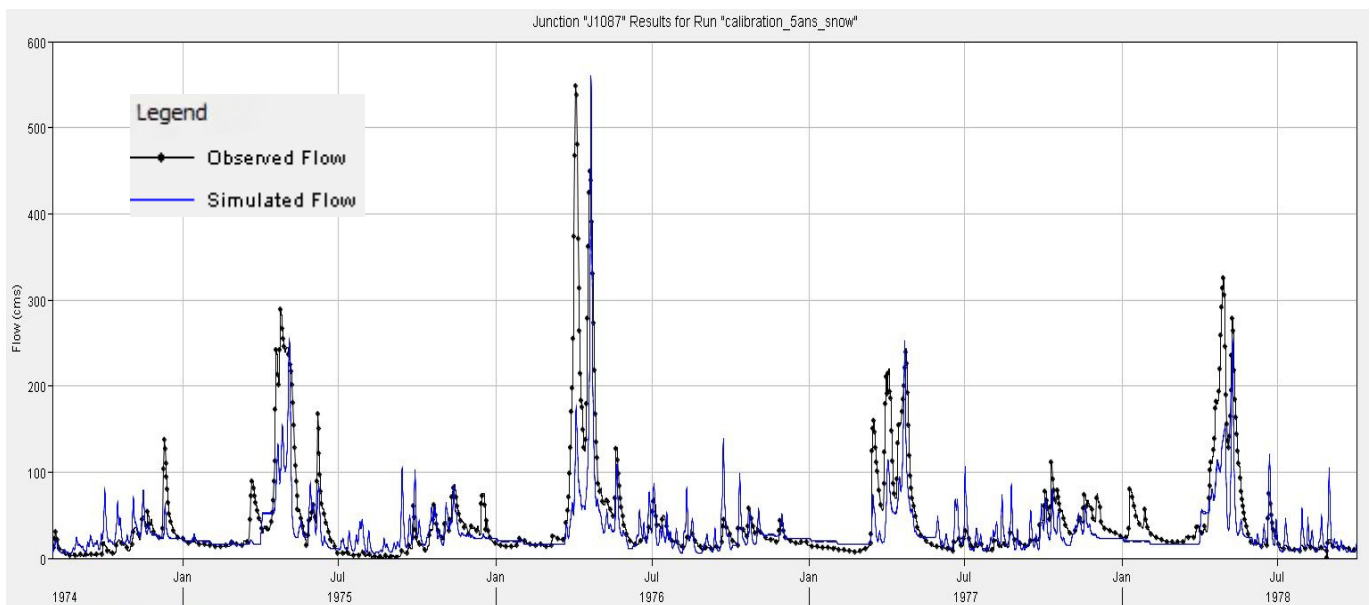


Figure 18: Observed and simulated flow at St-Andre after calibration by Hec-HMS

Table6: Comparison between observed and simulated flow after calibration in Hec-HMS

Observed Peak	549	m3/s	Observed Volume	2688.85	mm
Simulated Peak	560.8	m3/s	Simulated Volume	2049.1	mm
error	2.15	%	error	-23.79	%

Table7: Parameters calibrated by Hec-HMS and their values

	Before Calibration				After calibration			
Basin / Reach	Clark Storage coeff	Tc	infiltration rate	Lag Time	Clark Storage coeff	Tc	infiltration rate	Lag Time
	[h]	[h]	[mm/h]	[min]	[h]	[h]	[mm/h]	[min]
Noir	10		5		30		0.1	
Ste-Agathe up	10	7.216	5		30	10.98	0.1	
Ste-Agathe down	10		5		30		3.77	
Doncaster	10	13.348	5		30	31.02	2.509	
Mulet	10		5		30		1.138	
Simon	10				30			
St-Jerome	10				30			
Bellefeuille	10				30			
Bonniebrook	10				30			
Williams	10				30			
Lachute up	10				30			
Ouest	10				30			
Lachute down	10				30			
R700				422.7				954.56

### 3.2.5. Validation of the model

#### 3.2.5.1. Data for validation

To ensure that the model is not tuned only for the calibration period, but is also capable of doing correctly the rainfall-runoff transformation with other data, it is necessary to test it on another period where both precipitation and flow data are available.

For this project, the chosen period ranged from June 1<sup>st</sup> 1972 to December 31<sup>st</sup> 1973, with hourly precipitation data at St-Jerome and Ste-Agathe stations, hourly temperature data at St-Jerome, Ste-Agathe and Lachute stations and flow data at St-Andre, as for calibration.

#### 3.2.5.2. Results

The flow hydrograph resulting from this simulation is given in Figure 19, compared with the corresponding observed flow.

It can be noticed that the global pattern is correctly simulated, as far as peaks position is concerned. The magnitude of the peaks is also mostly correct, except for the three large peaks in the middle of the simulation, where the simulation poorly manages to represent them. This may be due to the fact that those three large peaks are very close to each other, and Hec-HMS has some difficulties dealing with it, and so underestimates the first two peaks and finally widely overestimates the last one. Moreover, as previously, some wrong data could also be part of the source of the differences between the observed and simulated flows. But excepted for this part, the results of the simulation are satisfying.

The model has therefore been declared properly calibrated, and validated for simulations.

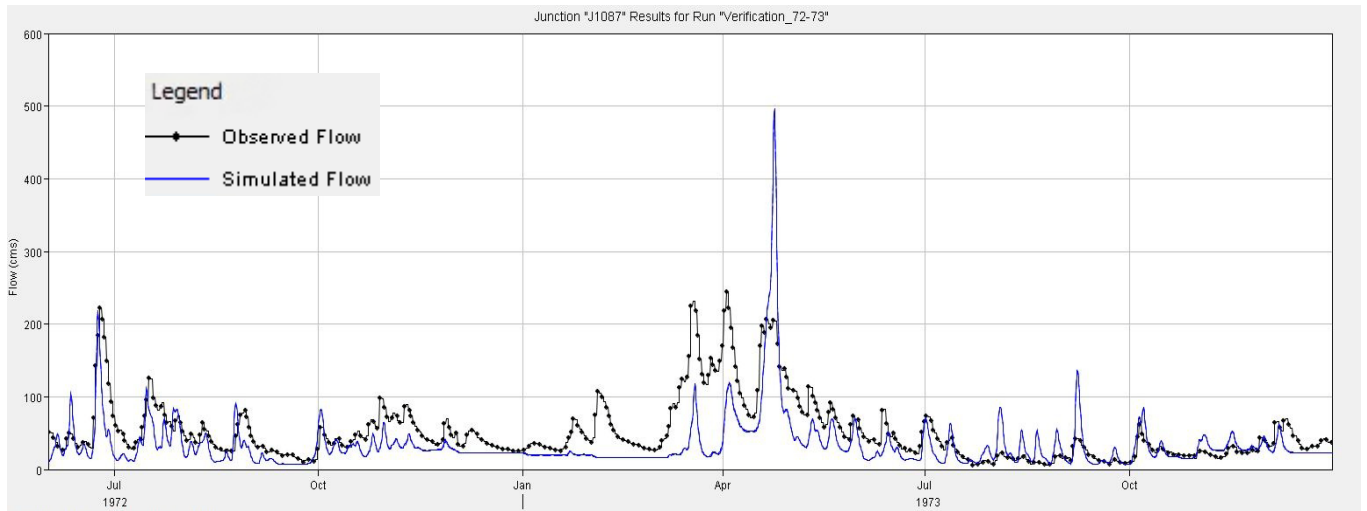


Figure 19: Observed and simulated flow at St-Andre with Hec-HMS (validation)

### 3.2.6. Simulation of the future 24h rainfall event

#### 3.2.6.1. Simulation

To simulate a future 24h rainfall event – and thus generate the flow hydrograph that will be the base of the hydrographs to be input into the simulation software – the rainfall histogram previously generated with the Chicago method has been used. Since the time step of this histogram was 15 min, the same time step has been required for the output hydrograph.

The simulation has been chosen to take place on April 15<sup>th</sup> 2050. April has been chosen because the large rainfall events causing inundations due to snow melt usually happens in this month. And the year 2050 has been chosen in line with the chosen percentage of increase for the rainfall taken from Mailhot et al (2007), which was related to SRES scenarios for the 2041-2070 period.

To enter the temperature data, mean values of April 1974 to 1978 have been taken, and have been increased of 3°C to take into consideration the climate change also for this parameter by 2050 (Ouranos, 2010). Evapotranspiration data also have been recalculated with this increase of temperature.

Contrary to the calibration and the simulation, which started in summer, this simulation takes place in early spring, when there is still snow on the ground. Therefore, an initial Snow Water Equivalent has been entered for each sub-basin, based on available past measured data in Ste-Agathe.

#### 3.2.6.2. Results

The hydrograph resulting from this simulation, corresponding to the flow at the outlet of the basin, is displayed on Figure 20 below. This hydrograph has a peak flow of 719.9m<sup>3</sup>/s, reached three days after the beginning of the rain, a baseflow around 60m<sup>3</sup>/s and a base time of 8 days. The full table of values of this hydrograph is available in Appendix 5.

To have a critical view on this simulation, the resulting hydrograph at the junction J1087 has been compared to past flow data on the Du-Nord River at St-Andre – same places than for the calibration and verification. The maximum value registered between 1972 and 1974 was a flow of 549m<sup>3</sup>/s. The simulated peak at that place was 702.7m<sup>3</sup>/s, therefore 28% larger. This seems logic since the simulation was done with a rare and large rainfall event – 24h of rain with 50 years of return period. A large peak value was therefore expected, within reasonable limits that seems respected.

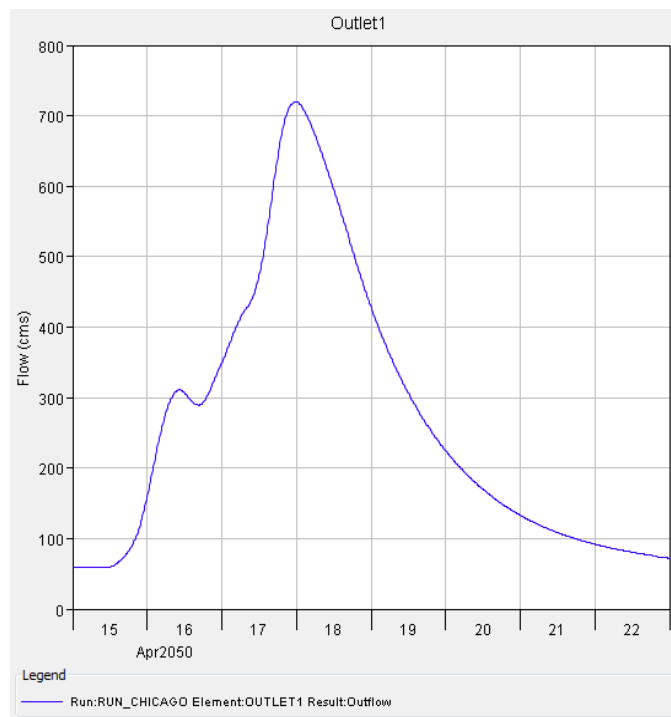


Figure 20: Simulated Hydrograph by Hec-HMS at the outlet of the Du-Nord Basin for a future 24h rainfall event

### 3.3. Hydrographs for the 1D and 2D hydraulic software

#### 3.3.1. Consideration of the Ottawa River and of the Lake of Two Mountains

Once the hydrograph at the outlet of the Du-Nord Basin has been determined, there is still some work to do to obtain the hydrographs to be entered into the simulation software, i.e. the hydrographs at the entrance of the Des-Prairies River and at its tributaries.

Indeed, the hydrograph at the entrance of the Des-Prairies River has to take into consideration the flow coming from the Ottawa River before the junction with the Du-Nord River, as well as the repartition of the water flowing out of the Lake of Two Mountains.

The flow of the Ottawa River has been estimated with historical data recorded at the Carillon Dam station of Environment Canada, just before the junction with the Du-Nord River. Monthly and annual flow rates data are available from 1962 to 1994, with a short statistical analysis to understand the trend and variations of the Ottawa River flow. Those data are available in Appendix 6.

It has been decided to take the mean flow rate in April, since the simulation was assumed to take place in this month, and since it was the maximum of the monthly mean flows. This value, 3510 m<sup>3</sup>/s, has therefore been added to the hydrograph at the exit of the Du-Nord River.

After its junction with the Du-Nord River, the Ottawa River flows into the Lake of Two Mountains. The water from this lake is then divided into the Mille-Ile River, the Saint-Lawrence River through the Vaudreuil and Sainte-Anne channel and the Des-Prairies River through two branches. This division, depending on the flow rate, has been estimated by the Quebec Center of Hydric Expertise (CEHQ, 2005), and is represented in Figure 21.

According to the CEHQ, the Lake of Two Mountains has a very little buffer effect, therefore the transmission of the peak discharge of the Ottawa River into its outlets has been considered instantaneous.

For the present study the flow rate evacuated, corresponding to the flow rate of the Ottawa River at its entrance, is around 3600 m<sup>3</sup>/s. Therefore it has been considered that 12% of the water of the Lake of Two Mountains flows into the Mille-Ile River, 26% into the Sainte-Anne channel, 19% into the Vaudreuil channel and 43% into the Des-Prairies River. To take into consideration the division of the Des-Prairies River around the Bizard Island, it has been estimated that 35% goes directly into the Des-Prairies River and 8% joins by the second branch after the Bizard Island – the first tributary.

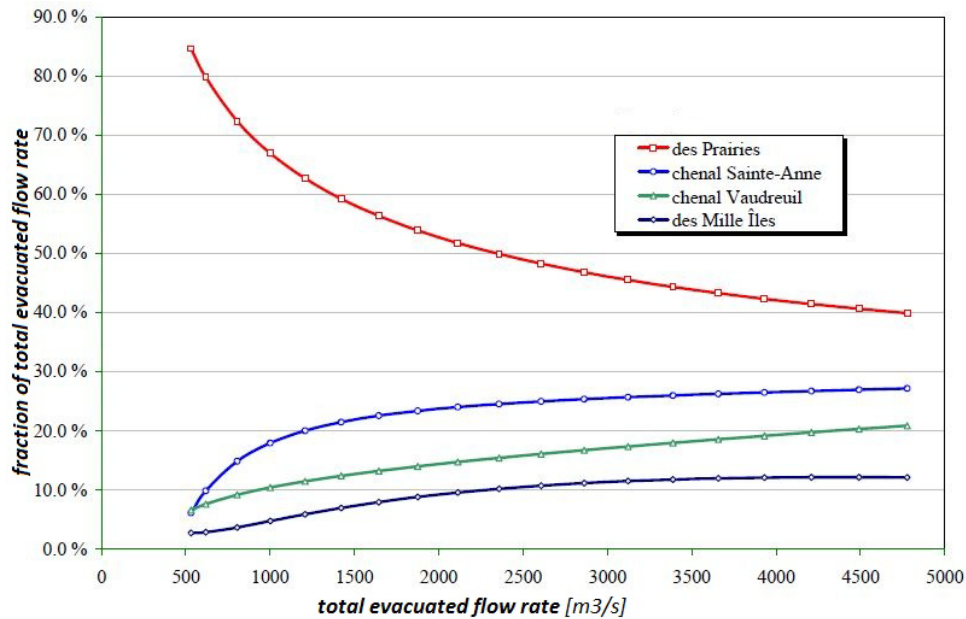


Figure 21: Repartition of the water of the Lake of Two Mountains [adapted from CEHQ, 2005]

### 3.3.2. Consideration of the Mille-Ile Basin

To be the more precise as possible, a rainfall-runoff transformation in Hec-HMS should have been done also in the Mille-Ile Basin, in order to calculate the contribution of this basin to the hyetograph of the Mille-Ile River.

However, it was not possible within the time-frame of the project. Therefore, in order to still take into consideration precipitations in this Basin, it has been done a comparison between the flows of the Du-Nord River and the flows of the Rivers of the Mille-Ile Basin, with recorded flow data (CEHQ, 2012b) and the report of the authority of the Mille-Ile Basin (COBAMIL, 2011). According to those studies, the four rivers of the Mille-Ile Basin represent 6% of the total flow of the Mille-Ile River, the rest coming from the water of the Lake of Two Mountains. The mean flow of the Mille-Ile River in April being 486 m<sup>3</sup>/s, the mean contribution of the Mille-Ile Basin is therefore 6% of this value, i.e. 29.16 m<sup>3</sup>/s. The mean value of flow in April in the Du-Nord River at St-Andre – near the confluence with the Ottawa River – is 157 m<sup>3</sup>/s. The Mille-Ile Basin can be thus considered contributing as 18.5% of the Du-Nord Basin. The hydrograph of the Du-Nord basin has therefore been multiplied by this coefficient and added to the hydrograph of the entrance of the Mille-Ile River to give the hydrograph resulting of a rainfall event in the Mille-Ile Basin.



### 3.3.3. Hydrographs for the simulation software

With all those considerations, all the hydrographs for the simulation software can be computed. The hydrograph at the entrance of the Des Prairie River and the hydrograph at the first tributary – just after the Bizard Island – are respectively 40% and 8% of the hydrograph at the entrance of the Lake of Two Mountains. The hydrograph of the Mille-Ile River tributary is the sum of the hydrograph of the Mille-Ile basin and of 12% of the hydrograph at the entrance of the Lake of Two Mountains.

All those hydrograph are represented in Figure 22, and the baseflow and peak values are reported in Table 8. The corresponding tables of values are available in Appendix 5.

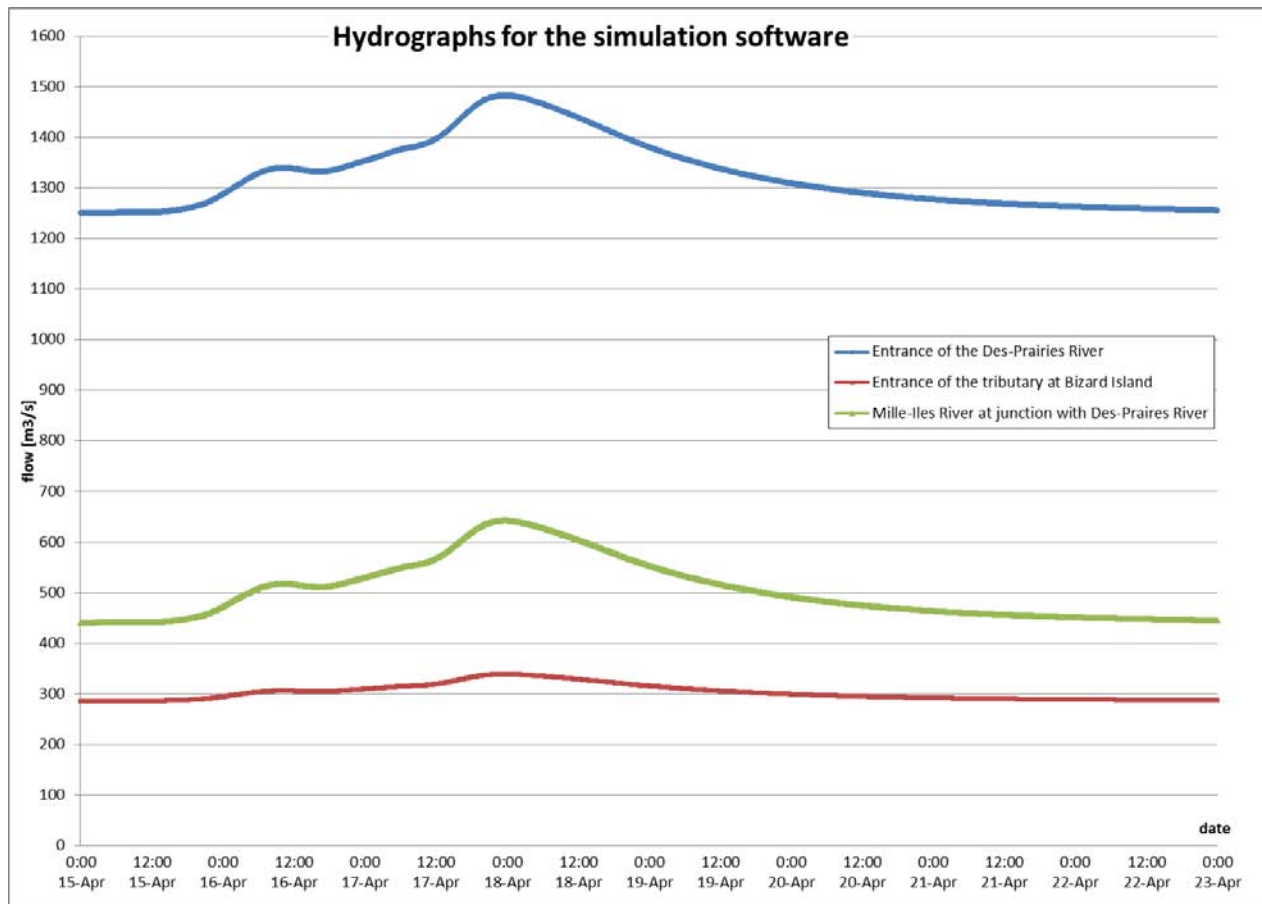


Figure 22: Hydrographs of the Des-Prairies River and of its tributaries for the simulation software

Table8: Baseflow and peak flow of the hydrographs of the Des-Prairies River and its tributaries

	Entrance of the Des-Prairies River	Entrance of the tributary at Bizard Island	Cheval Blanc Rapids	Mille-Iles River at junction with Des-Prairies River
baseflow [m3/s]	1248.91	285.46	1534.37	320.2
max flow [m3/s]	1480.47	338.39	1818.86	521.8



In order to validate those input hydrographs, it is important to compare them with recorded flow data over the past years. For this project, there was one station of the CEHQ in the area of study: the flow station number 043301 on the Des-Prairies River at the Rapids of Cheval Blanc – just after the junction with the first tributary – where data were available from 1923 to 2010. A short statistical analysis of those data has been done in order to understand the trend at this station, and is represented in Table 9.

For the simulated hydrographs, the flow at the Cheval Blanc rapids has been assumed to be the sum of the flow at the entrance of the Des-Prairies River and the flow at the entrance of the tributary at Bizard Island. The baseflow and maximum flows are given in Table 8.

The result of this comparison is satisfying, since the baseflow of the simulated hydrograph is close to the mean flow in April, which is the month with the highest flow rates, and way over the annual mean flow. Moreover, the peak flow of the simulated hydrograph exceeds the April mean flow, which seems logic since it results from a storm event. The hydrographs have therefore been validated.

*Table 9: Statistics on the flow rates at the Cheval Blanc Rapids in the Des-Prairies Rivers (data from 1923 to 2010)*

	Jan	Fév	Mars	Avr	Mai	Juin	Juil	Août	Sept	Oct	Nov	Déc	Annuel
monthly mean flows	943.1	930.9	1064	1682	1639	1236	993.5	835	789.4	896.3	1041	1035	1093.3
min of mean flows	530	541	518	977	712.4	619.1	595.2	547.9	572.9	588.4	638.8	592.2	777.7
max of mean flows	1403	1611	1887	2691	2773	2651	1579	1291	1282	1646	1769	1683	1466

## Chapter 4 – Determination of hydrodynamic conditions

The purpose of this part is to present the simulations done with the software, based on the flow hydrographs found in the previous part. First of all, some background about 1D and 2D modelling will be given, and the choice of the software used in the following will be explained. Besides, some information about the terrain data will be provided. For each of the two chosen software, the different steps of the simulation will then be explained. And finally, the results will be presented, analyzed and compared.

### 4.1. 1D and 2D modeling

#### 4.1.1. Introduction to 1D and 2D modeling

Hydraulic modeling consists in representing the processes occurring during a flood event. Not all the processes can be modeled, and a good compromise between the simplifications and assumptions taken and the computational time must often be found. Traditionally, hydraulic modeling was done with one-dimensional software. However, with the development of high resolution topographic data and the improvement of the computers calculation capability, two- and three- dimensional hydrodynamics models then appears.

The use of 1D or 2D model depends – among other things – on the type of river and flow that is modeled, and on the type of result that is expected.

Since in most of the time the river under study has a sub-critical flow regime, a 1D model is enough to simulate its behavior. However in case of super-critical flow – natural or induced by the presence of bridge, dam or other discontinuity – it can be useful to use a 2D model, in order to understand the influence of the second direction component. Sometime, a 1D model will be able to reproduce properly the behavior of the river in such conditions, but other times only a 2D model will catch it correctly. And to prove that the 2D component can be neglected or not, it is necessary to actually run a 2D model. For example, one can compare the velocity in the channel direction in 1D and 2D model, to understand if the 2D model gives noticeable difference.

Moreover, running a 1D model can also be helpful to set-up properly the initial condition of the 2D model.

That is why for this project it has been decided to use both a 1D and a 2D model.

#### 4.1.2. Main differences between 1D and 2D models

One of the biggest differences between the 1D and the 2D model is probably in the representation of the topography of the studied zone. Indeed, the 2D models use a continuous representation through a finite element mesh, whereas 1D models only represent the terrain as a sequence of cross-sections. Moreover, 1D models assume that all the water flows parallel to the channel direction. They cannot simulate the lateral interaction between the main channel and the flood plain. On the contrary, 2D models allow water to move both in the longitudinal and later direction, with negligible velocity in the vertical direction.

The type of results of those models is also very different. A 1D model will give as a result the elevation of the water level and the average velocity in each chosen cross section, whereas a 2D model will give the water level at each point of the mesh, and the velocity in the two directions.

It is worth noticing that the quality of the results of a 2D model depends a lot on the precision of the mesh – among others factors like the quality of the input data, topographic and bathymetric as well as boundary conditions. A poor mesh will result in very questionable results. But a very fine mesh means a long time of simulation, therefore a good compromise must be found in case such a model is used.

### **4.1.3. Comparison of different software**

There have been a lot of hydraulic software developed to model the behavior of rivers, both 1D and 2D. For the one-dimensional software, one can speak about Hec-RAS or Mike 11. As far as the modeling systems for 2D free-surface flow are concerned, the most known ones are River2D, Mike 21, Hydrosim and Telemac2D. A comparative study has been done on the software in order to make a well-informed choice. Table 10 summarizes the advantages and drawbacks of those programs (*DHI, 2006; DHI, 2012; Horritt & Bates, 2002; Marant, 2009; Steffler 2002a; Steffler 2002b; Steffler 2002c; Telemac 2010; USACE 2010c; USACE 2010d*).

### **4.1.4. Choice of the software**

For this project, the aim was to assess the response of the river to a future rainfall event, in term of water level rise, and the impact on the hydraulic structures on the river.

As it has been explained before, it has been decided to use both 1D and 2D model.

For the 1D model, the choice has been naturally directed on the Hec-RAS software: free, worldly used, for which I was already competent, and with results recognized by the scientific community. Moreover, since digitized data were available, it has been decided to use the GIS add-on Hec-GeoRAS.

For the 2D model, the non-free software has been dismissed, since powerful free ones were available. It has been thought to use both River2D and Telemac, to obtain quick results with the first one and to validate them with the second one, but it was not possible within the timeframe. Therefore, only River2D has been selected, since I was already familiar with it, and since the results it provides are also well recognized.

Table10: Comparison table of different 1D and 2D hydraulic software

	1D software			2D software			1D/2D
	Hec-RAS	Mike 11	Mike 21	Telemac2D	HydroSIM	River2D	
Developers	USACE (USA)	DHI (Denmark)	DHI (Denmark)	EDF (France)	INRS-Eau (Quebec)	University of Alberta (Canada)	DHI (Denmark)
Cost	Free	Not free	Not free	Free	Not free	Free	Not free
User-friendly	Yes	Yes	Yes	No	No	Yes	Yes
Documentation	Well furnished, active forum	Medium	Medium	Active forum	Medium	Well furnished, forum not active	Medium
Calculation time	Fast	Middle	Long	Long, can work in parallel	Very Long	Long	Middle
Calibration	Easy	Middle	Hard	Very Hard	Very Hard	Hard	Hard
Composition, pre- and post-processing	All-Included	Data viewer and calculator included. Add-on for sediment transport or water quality analysis	Data viewer, mesh generator and calculator included. Add-on for sediment transport or water quality analysis	Only calculator. Pre and post treatment in separated (BlueKenue, free)	Only calculator. Pre and post treatment in separated software (Modeleaur)	4 modulus (bed topography, mesh editor, ice editor, hydrodynamic simulator)	Coupling of Mike11 (in minor bed) & Mike 21 (in major bed)
GIS add-on modulus	Yes	Yes	Yes	No	Yes	No	Yes
Data requirement and format	Low, Manually entered or imported form ArcGIS	Low. From ASCII files or imported form Arc-GIS	High. From ASCII files	High, in special format prepared by pre-processing software	High, in special format prepared by pre-processing software	High. From ASCII files	Middle. From ASCII files
Flow	Steady & unsteady	Steady & unsteady	Steady & unsteady	Steady & unsteady	Steady & unsteady	Steady (gradually varied) & unsteady	Steady & unsteady
Bridges and dam multiple reach rivers	Good models	Good models	Good models	Good models	Some models	Poor models	Good models
Equations solved	Yes	Yes	Yes	Yes	Yes	Yes	Yes
Resolution method	1D Saint Venant (continuity&momentumeq)	1D Saint Venant (continuity&momentumeq)	2D incompressible Reynold averaged Navier-Stockes	2D Saint Venant + tracer conservation	2D Saint Venant	2D Saint Venant	1D & 2D St-Venant equations
	four-point implicit linearized finite difference scheme	implicit finite difference scheme	Cell-centred finite volume method, flexible mesh, triangular or quadrilateral elements	finite-element or finite-volume method, with triangular regular mesh elements	finite element	finite element, flexible mesh, triangular elements	Combination of the methods of Mike11 and Mike 21
Results	Water elevation and velocity at each cross-section	Time series of discharges and water level	At each mesh element: water elevation, velocities, flux densities, temperature, salinities, speed direction, wind velocity, eddy viscosity	Water elevation and depth averaged velocity (u,v) at each point of the mesh	Water elevation and depth averaged velocity (u,v) at each point of the mesh	Water elevation and depth averaged velocity (u,v) at each point of the mesh	Combination of the results of Mike11 and Mike 21

## 4.2. Preparation of the raw terrain data

For any simulation software, some information about the terrain is required as input in a terrain file, which can be of different formats according to the software – and usually some transformations of the raw terrain data are necessary to obtain this file in the adequate format. However, they are all based on georeferenced points, i.e. points with information about the x and y coordinates – which can be expressed in different coordinate systems – and the elevation z. This section presents the terrain model that has been used in this study and the different steps undertaken to get a raw but with enough precision terrain model

### 4.2.1. Available terrain data

For the studied zone – the Des-Prairies River and its surroundings – a Digital Elevation data Model (DEM) were available freely on the Geobase website, as it was for the Hec-HMS project.

For this project, four DEM have been downloaded, namely the NTS 031H058\_east, 031H12\_west, 031H12\_east and 031H11\_west. For those areas, the DEM were available with the best resolution, i.e. 0.75 arc seconds.

The problem of those DEM is that they were developed from aerial photography technique. Therefore, they give only the topography of the area under study – i.e. the relief of the area above water – but not the bathymetry – i.e. the relief of the river bed, under the water surface. In this model, the river elevation is taken constant on large polygons, with a value of one meter below the mean elevation of the bank. This is of course a problem in the context of the simulation of the river behavior, so the DEM could not be entered into the software without corrections. It was therefore necessary to get those bathymetric data.

Moreover, it has been noticed in previous projects with this terrain model in the same area of study that there are some errors in the topology, some wrong elevations in the banks near the river in the central zone of the studied area, which could distort the results of the simulation.

That's why it has been decided to ask for the help of Mr. Jean Belanger, professor of topology in Polytechnique Montreal. He gave us his advices to obtain the best terrain data possible, considering the time scale available and the cost restrictions, and helped us to get it. Its work is explained in the next paragraph.

### 4.2.2. Correction of the DEM

With the advices of Mr. Belanger, it has been decided to make a field study in the zone where the topology errors are located, in order to take some measured point, and to extract some bathymetric points from a paper bathymetric map to add them to the model, since no digital bathymetric model were available, and since it was not possible to make a field study to get the bathymetry because of the cost of such a huge undertaking.

#### 4.2.2.1. Field study

The topographic survey has been done in a zone of approximately 10 kilometers long and 500 meters wide on both Laval and Montreal sides, between the Bisson (A13) and Ahunatic-Viau Bridges. It took three days to survey the entire zone, and some more to make the post-processing of the data. I personally participated to this field survey on the second day, in order to familiarize myself with the material.

The survey has been done with a Real Time Kinematic (RTK) method. This technique was born in the early 1990's, and allows the user to obtain centimeter-level positioning in real time. It is based on the use of GPS signal measurements with a reference station providing real-time corrections.

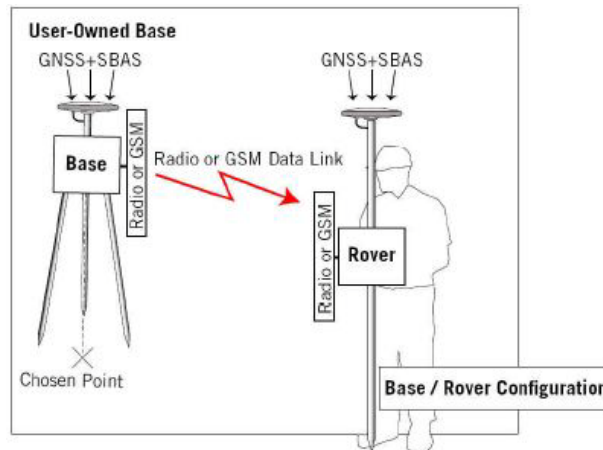


Figure 23: Principle of RTK method [resourcesupplyllc.com, 2012]

For this study, the antenna has been installed on the roof of a car, and the 10 km long area surveyed while driving, the system taking a measurement every seven meters, if the signal and the precision are enough. Indeed, some parts of the road are surrounded by trees, which hide the GPS signal and therefore affect the quality of the measurement. The records have been taken only if the precision at this point was smaller than one meter, to avoid really bad quality points. Most of the time the precision was below 50 cm, and often it was of the order of some centimeters.

Moreover, the parks near the river have also been surveyed while walking, taking a point every 20 steps, to get a better precision in those areas not accessible by car.

All those topographic points have then been post-processed by Mr. Belanger, in order to check their consistency, and to prepare them in an appropriate format.

#### 4.2.2.2. Bathymetric points

Since no computer bathymetric map was available, Mr. Bélanger bought a paper navigation map, displaying the elevation of the river bed at numerous points, also given in table form. Elevation data have been extracted at several cross sections all along the river, at regular distance, and in particular before and after each bridge.

For the refinement zone, more points have been taken, an interpolation has been made, and precise contour lines have been drawn.

### 4.2.3. Combination of the data

The result of the work of Mr. B elanger was an AutoCAD file containing, in different layers, the bathymetric points taken from the paper map, the topographic contour lines of the area of the field study, the bathymetric contour lines in the same area of the field study, and finally the delimitation line of the islands of Montreal and Laval, the Bizard Island and the islands on the Des-Prairies Rivers.

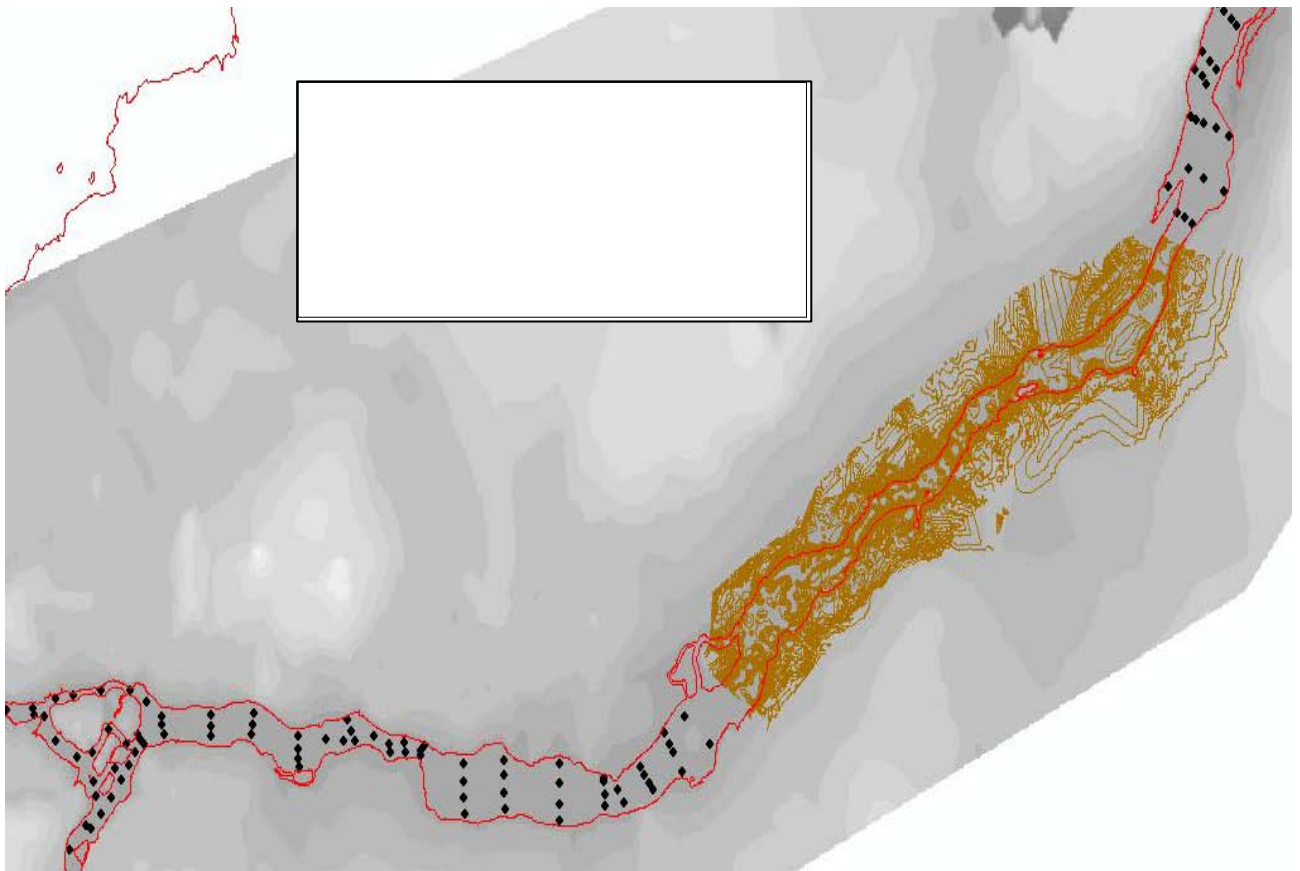
In order to be able to use those data for Hec-GeoRAS or River2D, they have been imported into an ArcGIS project. The bathymetric and topographic contour lines of the refined zone have been imported as a unique polyline shapefile, the bathymetric points as a point shapefile.

Besides, the four DEM taken from the Geobase website have been added to the project, as raster files. They have then been combined into one single raster. However, the part overlapping with the field study area has been deleted from the DEM, since the measured data are of better quality. The part corresponding to the river also has been deleted, since the elevations were wrong.

Moreover, all the data of a project need to be in the same coordinate system and the same projection. For this project, on one hand the files from AutoCAD have been created in the GCS\_North\_American\_1983 and projected in NAD\_1983\_UTM\_Zone\_18. On the other hand the downloaded DEM is in NAD83, with no defined projection. The latter layer has therefore been projected into UTM\_Zone\_18.

Figure 24 shows a portion of the raw terrain data thus obtained.

The detail of the manipulation done to transform those raw data into the proper format of each program will be explained in the following, within the corresponding paragraphs.



*Figure 24: Extract of the ArcGIS project with the data from all sources to form the raw terrain data.*

## 4.3. 1D Simulation with Hec-GeoRAS

### 4.3.1. Presentation of Hec-RAS and Hec-GeoRAS

#### 4.3.1.1. Hec-RAS

As it has been said previously the Hec-RAS – for Hydrologic Engineering Centers River Analysis System – software is designed to make one-dimensional hydraulic calculations in natural and constructed channels. Developed by the USACE as Hec-HMS, it is composed of four components for the steady flow water surface profile computations, the unsteady flow simulation for both sub- and super- critical flow, the movable boundary sediment transport computations and the water quality analysis.

For this project, it has been done an unsteady flow simulation.

The unsteady flow analysis is governed by the 1D equations of Saint-Venant (Eq.8): equations of mass conservation – continuity equation – and of momentum conservation, both partial differential equations. They are also known as shallow water or dynamic wave equations (*Haestad Methods et al, 2003; USACE, 2010c; USACE, 2010d*).

$$\begin{cases} \frac{\partial A}{\partial t} + \frac{\partial Q}{\partial x} = 0 \\ \frac{\partial V}{\partial t} + V \frac{\partial V}{\partial x} + g \frac{\partial y}{\partial x} - g(S_0 - S_f) = 0 \end{cases} \quad (8)$$

Those equations are based on the following assumptions:

- One dimensional flow
- Uniform velocity within the cross-sections and horizontal water level
- Incompressible fluid
- Gradually varied flow, prevailing hydrostatic pressure, negligible vertical acceleration
- Small curvature and small bottom slope of the channel
- Bed resistance effects described with Manning's equation

Moreover, in the resolution of those equations, horizontal water surface level is assumed at each cross-section normal to the flow direction, such that the exchange momentum between the channel and the flood plain are negligible, and that the discharge is distributed according to the conveyance.

With this assumption, the previous equations can be simplified.

The resolution is then based on a time and space discretization using a four-point implicit, linearized, finite difference scheme.

#### 4.3.1.2. Hec-GeoRAS

Hec-GeoRAS is “a set of procedures, tools, and utilities for processing geospatial data in ArcGIS using a graphical user interface (GUI)” (*USACE, 2011*). The aim is to prepare in ArcGIS all the geometric data required by Hec-RAS, and to export them in a geometry file that can then be read by Hec-RAS. This is particularly useful for complex studied systems, where the representation of the geometry in Hec-RAS can quickly become very complicated.

Moreover, this interface also allows the user to import the results of an Hec-RAS simulation into ArcGIS – in particular the water surface profile data and the velocity data – for floodplain mapping, flood damage estimation, flood preparedness, etc.



## 4.3.2. Preparation of the geometry file in ArcGIS

### 4.3.2.1. Creation of a TIN

To work with Hec-GeoRAS, it is required to have the terrain model in a TIN (Triangulated Irregular Network) or GRID (an ESRI format of raster data storage) format. For this project, it has been decided to work with a TIN, powerful vectorial representation of surfaces.

The slope and elevation data for the geometric file is extracted from this TIN, and the geometric layers are drawn on it.

It is possible to create a TIN with a special function of ArcGIS from features or raster data. However, all the data need to be of the same type. In this project, the data imported from AutoCAD were feature classes – points or lines – whereas the DEM was a raster. The latter layer has therefore been converted into a contour line feature class. The TIN has then been created.

### 4.3.2.2. Creation of the river, bank and flowpath layers

Once the TIN is created, one can create the river centerline, the bank and the flowpath layers with the Hec-GeoRAS toolbar, and then edit them with the editing function of ArcGIS.

The river is easily recognizable on the TIN, so the river multi-segment lines have been simply drawn by clicking point by point on the center of the river, reach by reach, from upstream to downstream. A name must then been assigned to each river and each reach. For this project, three rivers and five reaches have been created:

- The RDP River, with three reaches: the upper reach, the middle reach (after the junction of the Bizard Island) and the lower reach (after the junction with the Mille-Ile River).
- The tributary1 River, with only one reach named tributary1, which joins the RDP after the Bizard Island.
- The Mille-Ile River, with only one reach named tributary2.

The nodes representing the junction between two reaches of the river are created automatically by Hec-GeoRAS.

The banks have been drawn by following the delimitation lines of the islands of Montreal, Laval and of the Bizard Island, imported from AutoCAD. The right and left flow path have then been drawn in the floodplain, approximately parallel to the river centerline.

All those layers can be seen on Figure 27.

### 4.3.2.3. Creation of the cross sections

When the river, bank and flowpath layers are defined, one can create the cross section layers, and draw them with the editing section of ArcGIS, from the left to the right side of the river, crossing the bank and the flow path lines, for all reaches.

They have been placed regularly all along the rivers, and an attention has been paid to draw one just before and just after each bridge. In total, 65 cross-sections have been defined.

Once this layer is created, Hec-GeoRAS automatically assigns a river and reach name to each cross section, calculates the river and bank stations for each cross-section, and the cross-section elevation profiles.

Shape *	OID *	Shape_Length	HydroID	Station	River	Reach	LeftBank	RightBank	LLength	ChLength	RLength
Polyline	1	1437.24484	33	52215.688	RDP	upper_reach	0.14117	0.44476	1600.632	1061.334	764.122
Polyline	2	1505.410973	34	51154.355	RDP	upper_reach	0.50944	0.72961	855.047	1753.452	2263.65
Polyline	3	2395.306962	35	49400.902	RDP	upper_reach	0.31366	0.69804	900.838	1124.331	1379.844
Polyline	4	2434.043573	36	48276.57	RDP	upper_reach	0.22403	0.48315	1526.965	1811.633	2106.141
Polyline	5	2695.189527	37	46464.938	RDP	upper_reach	0.41895	0.59941	1179.903	1053.357	1054.94
Polyline	6	1441.486111	38	45411.582	RDP	upper_reach	0.24631	0.38506	328.886	263.184	188.725
Polyline	7	1482.260835	39	45148.398	RDP	upper_reach	0.25313	0.3945	751.259	857.629	1129.143
Polyline	8	1799.680921	40	44290.77	RDP	upper_reach	0.21066	0.57043	364.979	656.171	1060.237
Polyline	9	1082.75166	41	43231.367	RDP	upper_reach	0.47664	0.84909	1038.261	991.217	868.688
Polyline	10	1246.201181	42	43634.598	RDP	upper_reach	0.38047	0.6379	552.786	403.231	394.917
Polyline	11	833.524269	43	42240.148	RDP	upper_reach	0.3079	0.61322	1865.635	816.087	881.353
Polyline	12	693.214789	44	2726.8169	affluent	tributary1	0.52442	0.82096	426.008	552.832	742.074
Polyline	13	420.821402	45	2173.9851	affluent	tributary1	0.35366	0.61099	767.665	715.053	902.823

Figure 25: Extract of the attribute table of the XSCutLines layer

#### 4.3.2.4. Creation of the bridges and inline structures

The layers for the bridges and inline structures are created and edited like the cross-section layer, as multiple-segments lines, drawn from the left side to the right one. As previously, Hec-GeoRAS assigns automatically the river and reach name, and calculates the stationing for every bridge and inline structure. For each structure, it is then necessary to enter manually in the attribute table its name, the width at the top and the distance to the upstream cross-section.

For this project, 12 bridges have been defined, all of them on the RDP River, as shown in the attribute table reproduced in Figure 26. One inline structure also has been defined, the Des-Prairies River Dam, on the middle reach of the RDP.

Shape *	OID	Shape_Length	HydroID	River	Reach	Station	USDistance	TopWidth	NodeName
Polyline	1	1259.225334	159	RDP	upper_reach	45246.023	50	11.4	Bizard
Polyline	2	1623.916068	160	RDP	middle_reach	41268.18	20	10	Bigras_train
Polyline	3	1633.91777	161	RDP	middle_reach	34265.59	50	27.3	Bisson_A13
Polyline	4	2783.016362	162	RDP	middle_reach	30505.127	55	38.9	Lachapelle
Polyline	5	887.600648	163	RDP	middle_reach	28978.121	2	34.9	Mederic_Martin_A15
Polyline	6	796.957768	164	RDP	middle_reach	27579.934	25	10	Perry_train
Polyline	7	868.224226	165	RDP	middle_reach	25402.619	45	25.5	Ahunstic_Viau
Polyline	8	1776.077457	166	RDP	middle_reach	23208.213	30	27.3	Papineau_Leblanc_A19
Polyline	9	825.65427	167	RDP	middle_reach	20061.809	35	29.3	Pie9
Polyline	10	3610.180655	168	RDP	middle_reach	15352.394	65	29	A25
Polyline	11	1697.647218	169	RDP	lower_reach	3920.7969	60	27.7	CDG_A40
Polyline	12	2072.107534	466	RDP	lower_reach	1494.2675	60	21.4	Legardeur
Polyline	13	1215.798176	1493	RDP	middle_reach	23279.947	3	25	Papineau_leblanc

Figure 26: Attribute table of the bridges layer

#### 4.3.2.5. Assignment of the roughness coefficient

A roughness coefficient must be defined everywhere in the TIN. For that purpose, a land use file downloaded from the Geobase website has been used. It is represented in Appendix 7.

The land use file has been imported into the ArcGIS project. For the floodplains into consideration, 16 types of land use were present, which have been merged into 7 groups, and a Manning coefficient has been assigned to each of them, according to the Manning table available in the user's manual of Hec-RAS. As far as the channels are concerned, the Des-Prairies River and its tributaries are quiet clean rivers, with some pools and many islands. Therefore, a mean value of 0.035 has been chosen for the Manning coefficient in all the reaches. This value has then been refined in some places during the validation process in Hec-RAS.

Hec-GeoRAS then assigns the Manning value to the corresponding part of the cross-sections. The Manning table used is reported in Table 11.

*Table 11: Values of Manning's coefficient in floodplains*

Number in LandUse Layer	Description	Group	Manning coefficient
20	Water	Water	0.035
33	Sterile, with no vegetal	Sterile zone	0.02
34	Urbanized zones	Urbanized zone	0.2
51	Big shrubs	Shrubs	0.07
52	Small shrubs		
81	Humid wooded zone		
82	Humid zone planted with small trees		
83	Humid herbaceous zone	Herbs	0.03
100	Herbaceous plants		
121	Annual cultures		
122	Perennial cultures and pastry	Agricultural land	0.035
211	Dense conifer	Dense forest	0.15
221	Dense broad-leaved		
231	Dense mixed forest		
212	Open conifer	Open forest	0.09
222	Open broad-leaved		
232	Open mixed forest		

#### 4.3.2.6. Export to Hec-RAS

Once all the layers needed for the study have been created, Hec-GeoRAS exports the data into a geometry file, which Hec-RAS will be able to read.

The simulation with Hec-RAS is detailed in the next section.

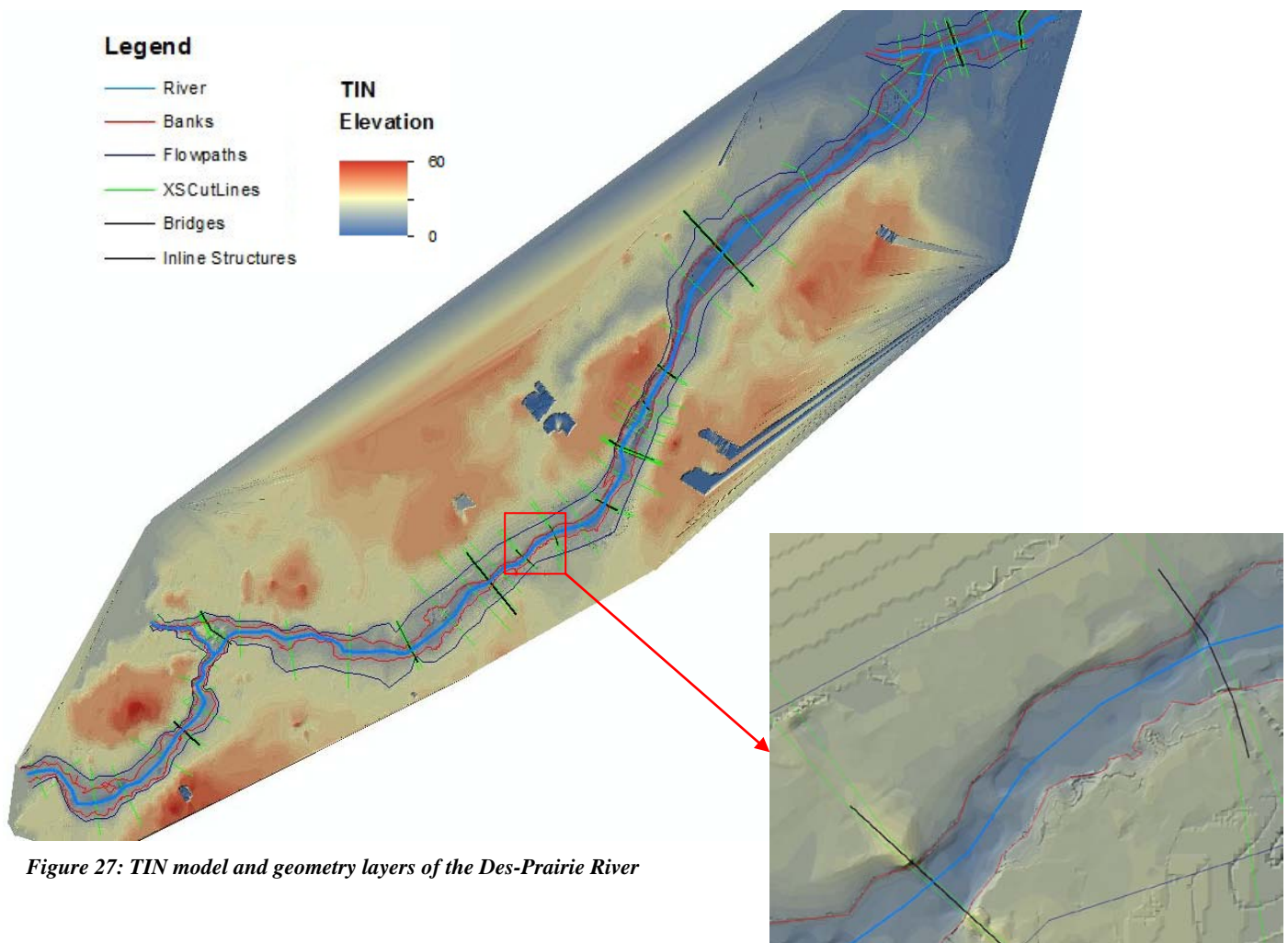


Figure 27: TIN model and geometry layers of the Des-Prairie River

### 4.3.3. Simulation in Hec-RAS

#### 4.3.3.1. Correction of the geometry, bridges and inline structures

Hec-RAS recognizes the geometry file created in ArcGIS. Its representation in Hec-RAS is available in Appendix 8. However, some information about the bridges and the inline structures are missing, and must be entered manually.

For the bridges, Hec-RAS knows their location, but the elevation of the decks must be defined, as well as the piers' location and geometry. Moreover, a type of weir crest shape and a weir coefficient has to be chosen, in case the bridge is submerged.

For this project, all the elevations have been taken from available construction plans. An example of plan is presented in Appendix 9. The bridges of this project were broad-crested. With no specific information, typical medium value of 2.8 has been taken as weir coefficient (*Haestad et al, 2003; USACE, 2010c; USACE, 2010d.*). Figure 27 shows the representation of the Lachapelle Bridge in Hec-RAS.

For the inline structure, the elevation of the deck must also be defined, as well as the geometry of the gates and of the spillway if relevant. This geometry has been entered according to the information furnished by Hydro-Quebec, and the resulting structure in Hec-RAS is shown in Figure 28.

- Power station: 200m long with 6 gates.
- Spillway: 220m long with 13 gates of 12.19m large and 7.37m height, the gate 13 being always open.

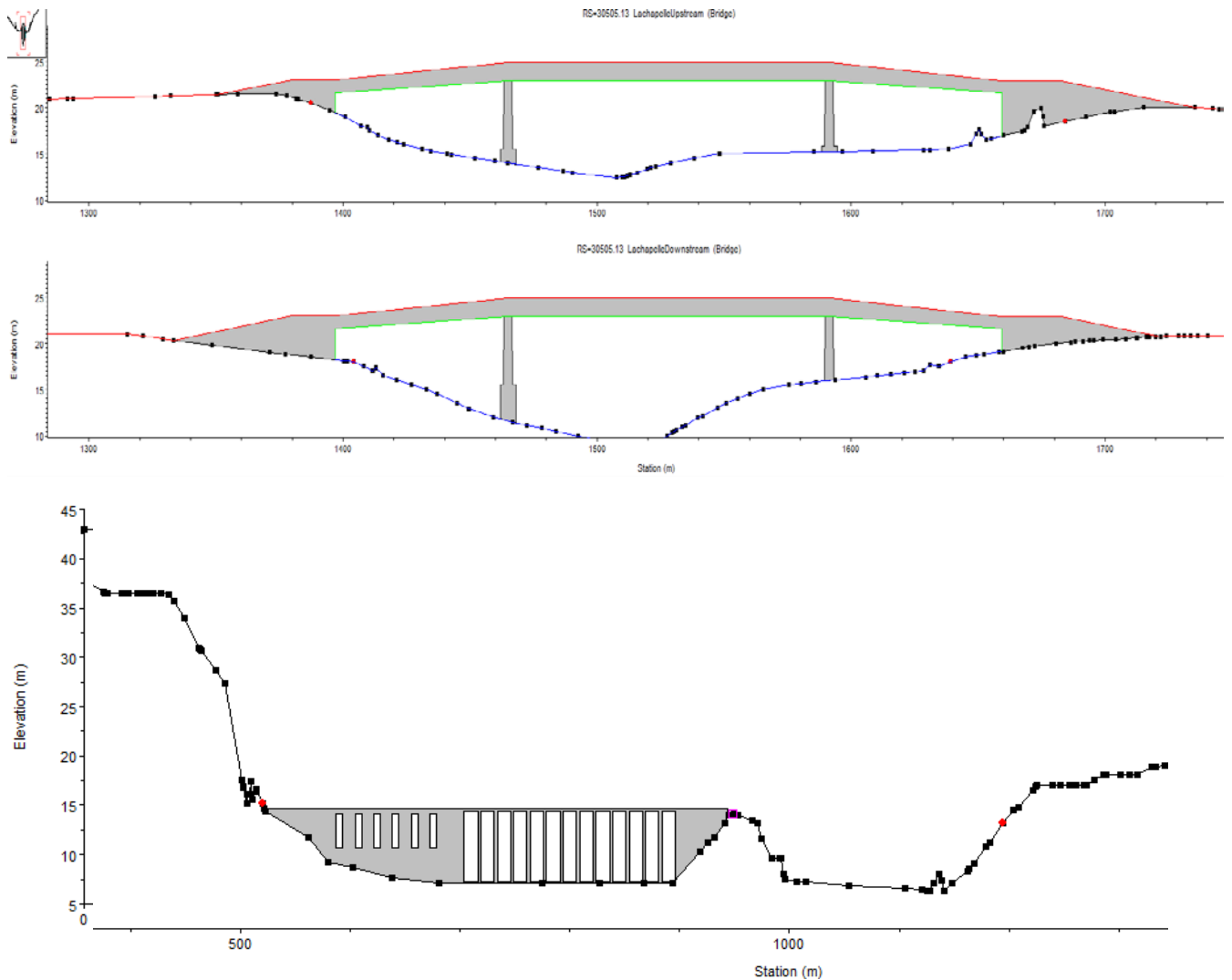


Figure 28: Representation of the Lachapelle Bridge and of the Des-Prairies dam in Hec-RAS

#### 4.3.3.2. Calibration and Validation of the model

To ensure that the model reproduces correctly the behavior of the Des-Prairies River, it has been tested in permanent conditions with input inflows for which known water surface elevations were available in many cross-sections (CEHQ, 2006). The calculated water levels of Hec-RAS have then been compared to the known ones. The Manning's coefficients of the Des-Prairie River have also been changed where necessary – lowered in most of the cases – based on some values given by the CEHQ and of indications of the USGS (2012) and in order to improve the model's precision. The results of this test after calibration are presented in Table 12.

It can be noticed that the errors are similar for both simulations. Upstream of the Des-Prairies dam Hec-RAS simulates well the water levels, with errors ranging from 0.28 to 3%, mostly overestimating the water levels. At some distances downstream of the dam, the results are also correct, with + 3 to +



5% of error. This global overestimation was expected, since it is a characteristic of simulations in steady flow (Haestad et al, 2003).

However, just after the dam, the model fails to catch the proper behavior of the river, with a very large error of nearly 50% of overestimation. This could be due to a flawed hydraulic representation of the dam and of the gates opening. However information about it – even if not complete – has been entered according to indications of Hydro-Quebec and of the CEHQ. Besides, the gates opening optimization process of Hec-RAS has been tested, in order to force a correct elevation in the cross-section just downstream, and failed to improve the results.

That is why it has been thought that the problem could come from the bathymetric data. And indeed, further discussions with the professor that prepared the topographic file showed that the bathymetric points used to make the terrain file should indeed be decreased of around 3 meters in order to better fit the reality in an influence zone of 2.5 km long after the dam. This corresponds to the four first sections of Hec-RAS after the dam. Moreover, in a small area of 400 meters just after the dam – which corresponds to the distance between the dam and the first section after the dam in Hec-RAS – there is a turbulence zone due to the dam, with no bathymetric reference available. The interpolation made in this area by the software to create the terrain file is therefore probably not correct.

Since those conclusions arrived at the end of the project, it was not possible to redo all the terrain file preparation and simulations with the corrected bathymetric data. However, this explains the very large errors in the calibration process in the area after the dam, and better results in this zone could probably be expected with the corrected bathymetry.

In the lower reach the simulated elevations are also wrong. This can be explained by the fact that the downstream boundary condition has been input just after the last bridge of interest, within the lower reach. Besides, for this test recorded flow and elevations were not available in the Mille-Ile reach. A reasonable guess has therefore been input, and that can impact on the results.

Despite of those two problematic zones, the model has been validated, since there was no solution in hand to solve that, and that the results in the other parts are totally acceptable. However, it must be known that the results in the lower reach and in the sections just after the dam may not be reliable.

*Table 12: Comparison between known water surface elevations and simulated ones by Hec-RAS after calibration*

location on RDP River	Hec-Ras nb.	CEHQ nb	22/04/2002				27/11/2003			
			flow [m <sup>3</sup> /s]	WS elevation [m]		error [%]	flow [m <sup>3</sup> /s]	WS elevation [m]		error [%]
				known	Hec-RAS			known	Hec-RAS	
beginning of upper reach	52215.69	31	1225	23.3	22.72	-2.489	1030	22.8	22.24	-2.456
middle of upper reach	46464.94	24	1225	22.85	22.64	-0.919	1030	22.4	22.16	-1.071
just before Bigras Island	42240.15	21	1225	22.5	22.2	-1.333	1030	21.85	21.76	-0.412
beginning of middle reach	40678.27	19	2356	21.3	21.54	1.127	1923	20.9	21.08	0.861
Bisson bridge	34319.33	14	2356	19.85	20.45	3.023	1923	19.3	19.86	2.902
Lachepelle bridge	30589.06	10	2356	19.6	20.15	2.806	1923	19.1	19.58	2.513
Viau Bridge	25461.29	9.4	2356	17.5	17.55	0.286	1923	17.3	17.38	0.462
just before dam	21566.02	9.1	2356	17.2	16.94	-1.512	1923	17.2	16.96	-1.395
just after dam	21168.85	9	2356	10.5	15.38	46.476	1923	10.1	15.05	49.010
between Pie9 and A25 Bridges	18582.18	7.5	2356	10.05	11.55	14.925	1923	9.7	11.36	17.113
between Pie9 and A25 Bridges	16827.11	7	2356	10	10.44	4.400	1923	9.7	10.07	3.814
A25 bridge	15419.11	6.5	2356	10	10.39	3.900	1923	9.7	10.03	3.402
Just before Pierre Island	11411.24	5	2356	9.3	9.83	5.699	1923	9	9.5	5.556
just before Mignerons Island	5614.082	2	2356	7.6	9.7	27.632	1923	7.1	9.39	32.254
CDG Bridge	4013.24	1.5	3097	7.4	9.59	29.595	2508	6.8	9.3	36.765

### **4.3.3.3. Input of the boundary and initial conditions for unsteady flow simulation**

A Boundary Condition (BC) must be defined at each free end of the reaches, upstream and downstream. For this project, there was four BC to set up, three upstream at the first cross-section of each river, and one downstream at the last section of the lower reach of the RDP.

The flow hydrographs calculated in the previous sections have been input for the three upstream boundary conditions, with a time step of 15 min. For the downstream one, a constant elevation has been entered. Indeed, it can be noticed (*CEHQ, 2006*) that the level of the Des-Prairies River at its downstream cross-section has little variation, even for large change of flow – it varies only from 6.5 to 7m for flow from 1900 to 2350 m<sup>3</sup>/s. An elevation of 7m has been chosen, since we are simulation high flow.

The gates of the dam have been controlled based on the elevation in the upstream cross-section, with a given start configuration – found from calibration in permanent conditions – and orders to open and close according to a certain level in the river.

Moreover, since the unsteady flow simulation is very sensitive to the opening of gates, and has a tendency to become unstable very quickly, an internal boundary condition has been entered: a constant elevation of 16.5 m has been input at the section just before the dam. Indeed, in period of high flow like the one that will be simulated, this will probably be the effect of the dam (*CEHQ, 2006*).

The initial conditions were taken equal to the first values of the input flow hydrographs.

## **4.3.4. Results**

### **4.3.4.1. In Hec-RAS**

The unsteady analysis has been run with the configuration previously described. A very small calculation time step of 2mn has been chosen, in order to ensure the stability of the analysis. The results have been required every hour. An arbitrary date of 15 April 2050, 00:00 has been set for the start of the simulation, and the ending time has been chosen 8 days after, on 23 April 2050, 24:00.

It has been verified that the flow always stays in sub-critical regime by looking at the Froude number, which stayed indeed smaller than one everywhere – and even smaller than 0.3. The only exception is in the very last section, where it reaches 2.5. But this is due to the downstream boundary condition imposed at this section.

The maximum water surface elevation has been reached on 17 April at 24:00, i.e. two days after the beginning of the simulation. The profiles of the initial and maximum water surface elevation are represented in Figure 29. The mean water rising is 56.3 cm, with a maximum value of 93 cm at Mederic Martin Bridge – disregarding the rising of 95 cm at Legardeur Bridge, too close to the downstream boundary condition to be reliable as said in the calibration part. The minimum water rising is 0 just before the dam, which was expected since the water level is forced to a constant value of 16.5m at this point. Table 13 presents the water rising in several cross-sections.



Looking at the water rise at each cross section, it can be noticed that all the bridges are high enough not to be flooded, i.e. that the water does not reach the lower part of the deck. Despite of the water rising, the clearance stays higher than 3 meter for all the bridges, ranging from 3.4m at Bizard, Lachapelle and Legardeur Bridges to 11.4 m at Pie9 Bridge.

However flooded zones are expected in the upper part of the Des-Prairies River, where water level exceed the bank level, like at the Bizard Island Bridge for example, as shown in Figure 30, or at the sections around. The flooded zone will be displayed more clearly in the next paragraph, were the results will be exported to ArcGIS.

Hec-RAS can also display flow and stage hydrographs at each section just before or after a bridge and each boundary section. An example at Bisson Bridge is given in Figure 31.

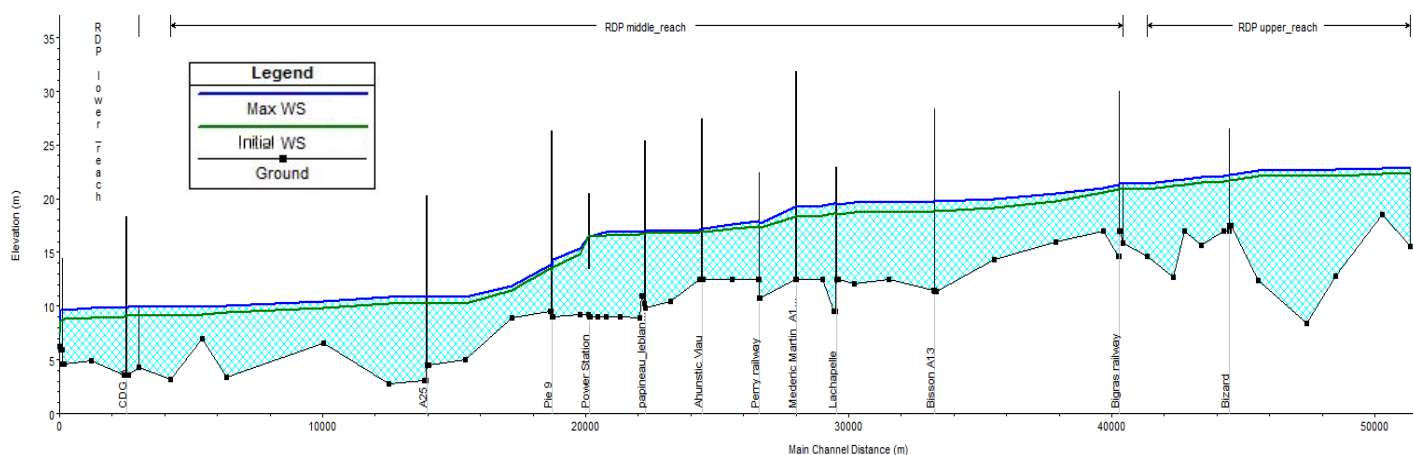
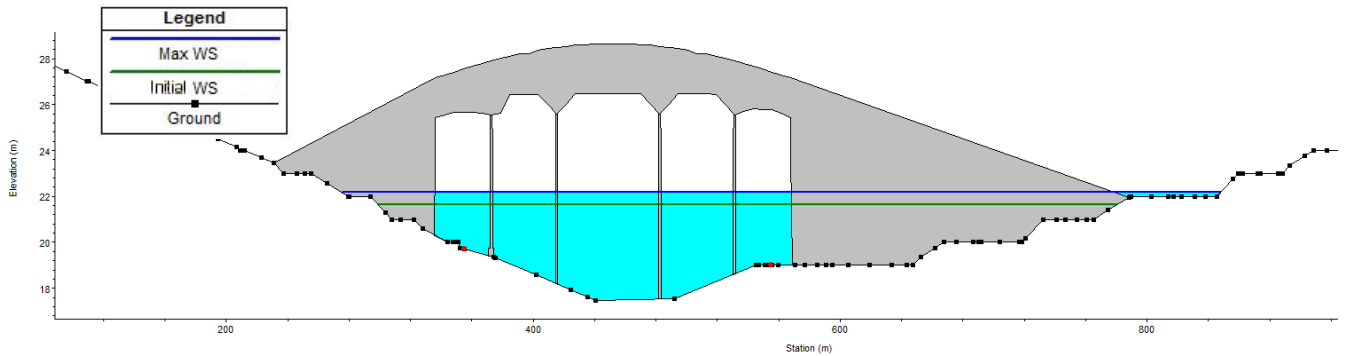


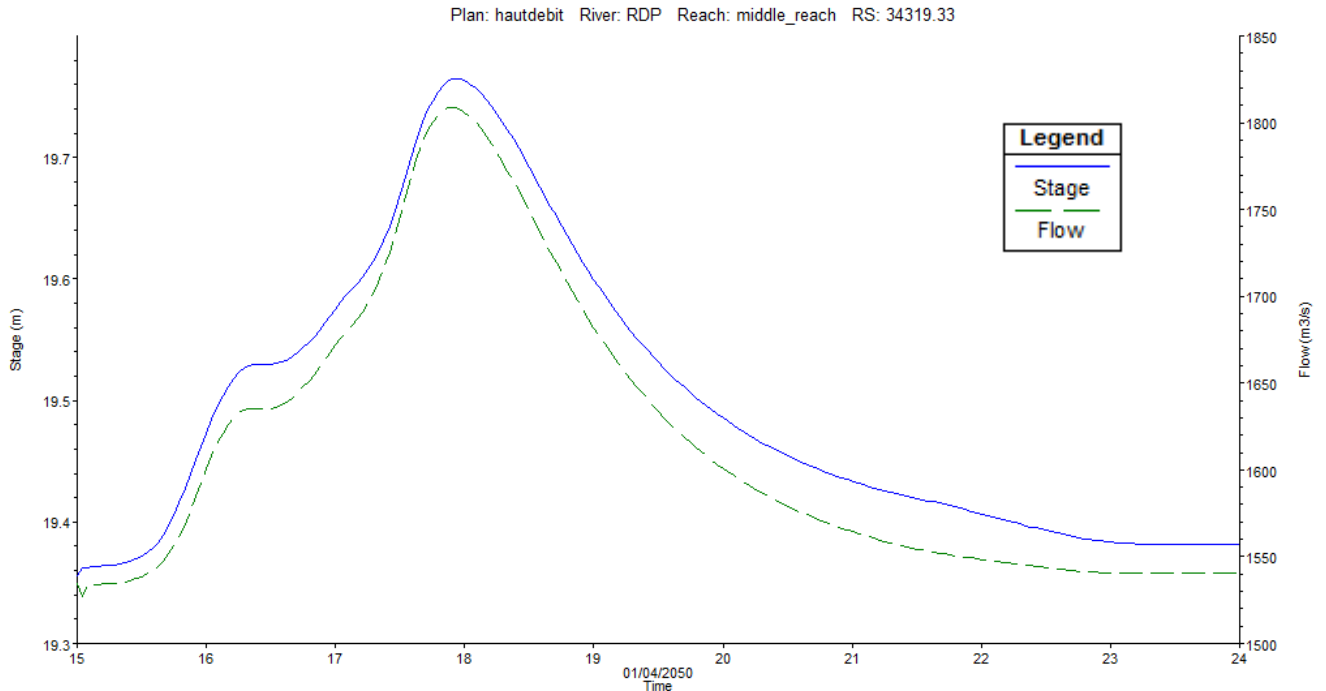
Figure 29: Initial and maximum water surface profile for the simulation of the future 24h rainfall event in Hec-RAS

Table13: Water rising at several cross-sections according to simulation in Hec-RAS

section		elevation [m]		difference
location	number	initial	max	[cm]
Beginning of upper reach	52215.69	22.38	22.87	49
Bizard Bridge	45246.02	21.6	22.11	51
just before Bigras Island	42240.15	20.96	21.37	41
Bigras railway Bridge	41246.25	20.86	21.32	46
beginning of middle reach	40678.27	20.53	21	47
Bisson bridge	34319.33	18.83	19.74	91
Lachepelle bridge	30589.06	18.58	19.5	92
Mederic Martin A15 Bridge	27971.25	18.35	19.28	93
Perry Island Railway Bridge	17539.73	17.43	17.88	45
Ahunistic Viau Bridge	25461.29	16.86	17.11	25
Papineau Leblanc Bridge	23238.97	16.67	16.8	13
just before dam	21566.02	16.5	16.5	0
just after dam	21168.85	14.82	15.32	50
Pie 9 Bridge	20028.22	13.46	13.87	41
between Pie9 and A25 Bridges	18582.18	11.49	11.86	37
A25 bridge	15419.11	10.27	10.82	55
Just before Pierre Island	11411.24	9.85	10.44	59
just before Mignerion Island	5614.082	9.09	9.89	80
CDG Bridge	4013.24	9.04	9.85	81
Legardeur bridge	1449.05	8.62	9.57	95



**Figure 30: Initial and maximum water elevation simulated by Hec-RAS at Bizard Island Bridge**



**Figure 31: Stage and flow hydrographs simulated by Hec-RAS just after Bisson Bridge**

In order to get a better idea of the reliability of this result, it is important to compare those elevations with past recorded water levels. On the CEHQ website, recorded monthly maximum, minimum and mean water levels, extracted from daily measures, were available at two stations.

- Station 043317, located 1.6km downstream the A25 bridge, with data from 1964 to 1981.
- Station 043319, located just before the Mignerons Island, with data from 1967 to 1975.

Unfortunately, no measured water level was available in the part upstream the dam. Table 14 shows the result of this analysis. It can be noted that for the station 043317, the maximum water elevation found by Hec-RAS – taken at section 12510.20 – ranges in the upper part of the recorded maximums, and that for the station 043319 – corresponding to the section 5614.082 – it is even way above, which is normal. Indeed, the event simulated is a future 24h rainfall episode with a return period of 50 years, which implies high flow and high water level expected. We could even have expected higher simulated levels, especially having in mind the results of the calibration test which showed a large tendency to overestimate the water level. However, the flow hydrograph that was input into the Des-Prairies River was not that huge, therefore the resulting water levels are high, but not incredibly.

*Table 14: Comparison of maximum water levels simulated by Hec-RAS with historical measured data at two stations of the Des-Prairies River*

	Station 043317	Station 043319
Maximum of the monthly max WS	11.001 m	9 m
Mean of the monthly max WS	9.34 m	6.97 m
Minimum of the monthly max WS	8.391 m	5.67 m
Minimum of the monthly min WS	8.101 m	5.32 m
Mean of the monthly mean WS	9 m	6.55 m
Hec-RAS max WS during simulation	<b>10.80 m</b>	<b>9.89 m</b>

Once again, it is important to remember that the large range of uncertainties in the process from the choice of a rainfall hyetograph to the determination of the maximum water surface elevation impacts a lot on the results.

#### 4.3.4.2. Export in ArcGIS

Since the project has been created in ArcGIS with the Hec-GeoRAS extension, the results of the analysis can also be exported back to the ArcGIS project in order to have a better graphical representation. For this project, the initial, final and maximum profiles have been exported, in term of water surface elevation and velocity in the main channel and overbanks. In ArcGIS, this information has been treated by Hec-GeoRAS tools in order to perform the inundation and velocity mapping (USACE, 2011).

The inundation mapping uses the water surface elevations imported from Hec-RAS at each cross-section to triangulate them into a TIN of water surface, which will be then rasterised and compared with the raster version of the digital terrain model, created for this occasion. The floodplain will be delimited by the area where the water surface grid is higher than the terrain grid, and the difference thus calculated gives the water depth. The resulting depth grid is presented in Figure 32.

However, this result should be taken carefully. Indeed, there can be many errors, due to imperfect topographic and bathymetric data. Since the program makes the comparison between the terrain and the water elevation files to determine the flooding zone and the water depth, any discrepancy in the terrain data will impact the final result, with incorrect values or abrupt changes in water depth, and wrong shape of flooding zone at some points.

Moreover, even with perfect data, the analysis done in 1D with HecRAS gives only constant water elevation at each cross-section. The interpolated result can then only be an approximation of the flooding zone and water depth and not a true 2D profile. And the more there are of cross-sections used, and the closer they are one from the others, the better the estimate will be. In this model, some cross-sections are far from each, and therefore some poor interpolation is expected.

The velocity mapping is done by interpolating the velocity data imported from Hec-RAS at each cross section. For that, it calculates the transition lines between cross-sections in the main channel and overbanks, for each point velocity on the cross-sections. It then interpolates the velocity data along the transition lines to create a velocity grid file, using the floodplain boundary previously found as a zero velocity boundary. The velocity distribution of the project is shown in Figure 33.

Once again, care should be taken in interpreting those results. It should not be forgotten that the analysis has been done in 1D, and this is just a practical representation of those 1D calculations, with an algorithm to interpolate the data that does not replace a true 2D analysis, and which cannot predict correctly the 2D behavior.

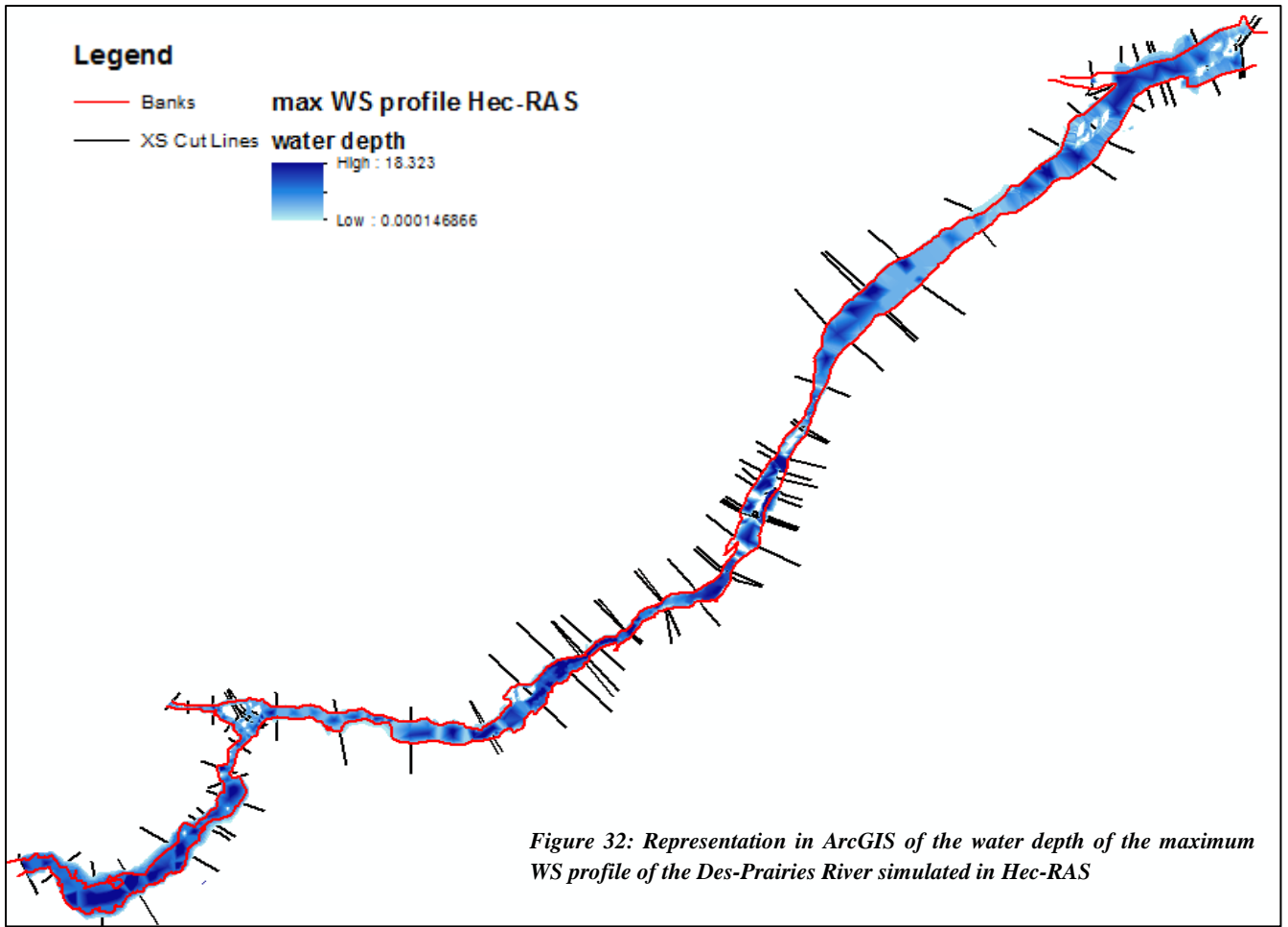


Figure 32: Representation in ArcGIS of the water depth of the maximum WS profile of the Des-Prairies River simulated in Hec-RAS

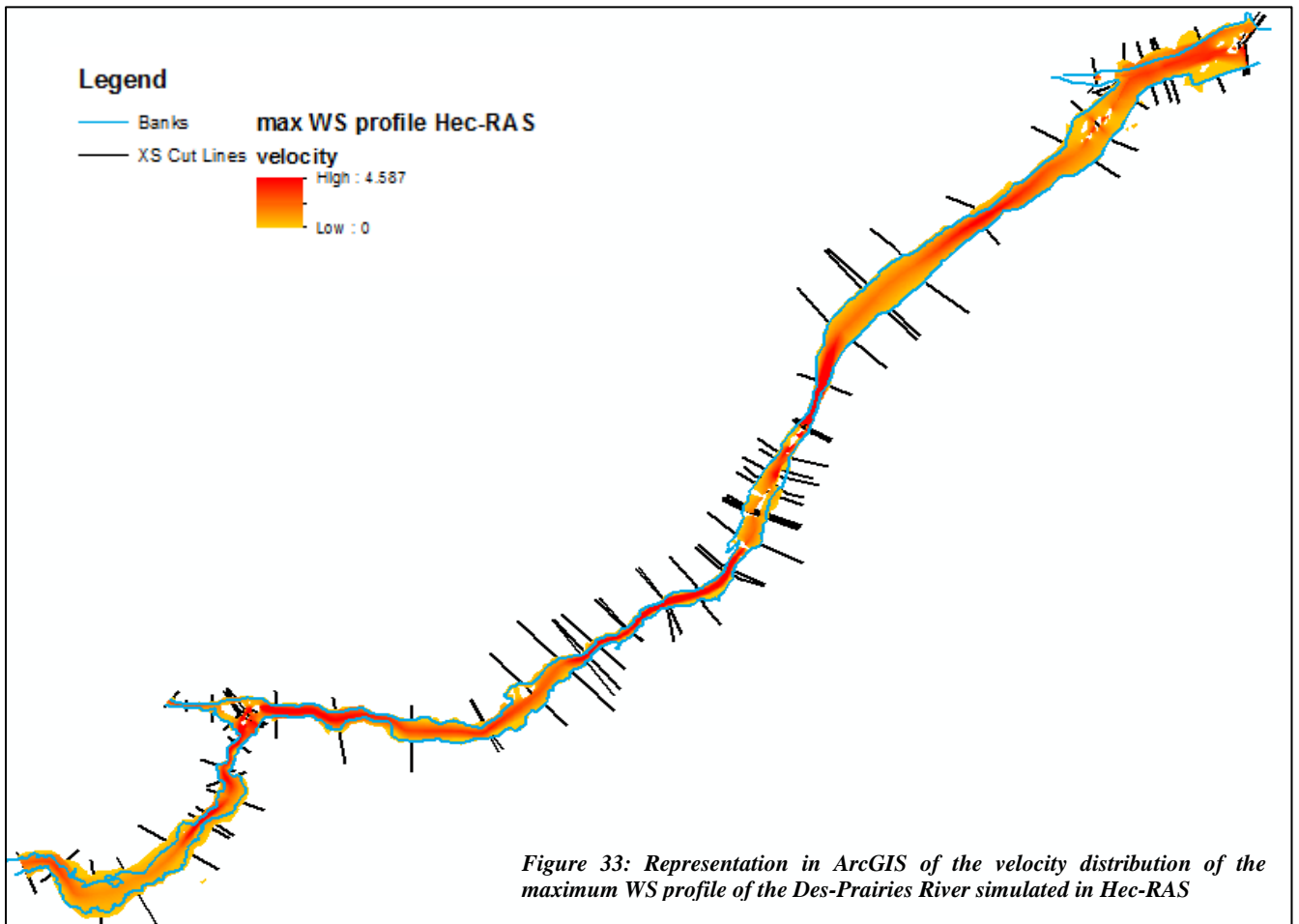


Figure 33: Representation in ArcGIS of the velocity distribution of the maximum WS profile of the Des-Prairies River simulated in Hec-RAS

The results of this mapping operation shows that water is expected in the overbank area in the upper reach of the Des-Prairies River, on both sides, and in the beginning of the middle reach. Moreover, the Pierre and Moulin Islands – just before the Mignerons Island, near the junction with Mille-Ile River – appear to be under water, as well as the overbank in this area. Finally, some flooding is also expected in the lower reach on Repentigny city side. Of course, the water depth is low in those flooding zones, and highest in the middle of the river bed. The maximum value displayed on the legend is 18.32 m. However it is due to a punctual error outside of the zone of interest, and the maximum value to take into consideration is 15.05m, in the upper reach, at the first turn of the river.

Some discrepancies can be observed as it was expected, resulting in abrupt color changing of strange form in the map. Moreover, there is even blank “no data” zones near the Visitation Island and in the Mille-Iles reach, due to problems in the interpolation process.

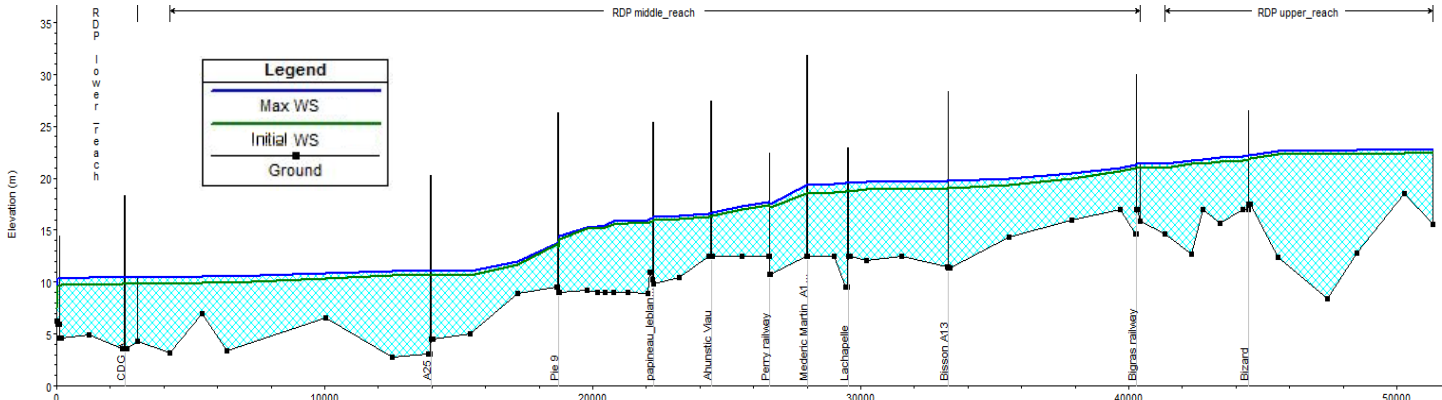
As far as the velocity distribution is concerned, the highest velocities are naturally found in the main channel, especially at places where there is a contraction, with a maximum value 5.78 m/s. As for the water depth, the true maximum velocity to consider is however 2.95 m/s. On the contrary, the velocity in the flooded overbank is nearly null. As for the water depth map, blanks can be observed at some places, due to problems during interpolation.

**4.3.4.3. Simulation without the inline structure**

In order to make conclusions on the use of 1D or 2D models for such a project, the results obtained with Hec-RAS will be compared with the ones obtained with River2D, in a next chapter. However, as it will be explained in the following, the Des-Prairies hydropower station could not be represented in River2D. Therefore, to have comparable results, a simulation in Hec-RAS has also been done without the inline structure. Of course, the results will be less precise, since it does not represent the reality. But it was done only in a comparison purpose, and the results of Hec-RAS to exploit for eventual adaptive measures would be the results with the inline structure given in a former paragraph.

As previously, the maximum water surface elevation is reached three days after the beginning of the simulation. The initial and maximum profiles are displayed in Figure 34.

Looking at the results of this simulation, that are described in Table 15, it can be seen that the error compared to the simulation with the inline structure is very small in the upper part of the river – less than 1.5% - and mostly in overestimation, but starts to increase from the AhunaticViau Bridge to reach nearly 8% just before the location of the dam, as expected with the suppression of the inline structure, and in underestimation. After the dam, the error decreases a bit, but becomes larger again in the lower reach of the river, in overestimation again.



**Figure 34: Initial and maximum water surface profile for the simulation of the future 24h rainfall event in Hec-RAS without the inline structure**

**Table 15: Water rising at several cross-sections according to simulation in Hec-RAS without the inline structure, and comparison with the simulation with the inline structure**

section		With Inline Structure			Without inline structure			error [%]	
		elevation [m]		difference	elevation [m]		difference	initial	max
location	number	initial	max	[cm]	initial	max	[cm]	initial	max
Beginning of upper reach	52215.69	22.38	22.87	49	22.5	22.87	37	0.54	0.00
Bizard Bridge	45246.02	21.6	22.11	51	21.83	22.19	36	1.06	0.36
just before Bigras Island	42240.15	20.96	21.37	41	21.03	21.36	33	0.33	-0.05
Bigras railway Bridge	41246.25	20.86	21.32	46	20.98	21.32	34	0.58	0.00
beginiing of middle reach	40678.27	20.53	21	47	20.65	21	35	0.58	0.00
Bisson bridge	34319.33	18.83	19.74	91	19.04	19.76	72	1.12	0.10
Lachepelle bridge	30589.06	18.58	19.5	92	18.76	19.53	77	0.97	0.15
Mederic Martin A15 Bridge	27971.25	18.35	19.28	93	18.48	19.32	84	0.71	0.21
Perry Island Railway Bridge	17539.73	17.43	17.88	45	17.3	17.57	27	-0.75	-1.73
Ahunstic Viau Bridge	25461.29	16.86	17.11	25	16.28	16.57	29	-3.44	-3.16
Papineau Leblanc Bridge	23238.97	16.67	16.8	13	15.93	16.2	27	-4.44	-3.57
just before dam	21566.02	16.5	16.5	0	15.19	15.35	16	-7.94	-6.97
just after dam	21168.85	14.82	15.32	50	15.14	15.29	15	2.16	-0.20
Pie 9 Bridge	20028.22	13.46	13.87	41	13.25	13.75	50	-1.56	-0.87
between Pie9 and A25 Bridges	18582.18	11.49	11.86	37	11.69	11.94	25	1.74	0.67
A25 bridge	15419.11	10.27	10.82	55	10.62	11.06	44	3.41	2.22
Just before Pierre Island	11411.24	9.85	10.44	59	10.3	10.8	50	4.57	3.45
just before Mignerons Island	5614.082	9.09	9.89	80	9.83	10.49	66	8.14	6.07
CDG Bridge	4013.24	9.04	9.85	81	9.82	10.47	65	8.63	6.29
Legardeur bridge	1449.05	8.62	9.57	95	9.64	10.35	71	11.83	8.15

## 4.4. 2D Simulation with River2D

### 4.4.1. Presentation of River2D

River2D is a free two-dimensional, depth average hydrodynamic model for natural stream and rivers developed by the University of Alberta.

The hydrodynamic model is based on the 2D, depth averaged St-Venant equations (Eq.9, Steffler et al., 2002c):

$$\begin{aligned}
 & - \text{Mass conservation equation: } \frac{\partial H}{\partial t} + \frac{\partial HU}{\partial x} + \frac{\partial HV}{\partial y} = 0 \\
 & - \text{Momentum equations: } \begin{cases} \frac{\partial HU}{\partial t} + \frac{\partial HU^2}{\partial x} + \frac{\partial HUV}{\partial y} + gH \left( \frac{\partial H}{\partial x} + S_{0x} - S_{fx} \right) = \frac{1}{\rho} \left( \frac{\partial H\tau_{xx}}{\partial x} + \frac{\partial H\tau_{xy}}{\partial y} \right) \\ \frac{\partial HV}{\partial t} + \frac{\partial HUV}{\partial x} + \frac{\partial HV^2}{\partial y} + gH \left( \frac{\partial H}{\partial y} + S_{0y} - S_{fy} \right) = \frac{1}{\rho} \left( \frac{\partial H\tau_{yx}}{\partial x} + \frac{\partial H\tau_{yy}}{\partial y} \right) \end{cases} \quad (9)
 \end{aligned}$$

Where  $S_{fx} = \frac{\tau_{bx}}{\rho gH}$  (10) is the friction slope, calculated with the two-dimensional form of the

Manning's equation (Eq.11):  $S_{fx} = \frac{n^2 U \sqrt{U^2 + V^2}}{H^{4/3}}$  (11), and  $\tau_{xy}$  the transverse shear, calculated with

the Bousinessq type eddy viscosity (Eq.12):  $\tau_{xy} = \nu_t \left( \frac{\partial U}{\partial y} + \frac{\partial V}{\partial x} \right)$  (12)

Those equations are solved numerically, with a finite element model, based on the conservative upwind Petro-Galerkin weighted residual formulation. River2D can use a direct or iterative solver for solving those equations. In this project the iterative solver – working with the Generalized Minimal Residual method – has been used, because of the very large size of the matrix that would be involved with the direct solver.

Moreover, the following assumptions are made:

- Shallow water:  $H/L \ll 1$
- Incompressible fluid
- Fully turbulent flow
- Hydrostatic vertical distribution of the pressure
- Constant distribution of horizontal velocity over depth
- Coriolis and wind forces negligible

Therefore, the utilization of this model should be limited to channel with mild slope, not too large (no lakes or estuaries).

#### 4.4.2. Preparation of the data in Arc-GIS

R2D\_Bed, the first modulus of River2D software dealing with the river bed topography editing, requires as input file an ASCII file – i.e. a text file – of five columns, respectively the number of the point, its X and Y coordinate, its elevation and its associated roughness.

Arc-GIS can export a point feature class into an ASCII file. Therefore, all the layers of the raw terrain model have been transformed to points. Then, the land use layer used with the Hec-GeoRAS project has been added, with the same values of the roughness coefficient chosen, in order to assign to each point its corresponding manning coefficient. However, River2D uses the roughness height instead of the Manning's coefficient. A conversion has therefore been necessary, done with the Equation 13 (Steffler *et al.*, 2002a). Those data have then been exported into an ASCII file.

$$k_s = \frac{12 * R}{e^m} \quad \text{with} \quad \begin{cases} m = \frac{R^{1/6}}{2.5 * n * \sqrt{g}} \\ R = A/P \cong H \end{cases} \quad (13)$$

where  $k_s$  is the roughness height,  $n$  the manning's coefficient,  $g$  the gravity constant,  $A$  the area of a cross section,  $P$  the wetted perimeter,  $H$  the water depth and  $R$  the hydraulic radius.

#### 4.4.3. Simulation with River-2D

##### 4.4.3.1. Bed topology with R2D-Bed

The text file created by ArcGIS is imported into the R2D-Bed modulus, where the points are displayed. In this modulus, some points can be added or removed, break lines can be drawn and the outside boundary is defined. All those steps allow generating a topographic mesh. For this project, several breaklines have been defined in the bottom of the river bed, to ensure a proper representation of the later by forcing a linear interpolation along the defined breakline. The resulting topographic mesh is displayed in Figure 35, and a zoom has been done in a small part in Figure 36 to distinguish the different elements that compose it.

It is important to note that River2D cannot consider the dam, therefore it has not been represented. Moreover, the bridges have not been represented neither. It would have been possible to take them into consideration by creating some small internal boundaries corresponding to the piers. However this would have been a complicated process, whereas the piers of the bridges are very small compared to the width of the river, and therefore their effect on the flow can be considered negligible.



#### 4.4.3.2. Mesh generation with R2D-Mesh

First of all, the boundary has been discretized, by creating boundary nodes all along, with a spacing of 80m. A rough mesh has then been generated in the entire calculation domain, with a uniform node fill of spacing 80m. The critical zones – around the islands, at the junction of two reaches, in places where there is abrupt contraction – have then been refined, and a first triangulation has been done. Some steps of smoothing, adding and deleting nodes and breaklines have then been done, in order to improve the quality of the mesh. This quality can be measured by the Quality Index (QI), which represents the minimum “triangle quality” – ratio of the triangle area by the circumcircle area normalized by corresponding ratio for an equivalent equilateral triangle (Steffler *et al.*, 2002b). An ideal mesh would have a QI of one, however values ranging from 0.15 to 0.5 are considered acceptable. Moreover, the “bad” triangles (with a low QI) and the generated contour lines can be displayed and compared with the topography contour lines, which gives a good idea of the quality of the mesh and of the places to refine.

The final mesh, that will be used in the simulations, has 19375 nodes, 1985 boundary segments and 38713 elements, with a quality index of 0.22. A portion of this resulting mesh can be seen on Figure 37. More detailed meshes – with more nodes and elements – have been tested, but the corresponding time of calculation was not acceptable – more than one week to get a result.

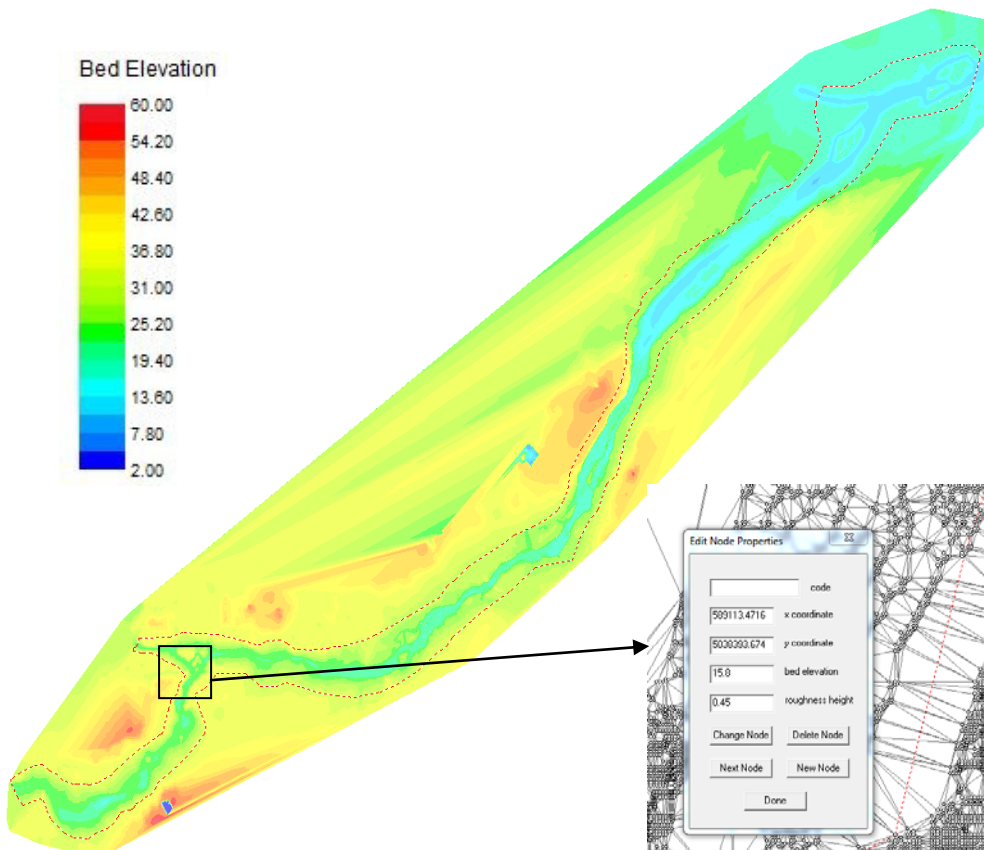


Figure 35: Bed elevation of the Des-Prairies River after triangulation in R2D-Bed

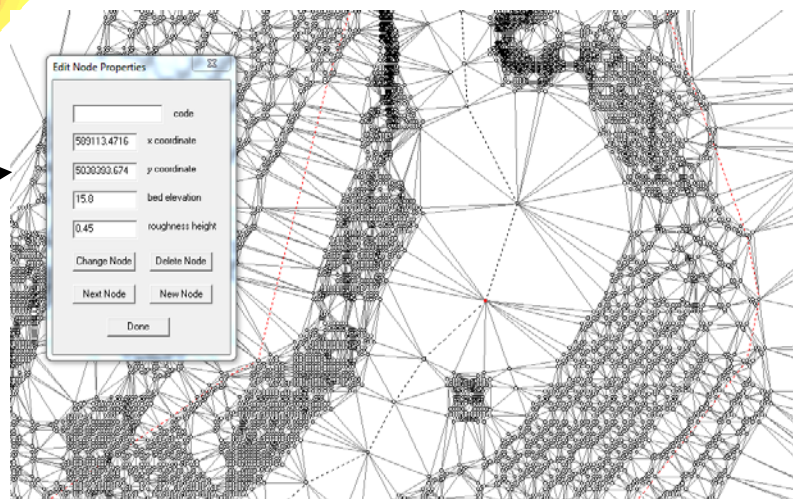
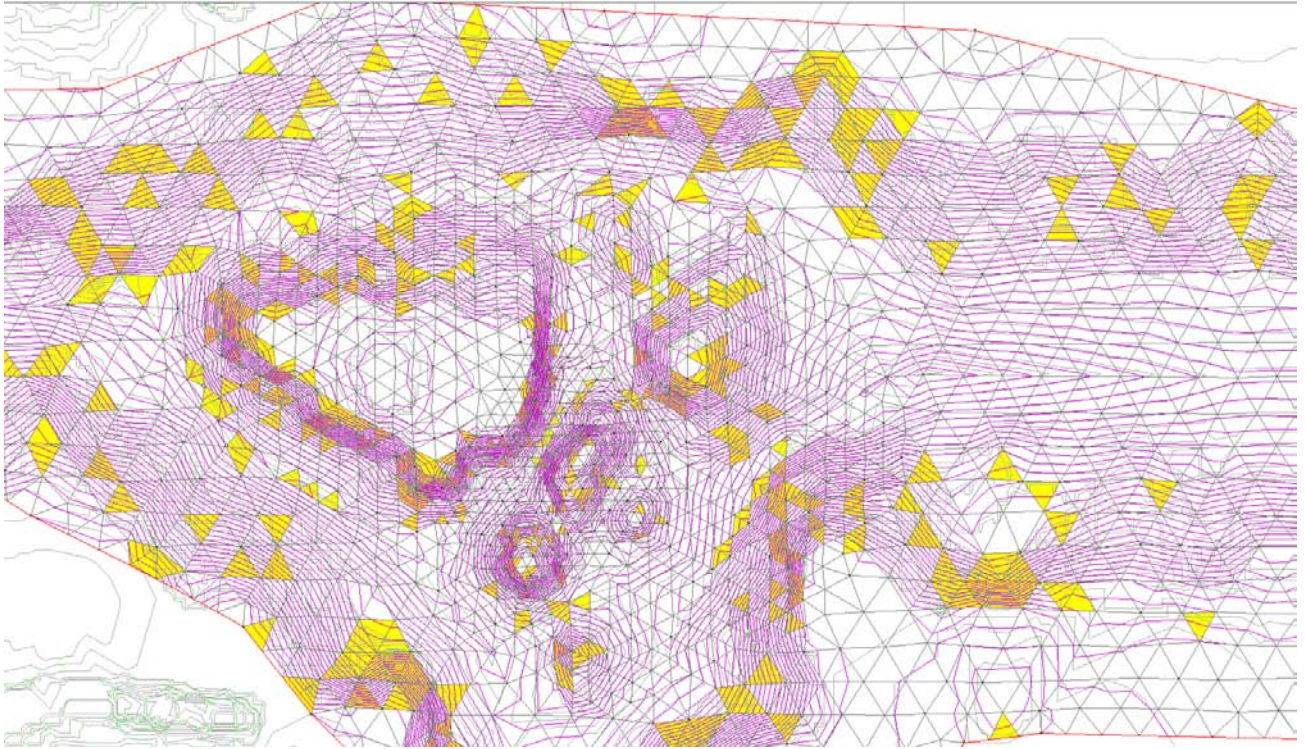


Figure 36: Zoom on a small portion of the topographic mesh of the Des-Prairies River (nodes and triangulated elements in black, breaklines in dotted lines, external boundary in red).



**Figure 37:** Zoom on the hydrodynamic mesh of the Des-Prairies River around Bigras Island in R2D-Mesh (hydrodynamic mesh in black triangles, external boundaries in red, topographic contour lines in black, generated contour lines in pink, large elevation triangles in yellow)

#### 4.4.3.3. Calibration and validation of the model

As it has been done with Hec-RAS, the model has been tested in permanent conditions in the River2D modulus with input inflow corresponding to known water surface elevations. The roughness height has then been changed where necessary in order to obtain simulated water level as close as possible to observed ones. The results after calibration are shown in Table 16.

**Table 16:** Comparison between known water surface elevations and simulated ones by River-2D after calibration

location on RDP River	CEHQ nb	22/04/2002				27/11/2003			
		flow [m <sup>3</sup> /s]	WS elevation [m]		error [%]	flow [m <sup>3</sup> /s]	WS elevation [m]		error [%]
			known	River2d			known	River2d	
beginning of upper reach	31	1225	23.56	23.6	0.170	1030	23.01	23.15	0.608
middle of upper reach	24	1225	23.02	23.4	1.651	1030	22.39	23	2.724
just before Bigras Island	21	1225	22.35	23.1	3.356	1030	21.69	22.6	4.195
beginning of middle reach	19	2356	21.28	22.6	6.203	1923	20.75	22.15	6.747
Bisson bridge	14	2356	19.85	21.5	8.312	1923	19.55	21	7.417
Lachepelle bridge	10	2356	19.6	21	7.143	1923	19.05	20.4	7.087
Viau Bridge	9.4	2356	17.52	18.7	6.735	1923	17.4	18.6	6.897
just before dam	9.01	2356	17.15	18.1	5.539	1923	17.15	17.8	3.790
just after dam	9	2356	10.55	17.9	69.668	1923	10.11	17.7	75.074
between Pie9 and A25 Bridges	7.5	2356	10.05	12.6	25.373	1923	9.7	11.5	18.557
between Pie9 and A25 Bridges	7	2356	10	11.7	17.000	1923	9.64	11.35	17.739
A25 bridge	6.5	2356	10	11.6	16.000	1923	9.7	11.2	15.464
Just before Pierre Island	5	2356	9.33	11.5	23.258	1923	8.99	10.2	13.459
just before Migneron Island	2	2356	7.62	9.8	28.609	1923	7	9.4	34.286
CDG Bridge	1.5	3097	7.35	9.3	26.531	2508	6.74	9	33.531
Legardeur Bridge	0.5	3097	7.17	7.4	3.208	2508	6.58	6.9	4.863

It can be noticed that even after the calibration process, there is a global tendency to overestimate the water surface elevation, in both simulations. Several trials of adjustment of the roughness height have been done, and the results have been improved, but it has not been possible to obtain better results than the presented ones. Therefore, it is probable that this global overestimation of the water level results from a too rough hydrodynamic mesh. However, as it has been explained before, it was not possible within the time frame of the project to work with a more refined mesh.

Moreover there are still some large errors, especially in the part downstream the location of the dam. As explained previously (paragraph 4.3.3.2.), this is probably due to wrong bathymetry in this area. The error is even larger than in Hec-RAS, which can be explained by the fact that the dam is not represented in River2D. And even if this is a run-of-river power station, its effect is probably not totally null on the flow.

As far as the overestimation in the lower part of the river is concerned, it can be explained by both a poor bathymetry in this part, and the fact that the inflow of the Mille-Ile River for the calibration was not known, and so the estimate input might be wrong – as for the calibration in He-RAS.

Despite of those problems, the model has been validated, since there was no solution in hand to solve them in the frame time of the project with the resources available. Moreover, as it has been said before, the objective of this project was not to produce exact and certified results, but rather to make a complete study of the entire process and to make comparison and recommendations about the different available methods at each step.

#### **4.4.3.4. Hydrodynamic simulation with River2D**

The transient simulation of River2D is based on an iterative procedure and can be quiet time-consuming, especially if the initial guess is not precisely input. This initial guess of water level at each point of the mesh is calculated by River2D by linear regression from the input water level at the inflow sections and the downstream elevation, input as boundary condition. However, this method leads to a rough estimation of the water surface.

That is why first of all the model has been run in permanent flow conditions, in order to get a better estimation of the water surface. The permanent simulation has been run with a flow value equal to the value at the beginning of the flow hydrographs that will be input in the transient simulation – for a duration approximately equal to the double of the time for the water to go through the modelled reach, until the stabilization of the solution, when the inflow and the outflow are stable and approximately equal. The downstream elevation has been chosen equal to 7m, as in Hec-RAS. The initial upstream elevation has been chosen equal to 23m, a little overestimated compared to the report (*CEHQ, 2005*), because the program has more facilities to do the drying process than the wetting one. The result of this simulation has then been taken as the initial conditions of the transient flow simulation.

The transient simulation has been run with the results of the permanent simulation as initial condition. The same boundary conditions than in Hec-RAS have been used: same flow hydrographs upstream and same constant elevation downstream. The tolerance of the iterative method has been set to 0.1, in order to reduce the very long time of computation. The implicitness  $\theta$  has been chosen equal to 1 – to get the most stable and with fastest convergence – which means that a fully implicit scheme has been used. A value of 0.5 would have given more accurate results, but it was not necessary since I was interested into the general trend of the water lever, in a large scale phenomenon, and not in modeling small flow features. The Goal  $\Delta t$  – time interval at which results will be displayed, the true calculation



time can be smaller for convergence reasons – has been set to 900s (15mn), which corresponds to the time step of the input hydrographs.

The results given by River2D that were interesting for this project were the water surface level, the water depth and the velocity. They have been saved automatically at each goal time step for each point of the mesh, in a .cdg file. They can then be extracted in excel at the sections of interest.

It is important to note that the results of such a simulation near the boundary conditions can be strongly influenced by the choice of the latter. That's why it is recommended to place the boundary conditions far away from the domain of interest. However in this case it was not possible, since no information about the bathymetry was available before and after the Des-Prairies River. The global results will not be affected, but it should be in mind for the interpretation of the results that near the boundaries, they can be biased.

#### 4.4.4. Results

The maximum water surface elevation has been reached around time 270000s, i.e. 75 hours after the beginning of the simulation. At this moment, the total inflow in the system is 2387.6 m<sup>3</sup>/s and the outflow is 2379.962 m<sup>3</sup>/s. The maximum water surface elevation is displayed in Figure 38. The water depth at the same moment is displayed on Figure 39 and the velocity distribution and vectors are shown on Figure 40, the two later with a zoom to see the distribution better.

Looking at the water surface elevation, it can be seen that it ranges from 23.51m at the beginning of the river to 6.95 at the lower end, which seems reasonable values. It is not possible to display the banks in River2D, in order to visualize the flooded zones. However, the maximum water extent has been exported into ArcGIS, where it has been superimposed with the banks. It can be noticed several flooding zones, in the upper reach of the river in both sides, in the beginning of the middle reach in Montreal side and near Patton Island on Laval side, where Tremblay island appears under water. They can be observed on Figure 41.

It is worthy noticing that the position of the bank in ArcGIS should also be taken carefully. Indeed, they have been created manually – by following point by point the contour lines of the different islands – which can lead to imprecisions, and thus some errors in the flooded zones.

Looking at the velocity distribution, it can be observed that it is nearly null outside of the river bed, in the flooded zones, which was expected. Moreover, the velocity tends to increase where there is a contraction of the river, which is also normal, with a maximum value of 9.89 m/s. However, this value is reached only in one point, and seems to be an error. Therefore, looking at the velocity distribution in global, the maximum velocity to consider would be around 3.8 m/s, in the contraction zone just after Pie9 Bridge.

As far as the water depth distribution is concerned, the highest depths are of course located on the middle of the river bed, with a maximum of 15.35m in the upper reach, at the first curve of the river. And naturally, there is little water depth in the flooded zones.

Water Surface Elev

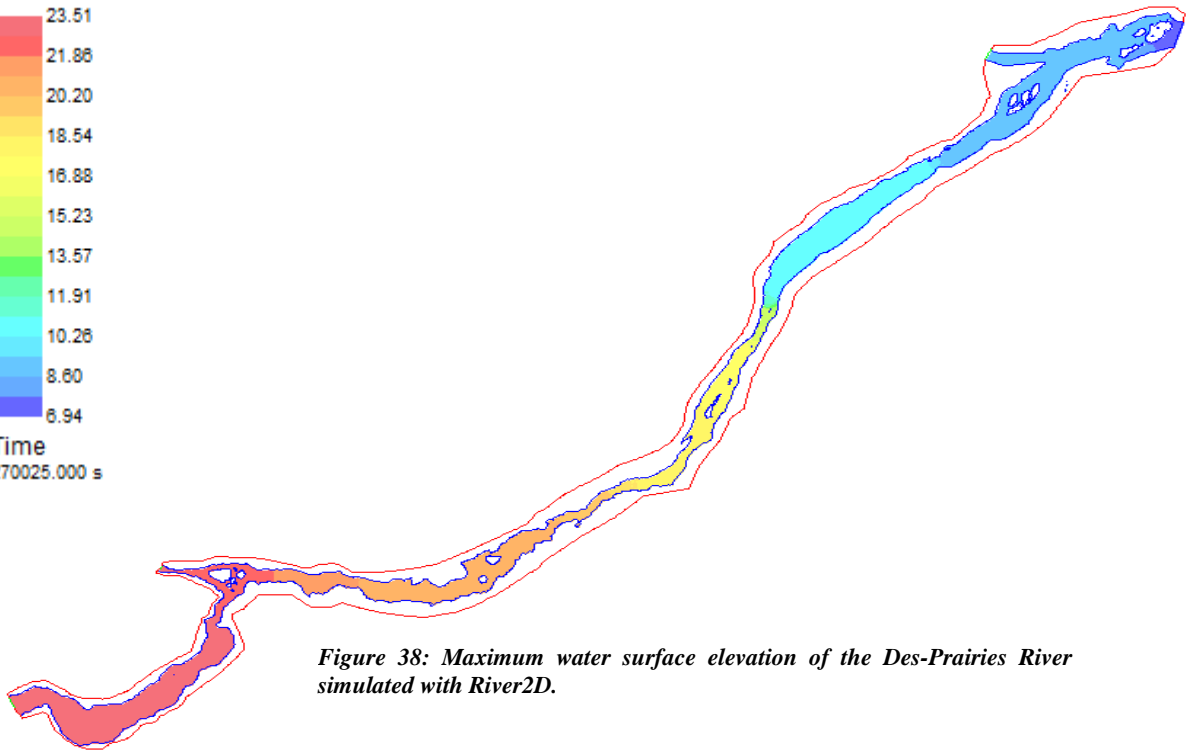
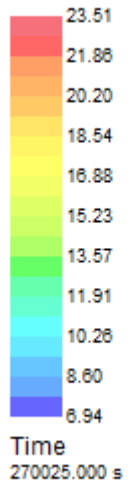


Figure 38: Maximum water surface elevation of the Des-Prairies River simulated with River2D.

Depth

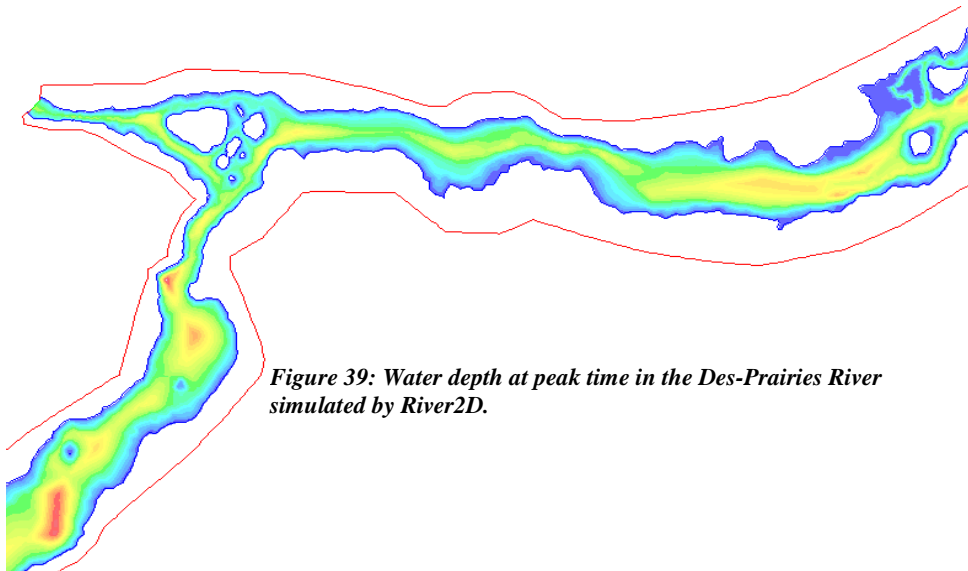
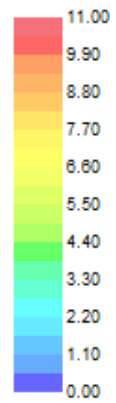


Figure 39: Water depth at peak time in the Des-Prairies River simulated by River2D.

Velocity

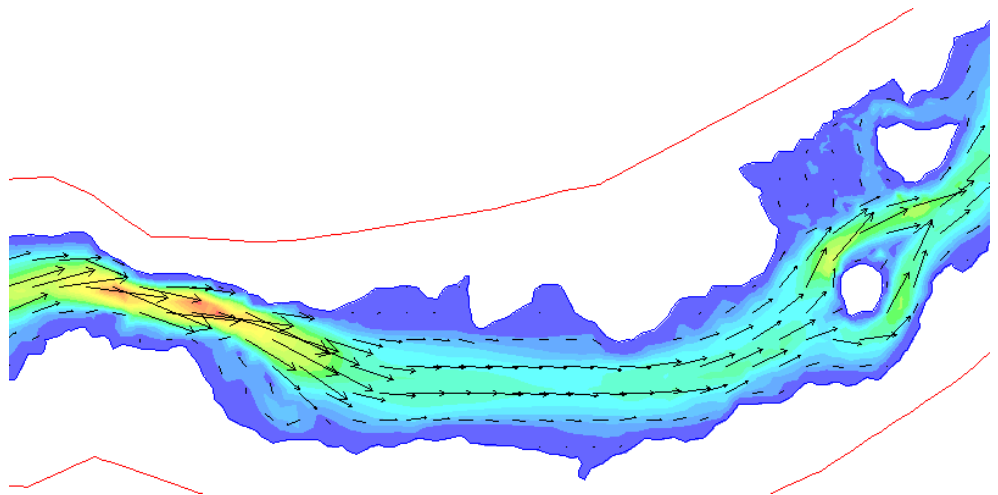
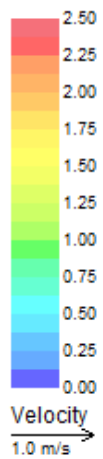
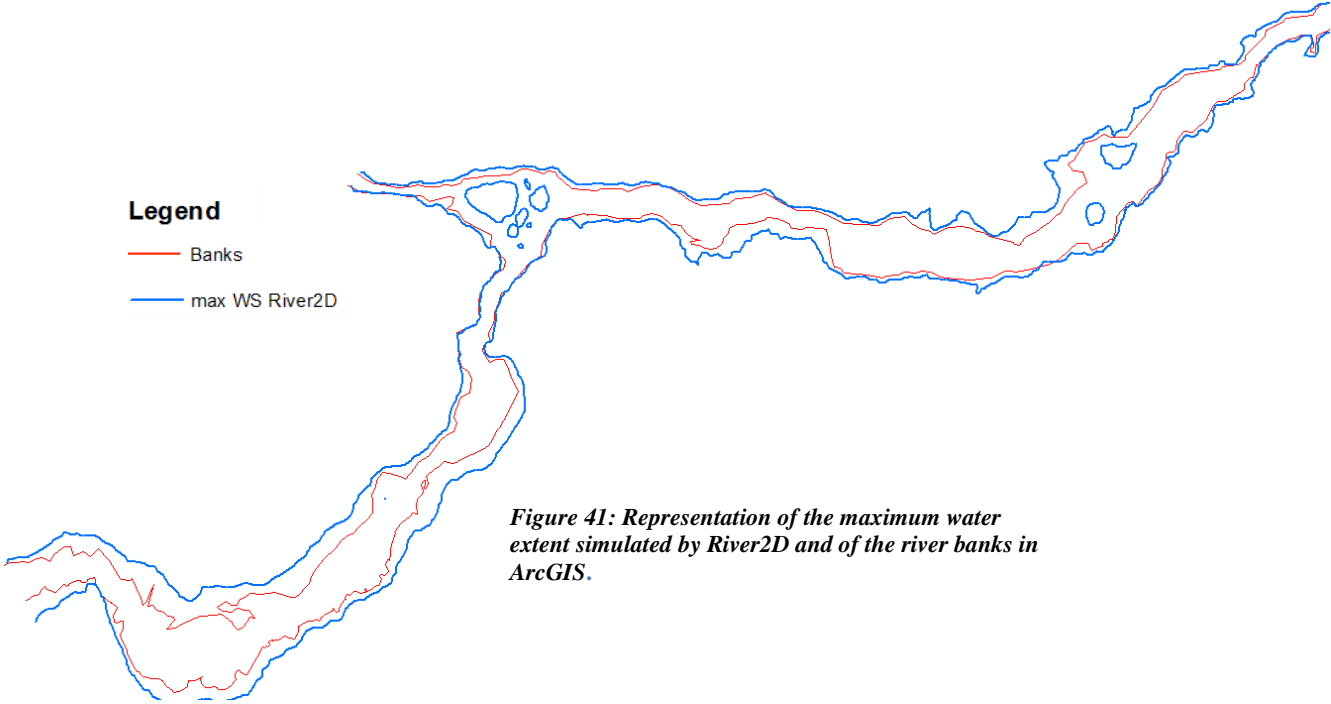


Figure 40: Velocity distribution and vectors at peak time in the Des-Prairies River simulated by River2D.

The initial and maximum water levels have been taken at several cross-sections, and are reported in Table 17. However those results must be taken carefully, because they have been taken manually, by pointing the mouse on an estimated location on the results map in River2D. However, it is difficult to be absolutely sure of the location. And in some places, like around the Pie9 Bridge for example, there are very rapid changes in water surface elevation. Moreover, the water level is not constant on each cross section. Here, the level of the middle of the river bed has been taken.

*Table 17: Water rising at several cross-sections according to simulation in River2D*

section's location	elevation [m]		difference [cm]
	initial	max	
Beginning of upper reach	23.11	23.47	36
Bizard Bridge	22.85	23.2	35
just before Bigras Island	22.18	22.5	32
Bigras railway Bridge	21.68	22.08	40
beginiing of middle reach	21.65	21.9	25
Bisson bridge	20.46	20.82	36
Lachepelle bridge	20.05	20.34	29
Mederic Martin A15 Bridge	19.51	19.71	20
Perry Island Railway Bridge	18.78	19.12	34
Ahunstic Viau Bridge	18.05	18.35	30
Papineau Leblanc Bridge	17.52	17.76	24
just before dam	17.47	17.7	23
just after dam	17.34	17.66	32
Pie 9 Bridge	16.49	16.9	41
between Pie9 and A25 Bridges	11.02	11.25	23
A25 bridge	11.01	11.24	23
Just before Pierre Island	9.32	9.65	33
just before Mignerons Island	9.15	9.4	25
CDG Bridge	8.84	9.08	24
Legardeur bridge	7.32	7.37	5



*Figure 41: Representation of the maximum water extent simulated by River2D and of the river banks in ArcGIS.*

As with Hec-RAS, the results of this simulation have been compared with past recorded water levels, at the same two stations of the CEHQ. Table 18 shows the result of this analysis.

It can be noted that for both stations, the maximum water elevation found by River 2D is above the recorded maximums, which is normal. Indeed, the event simulated is a future 24h rainfall episode with a return period of 50 years, which implies high flow and high water level expected. Moreover, the calibration test showed a very large tendency to overestimate the water level, especially in the part downstream of the dam, therefore those high flow are logic.

Once again, it is important to remember that the large range of uncertainties in the process from the choice of a rainfall hyetograph to the determination of the maximum water surface elevation impacts a lot on the results.

*Table 18: Comparison between maximum water levels simulated by River2D and historic ones at two stations of the Des-Prairies River*

	Station 043317	Station 043319
Maximum of the monthly max WS	11.001 m	9 m
Mean of the monthly max WS	9.34 m	6.97 m
Minimum of the monthly max WS	8.391 m	5.67 m
Minimum of the monthly min WS	8.101 m	5.32 m
Mean of the monthly mean WS	9 m	6.55 m
River 2D max WS during simulation	<b>11.2 m</b>	<b>9.4 m</b>



## Chapter 5 – Results Processing

In this chapter, the results obtained with Hec-RAS and River2D, already commented in the previous chapter, will be compared, in order to make conclusion on one hand on the level rise of the Des-Prairies River, and on the other hand on the use of 1D and 2D model for such simulation.

### 5.1. Results discussion

#### 5.1.1. Comparison between 1D and 2D results

In order to visualize easily the differences between Hec-RAS – without inline structure – and River2D simulated flooded zones, the two corresponding maximum extent of water have been superimposed in ArcGIS. The result is displayed in Figure 42, zoomed in the part downstream of the Lachapelle Bridge, since most of the flooded zones are in this area.

One can remarks that the two results look very similar, with the same trends, and flood expected in the same areas, except in some places – like near Tremblay Island, which is under water with River 2D and not with Hec-RAS. And in overall, Hec-RAS seems to have a tendency to simulate water levels a little bit lower than River2D. This seems logic, since it has been seen during the calibration test that River2D has a strong tendency to overestimate the water level. The only exception is in the lower reach, where Hec-RAS largely overestimate the water level, and seems to have convergence problems due to the near boundary condition. Besides, it is important to remind that between two cross-sections, the delimitation of the floodplain from Hec-RAS is done by interpolation – which explains its angular shape – and is therefore only an approximation.

However, looking in Table 19 at the water levels taken at several sections, it can be noticed that the difference in water level between the two software is quiet large – always more than 60 cm, and up to 2 meters just after the dam. This can be explained by the topography of the banks. Indeed, in case of steep bank, a large difference in water surface elevation will result only in a few differences in water extend on the map, since the topographic contour lines are close to each other's. Moreover, this is also due to the fact that Hec-RAS simulates horizontal water level on each section, while River2D allow variations – even if they are small – on a cross-section, with maximum value in the middle of the river bed – where it has been taken for the values of Table 19 – and minimum value in the overbanks. And finally, it should not be forgotten that Figure 42 presents the results at a very large scale, at which a difference of 1 meter can look very small. A zoom at smaller scale can show better the differences between the two simulations.

Those differences between Hec-RAS and River 2D simulations can be explained by the fact that even if the topographic and bathymetric data were the same at the beginning, each software – Hec-GeoRAS and River2D – made its own algorithm to generate the terrain file used in the simulation, and thus created differences in river bed and floodplain elevations. An example is given in Figure 43 in a cross-section at the beginning of the middle reach of the Des-Prairies River. Those bed elevation differences could have been avoided – or at least reduced – with more bathymetric data. Indeed, with precise bathymetric data the two algorithms for terrain file creation would probably have converged to a closer solution. And of course, those differences are also simply due to the intrinsic differences between one- and two-dimensional simulations.

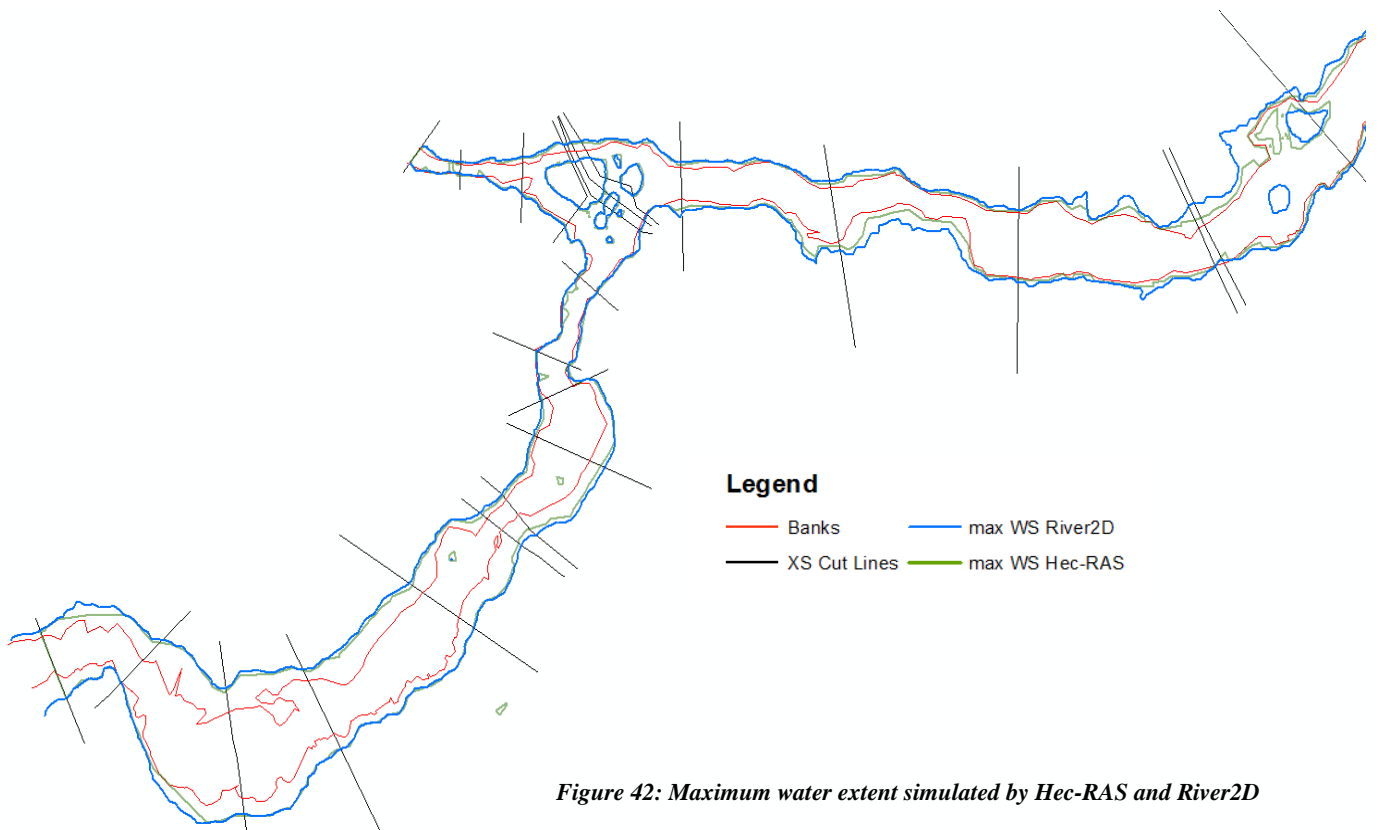


Figure 42: Maximum water extent simulated by Hec-RAS and River2D

Table19: Comparison between water surface elevations simulated with Hec-RAS and River2D.

section's location	Hec-RAS number	Hec-RAS			River2D			Difference (River2D compared to Hec-RAS)		
		elevation [m]		water rise [cm]	elevation [m]		water rise [cm]	elevation [m]		water rise [cm]
		initial	max		initial	max		initial	max	
Beginning of upper reach	52215.69	22.5	22.87	37	23.11	23.47	36	0.61	0.6	-1
Bizard Bridge	45246.02	21.83	22.19	36	22.85	23.2	35	1.02	1.01	-1
just before Bigras Island	42240.15	21.03	21.36	33	22.18	22.5	32	1.15	1.14	-1
Bigras railway Bridge	41246.25	20.98	21.32	34	21.68	22.08	40	0.7	0.76	6
beginiing of middle reach	40678.27	20.65	21	35	21.65	21.9	25	1	0.9	-10
Bisson bridge	34319.33	19.04	19.76	72	20.46	20.82	36	1.42	1.06	-36
Lachepelle bridge	30589.06	18.76	19.53	77	20.05	20.34	29	1.29	0.81	-48
Mederic Martin A15 Bridge	27971.25	18.48	19.32	84	19.51	19.71	20	1.03	0.39	-64
Perry Island Railway Bridge	17539.73	17.3	17.57	27	18.78	19.12	34	1.48	1.55	7
Ahunstic Viau Bridge	25461.29	16.28	16.57	29	18.05	18.35	30	1.77	1.78	1
Papineau Leblanc Bridge	23238.97	15.93	16.2	27	17.52	17.76	24	1.59	1.56	-3
just before dam	21566.02	15.19	15.35	16	17.47	17.7	23	2.28	2.35	7
just after dam	21168.85	15.14	15.29	15	17.34	17.66	32	2.2	2.37	17
Pie 9 Bridge	20028.22	13.25	13.75	50	16.49	16.9	41	3.24	3.15	-9
A25 bridge	15419.11	10.62	11.06	44	11.01	11.24	23	0.39	0.18	-21
Just before Pierre Island	11411.24	10.3	10.8	50	9.32	9.65	33	-0.98	-1.15	-17
just before Mignerion Island	5614.082	9.83	10.49	66	9.15	9.4	25	-0.68	-1.09	-41
CDG Bridge	4013.24	9.82	10.47	65	8.84	9.08	24	-0.98	-1.39	-41
Legardeur bridge	1449.05	9.64	10.35	71	7.32	7.37	5	-2.32	-2.98	-66

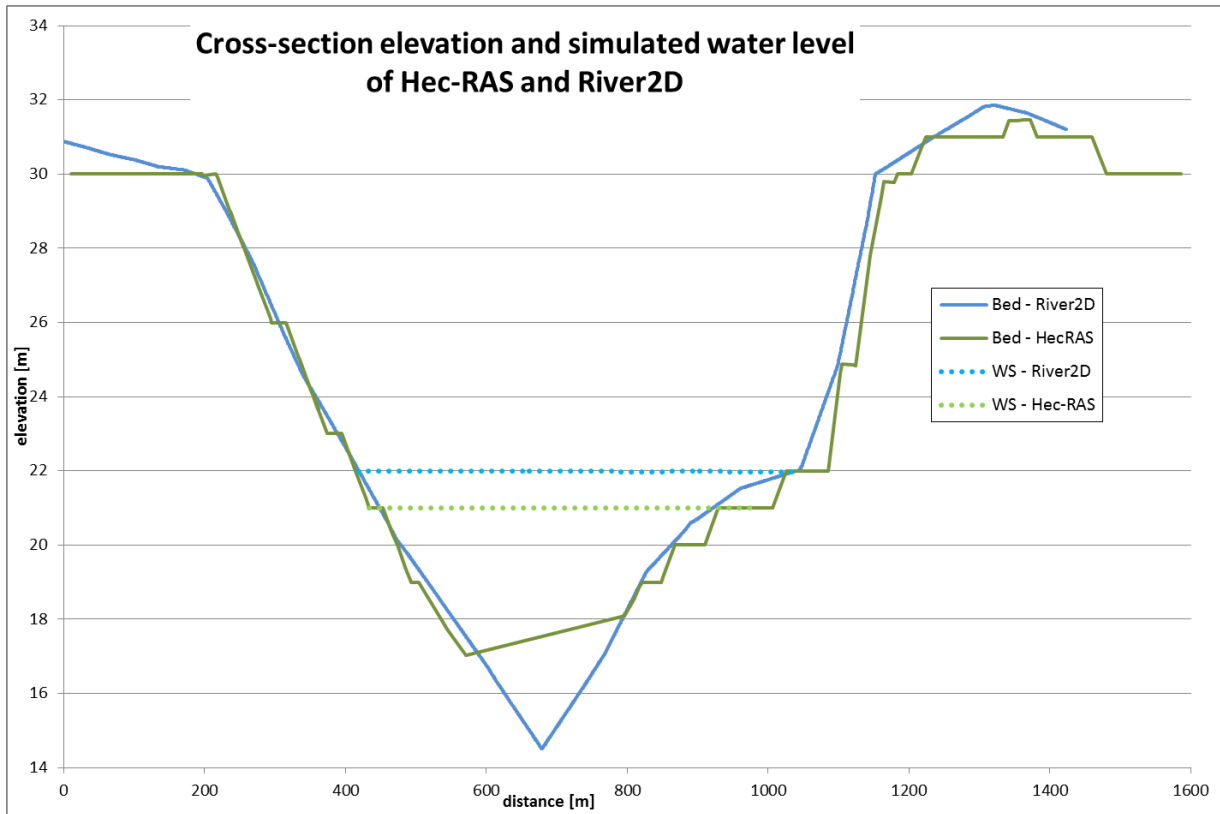


Figure 43: Comparison of cross-section's elevation and simulated water level between Hec-RAS and River2D at the beginning of the middle reach (section 40678.27).

The velocities of Hec-RAS and River2D could not be superimposed and ArcGIS, because it was not possible to export the results of River2D. However, looking at the results in their corresponding chapter, it can be observed that the global pattern were the same: high velocity in the main channel and especially in places where there is a contraction of the river, and nearly null value in the floodplains. Moreover, the maximum velocity is reached at the same place, with a similar value: 3.15 m/s for Hec-RAS and 3.8 m/s for River2D.

### 5.1.2. Results Uncertainties

As it has been said all along this report, there are a lot of uncertainties involved in the building of the hydrographs used by the Hec-RAS and River2d, mainly from climate models and determination of future rainfall data, and of course increased in Hec-HMS. However, the current level of knowledge on the subject does not permit to evaluate them with significant accuracy, and one could wonder what would happen if the flow is higher than what was simulated in Hec-HMS.

Therefore, in order to have a quick idea about the sensitivity of the results to uncertainties in flow hydrographs, a simulation has been done in Hec-RAS by increasing the previous hydrographs of 10 then 20%. The results are presented in Table 20. To be more precise, a proper sensitivity analysis should have been done, with simulations in both Hec-RAS and River2D, and with several different hydrographs. However, it was not possible within the frame time of this project.

Table 20: Maximum water surface elevation simulated by Hec-RAS with increased hydrographs of 10 and 20%

section's location	Max WS elevation with different hydrographs			Difference with initial hydrographs [cm]	
	init	+10%	+20%	+10%	+20%
Beginning of upper reach	22.87	23.09	23.31	22	44
Bizard Bridge	22.11	22.37	22.58	26	47
just before Bigras Island	21.37	21.56	21.74	19	37
Bigras railway Bridge	21.32	21.56	21.7	24	38
beginiing of middle reach	21	21.19	21.38	19	38
Bisson bridge	19.74	19.99	20.24	25	50
Lachepelle bridge	19.5	19.71	19.94	21	44
Mederic Martin A15 Bridge	19.28	19.49	19.7	21	42
Perry Island Railway Bridge	17.88	17.93	18.07	5	19
Ahunstic Viau Bridge	17.11	17.33	17.45	22	34
Papineau Leblanc Bridge	16.8	16.86	16.92	6	12
just before dam	16.5	16.5	16.5	0	0
just after dam	15.32	15.43	15.54	11	22
Pie 9 Bridge	13.87	13.92	14.01	5	14
A25 bridge	10.82	11.04	11.31	22	49
Just before Pierre Island	10.44	10.69	11	25	56
just before Mignerons Island	9.89	10.23	10.64	34	75
CDG Bridge	9.85	10.22	10.63	37	78
Legardeur bridge	9.57	10	10.47	43	90

It can be noticed that the more the hydrographs are increased the highest is the maximum water level simulated by Hec-RAS, as expected. Except at the station just before the bank where the water level is imposed by an internal boundary condition. And those results show that if the hydrograph found with Hec-HMS are underestimated of 10% or 20%, then an average additional increase of respectively 20cm or 40cm is expected – except in the zone just before the dam – which could cause an increase of the flooding zone and of the water depth in it.

### 5.1.3. Conclusion on 1D and 2D models

As it has been seen in the previous paragraph, the global trend of the results of the 1D and 2D simulations are similar – which is reassuring – however some differences have been noted, even large ones speaking about water surface elevations. And one could wonder which results are the most reliable, and when to use 1D or 2D models.

First of all, as it has been said all along the comments of the results, the latter are strongly influenced by the quality of the topographic and bathymetric data input in the models, especially in the two-dimensional simulation. That is why there is no use of a 2D model in case no precise terrain data is available. Indeed, the results would be of poor precision – probably worse than with a 1D model where the sections have been chosen carefully – and there is only the risk to be misled by attractive and colorful but wrong results.

And as it has been shown, the results of a 1D model can be displayed on a map with GIS add-on, in a similar way to the 2D results. However, one should never forget that as nice as the results seem, they are only an interpolation of 1D results, and do not substitute full two-dimensional calculations. Besides, if it gives a nice way to visualize the results, it can also be the source of many errors during the interpolation process if there was not enough cross-sections defined and so they were too far from each other.

Another important limitation of the 1D models is that they suppose the water level constant on a cross-sections. If this assumption fits well the simple cross-sections, it may be a source of problems in case of more complicated geometry, where the river is divided around an island or when natural dikes are present on the banks for example. In this project for example, Hec-RAS could not simulate correctly the water at the level of the Visitation Island, since in the reality the elevation on the right side is lower than in the left side, but Hec-RAS automatically calculated a horizontal level for the entire section.

However, a 1D model is relatively easy to calibrate, and very rapid to make simulations. Therefore it is possible to run many simulations, to test different configurations – for example to see the impact of possible adaptive measures.

On the contrary, to simulate an entire river as it has been done with the Des-Prairies River requires a very long time of calculation with the 2D model, which does not allow making as much simulations or calibration steps as wanted. And in order to speed up the simulation, it is often necessary to increase the tolerance of the calculations – as it has been done in this project – which of course reduces the precision of the results.

However, if properly calibrated and with sufficient data, the two-dimensional models undoubtedly give more detailed results about the extent of the floodplain, the water depth in it and the velocity distribution.

Therefore, for such problem where one want to simulate an entire river system to delimitate flooding zones and endangered structures, it could be interesting to use both 1D and 2D software, but not at the same level. Indeed, the 1D model could be used to make a first simulation on the entire river, to get a quick and easy rough estimation of the response of the system, and to localize critical zones that may be flooded. Then, the 2D software could be run only in those restricted zones, to have refined results concerning the precise delimitation of the flooded zone and the water depth and velocity repartition.

Moreover, the 1D software also furnish detailed results about the behavior of the hydraulic structures – like culverts, dam, gate openings, etc. – which could not be done with River 2D. Of course, some other 2D simulation software can take into consideration those structures, like Telemac2D. It would have been interested to run a simulation with this software for this project, but it was not possible within the frame time.

Finally, in some cases it can be important to run a 2D model, even a rough simulation, when the 1D simulation indicates that the flow pass in supercritical regime – or is likely to. Indeed, a comparison with a 2D model in this situation will show if the transverse component is negligible or if it plays an important role.

Table 21 recapitulates those recommendations of utilization.

Table 21: Fitting of 1D and 2D models to different criteria of simulation

Criteria	1D model	2D model
Terrain data required	Good	Very precise
Geometry	Simple	Complex (islands, dikes)
Time available	Very quick calibration and simulations	Very long calibration and simulations
Extent of the study	Entire River System	Precise local study
Expected flow regime	Sub-critical	Sub- and super- critical
Hydraulic structures (bridges, culverts, dam)	Complete representation	Depends on the model chosen. With River2D: no representation
Type of result	Constant Water level and 3 points of velocity at each cross section	Water level and velocity at each point of the mesh (better for floodplain analysis)

## 5.2. Impacts of climate change on the Des-Prairies River

### 5.2.1. Expected consequences on the Des-Prairies River

#### 5.2.1.1. Bridges

There are two types of damages that a bridge can suffer during a flood event: direct damages due to the force of the water – bridges submerged or swept away, embankment eroded leading to failure, etc. – and indirect damages due to the impacts of large debris floating in the river in case of reduced clearance.

For this study, the water velocity is not expected to be too large – maximum of 3.8 m/s – and the predicted rising of the water level in the Des-Prairies River is not so high that the Bridges will be flooded, i.e. that the water would reach the lower part of the deck. Therefore it is not expected to have any bridge taken by the flow or submerged. Moreover, the clearance is expected to be always larger than 3 meters, which is enough to allow debris – even large ones like trees' branches or cars – to pass under the bridge without damaging it.

However, in some sections the water level reaches the embankment of the bridge, and therefore may erode it – and eventually cause the destruction of the road in extreme cases. This is the case for the Bizard Island and Lachapelle Bridges on both sides, for the Bisson Bridge on Laval side, for the Charles-de-Gaulle and Legardeur Bridges on Repentigny side, and for the Perry and Ahunistic-Viau Bridges on Montreal side.

And finally, a large flow rate always causes an increasing of the scouring of the river bed around the bridges piers. And even if it does not cause perceptible damage during the event – except for an event so large that it would directly cause the failure of the pier, but it is not expected in this case – it contributes to the fragility of the pier. And after a certain number of such events, this phenomenon could cause the failure of its foundations.

### **5.2.1.2. Floodplain**

According to the results of the simulations, some areas are expected to be flooded. The land use file used previously as well as aerial photography of the concerned zones have been used to determine the kind of damages that could be expected. Indeed, green areas and agricultural zones present less exposure to flood than residential areas, where people, goods and buildings can be damaged.

The main problematic zone is located on the upper reach of the Des-Prairies River, where flood is expected on both sides on a distance varying from 60 to 300 meters, from the beginning of the Des-Prairies River until the Bizard Island Bridge, and then only on Montreal side for yet one kilometer. At the beginning, this area is mainly characterized by forest, herbaceous zones and cultures, corresponding to the Natural Park of Cap-Saint-Jacques on Montreal side and of the end of the Bizard Island on the other side. Those are therefore not areas of high exposure. However, a little bit before the Bizard Island Bridge the land use changes to residential area, with individuals separate houses, therefore with higher exposure. The simulated water depth at those places is around 3 meters just outside of the river bed, and decreases going away from the river, reaching around 1 meter at 100 meters of the river.

The second flooded zone was at the start of the middle reach, on both sides, on a smaller distance of 25 to 200 meters, with a water depth smaller than one meter. Just at the beginning of this zone, there is also a park on Montreal side, but then once again it turns to residential areas, like in the opposite side.

Then, a flood was also predicted in the area near the Bisson Bridge on Laval side, but this is a green area. However the residential Tremblay Island just after may be flooded too – the results of Hec-RAS and River2D diverge on this point – with around 60 cm of water.

Finally, taking the results of River 2D, a flood is anticipated in Repentigny side, just after the junction with the Mille-Ile River, in an agricultural zone, with 2 meters of water depth. The results of Hec-RAS seemed not reliable in this zone and have therefore not been considered.

## **5.2.2. Adaptive measures**

There are two kinds of measures that can be undertaken in order to reduce the expected damages of a flood event: the protective measures, which try to reduce the adverse consequences in case of a flood event by diminishing its magnitude, and the preventive measures, which aim to reduce the probability of a flood event to happen in a given area.

### **5.2.2.1. Protective measures**

In order to reduce the damages in case of a flood event, some structural measures can be done. First of all, regular verification of the solidity of the bridges embankment is recommended, with consolidation if needed. In that way, they should resist better during a flood event. Then, some dikes could be built where the floodplain is threatened to be flooded, planned to force the water into the main channel, or to flood a green area instead of an urbanized one. In some river systems, deviation of the flow can be considered. However, in such an urban context, this is not possible.



As far as the non-structural measures are concerned, the revision of the urbanization plan could be considered. This is obviously a long term measure, and often the areas concerned are already being used, as it is the case in this project. However it is interesting to start thinking about it and planning a more adapted urbanization plan, so that when construction and rehabilitation work will be considered, they can be done in a way that reduce the risk rather than the contrary.

Finally, the development of an emergency plan is always an important measure, even if there should not be any life in danger in the scenario simulated or any important damages. Indeed, preparedness is a key to risk mitigation, and the development of an emergency plan often permit to gather ideas and experiments from many people, and thus to raise crucial issues that could have been forgotten otherwise, and even to find other preventive or protective measures to implement. Moreover, if done seriously, it is an efficient way to make sure that all the actor that could be implicated in such an event are aware of the risks in question and of the actions they have to do, from the population to the public authorities passing through the rescue services, the lifeline companies, etc.

#### **5.2.2.2. Preventive measures**

To prevent a flood to happen, a way is to increase the conveyance of the river, by cleaning regularly the river bed, in order to avoid the accumulation of sediments. In a similar way, cleaning the parks near the river also prevent branches to go into the river, thus blocking the bridges.

Moreover, the regulation of the flow by the existing dams is of course very helpful. In the case of study, the Carillon and the Des-Prairies hydropower installations can be used. However, they are run-on-river stations, and therefore can have less impact on the flow than reservoir dams. Besides, care should be taken in such regulations not to cause flood upstream of the dam by trying to avoid it downstream.

In certain situation this solution can be hard to implement, if the company owning the installations is more interested by regulating it to maximize their profit rather than to avoid inundations. However in Quebec the law at this subject is well developed in favor of inundation prevention.

Finally, more rain and flow gauges could help to understand better the phenomenon and to make more precise prediction. Besides, real time gauges allow to have better idea of what is happening and to be able to make real time forecasting.

Currently, there are three flow gauges in the Mille-Ile River, two in the Du-Nord River, one in the Doncaster River and eight level gauges distributed in the Du-Nord Basin. However, there is only one real-time flow gauge in the Des-Prairies River, at the Cheval Blanc Rapids, which seems few.

# Conclusion and recommendations

---

## **Conclusion**

Several models to predict future climate and to downscale than at the desired precision were presented in this report, with their respective strengths and weaknesses. For the project – because of the high uncertainties of the results of those models, the lack of data to use them and the limited time available – those models have not been directly used. Instead, an expected percentage of increase of the precipitations' intensity in Southern Quebec for 2041-2070 – obtained by the CRCM model with SRES-A2 scenario – was taken from Mailhot et al. (2007). This percentage was then applied to the hyetograph of a 24h rainfall event with a return period of 50 years built with Chicago method from IDF curves available in the Du Nord Basin, to obtain future precipitation data.

Different methods to make the rainfall-runoff transformation were then exposed. In this project the Hec-HMS software was used, with its extension in ArcGIS to calculate the basin's characteristics. Among the different models available in Hec-HMS, the deficit and constant method was chosen for the loss evaluation, the Clark Unit Hydrograph was used for the rainfall-runoff transformation, constant monthly average values were entered as base flows, and the lag time method was taken for the routing calculations. The evapotranspiration were estimated with the Thornthwaite formula, and the snowmelt model was based on the temperature index method. After the calibration and validation of the model with past data over several years, the future hydrograph at the outlet of the Du-Nord Basin was obtained.

After that, several utilities for hydrodynamic simulation were compared. It was decided to use both 1D and 2D models, to be able to make conclusion on their use and to compare the results. Hec-RAS – with its extension in ArcGIS for the terrain processing and the determination of the geometry of the river and the display of the results – and River2D were chosen, and theoretical background was given. The models were calibrated with known water levels and flows, and simulations were done in the Des-Prairies River. The results showed that flood is expected in some areas, some of them parks or agricultural zones, but others residential ones, with high exposure. Besides, the bridges are not expected to get submerged or swept away, however erosion of the embankment or of the river bed near the piers is always possible. Some ideas about adaptive measures – preventive or protective, structural or not – were then given. The comparison between 1D and 2D results showed a similar trend, with however constant tendency of River2D to predict higher water level than Hec-RAS. As far as the use of 1D or 2D model is concerned, it was seen that the choice should be based on the terrain data available, the complexity and the extent of the area to study, the expected flow regime, the presence of hydraulic structure and the type of results wanted.

## **Recommendations**

This report gives an overview of the different methods to assess the impact on the Des-Prairies River of a heavy rainfall event aggravated by climate change, from the determination of future precipitation data to the hydrodynamic simulations, passing by the rainfall-runoff transformation, with a critical view on the models available at each step and on the results. Through the realization of this process, several crucial points and weaknesses have been noticed, and therefore some recommendations can be made if one wanted to go on more in depth into this subject to give more precise results or to assess better the uncertainties.

First of all, it was seen that the uncertainties related to this kind of study are very high, and that a large part comes directly from the climate models. There are indeed a lot of different models, based on different hypothesis and equations, with different calibration and validation procedures, and that can use different climate change scenarios. That is why the results of those models are very variable. It could therefore be interesting to use several of them to build the future precipitation data – with different downscaling techniques to obtain the value at the exact desired scale –, and to present the result not as a fixed value but as a range of possible values, in the same principle of a confidence interval.

Then, in the rainfall-runoff transformation only one method for each step was tested. It would be worthy to try more methods and to compare the results, in order to have a better idea of the uncertainties related and maybe to improve the quality of the results by getting a better convergence during the calibration process. However, some of the models require additional input data that were not available, so field studies to determinate them would be necessary.

Finally, it would be constructive to redo the hydrodynamic study with better bathymetric data. River2D would give more precise results, and it would be possible to extract more cross-sections for Hec-RAS, therefore obtaining better results too, and a better representation of the results in ArcGIS. It could also improve the calibration of the models, which was not perfect in this project. Moreover another 2D software taking charge of the hydraulic structures could be tested – like Telemac– in order to compare the results, and maybe gain in precision.

Climate change is a reality. It is important to accept it and to study its possible consequences, in order to get ready to face its impacts. This is the aim of such projects, even with limited resources, and they should be more numerous and developed further.

# Bibliography

---

**Abrinord, 2008:** *Portrait et diagnostic du bassin versant de la rivière du Nord*, 294p., downloaded from the Abrinord website in May 2012. <http://www.abrinord.qc.ca/index.html>

**Anctil et al, 2005 :** F.Anctil, J. Rousselle, N. Lauzon, *Hydrologie: cheminements de l'eau*, Presses Internationales Polytechniques, 317p.

**Bertrand-Krajewski, 2006a:** *La Pluie*, Notes of Hydrologie Urbaine, 2006, INSA de Lyon, France. Downloaded on May 2012 : <http://jlbkpro.free.fr/teachingmaterial/>

**Bertrand-Krajewski, 2006b:** *Les Pertes avant ruissellement*, Notes of Hydrologie Urbaine, INSA de Lyon, France. Downloaded on May 2012: <http://jlbkpro.free.fr/teachingmaterial/>

**CCCma, 2012:** website of Environment Canada, pages dedicated to the Canadian Centre for Climate Modeling and Analysis, consulted on April 2012.  
<http://www.ec.gc.ca/ccmac-cccma/default.asp?lang=En&n=4596B3A2-1>

**CCIS, 2012:** website of the Canadian Climate Impacts Scenario, consulted on April 2012.  
<http://www.cics.uvic.ca/scenarios/index.cgi>.

**CEHQ, 2005:** JF. Cyrin and M. Fontin –, *Rivière des Mille-Iles – Etude des solutions de soutien des étiages critiques*, 253p, downloaded on May 2012 on the CEHQ website:  
<http://www.cehq.gouv.qc.ca/debit-etiage/mille-iles/index.htm>

**CEHQ, 2006 :** S.Dubé, W. Larouche, JF. Cyr – Centre d'Expertise Hydrique du Québec – Direction de l'expertise et de la gestion des barrages publics, *Rivière des Prairies – Villes de Charlemagne, de Laval, de Montréal, de Repentigny et de Terrebonne – Révision des cotes de crues*, 98p.

**CEHQ, 2012a:** website of the CEHQ, page of the real-time hydrology data of the stations of the Ottawa and Montreal Basins, consulted on June 2012.  
<http://www.cehq.gouv.qc.ca/suivihydro/ListeStation.asp?regionhydro=04&Tri=Non>

**CEHQ, 2012b:** website of the CEHQ, page of the level and flow history of the stations of the Ottawa and Montreal Basins, consulted on June 2012.  
[http://www.cehq.gouv.qc.ca/hydrometrie/historique\\_donnees/ListeStation.asp?regionhydro=04&Tri=Non](http://www.cehq.gouv.qc.ca/hydrometrie/historique_donnees/ListeStation.asp?regionhydro=04&Tri=Non)

**Cobamil, 2011:** the Conseil des Bassins Versants des Mille-Iles, *Plan directeur de l'eau – portrait préliminaire de la zone de gestion intégrée des ressources en eau des Mille-Iles*, 104p., Downloaded from the website of the COBAMIL in May 2012:<http://www.cobamil.ca/>.

**Daynou&M. Fuamba, 2008:** *Determination of Overflow Risk for Stormwater Systems*, Reliable Modeling of Urban Water Systems – Monograph 16 (pp. 19-34), 485p., Computational Hydraulics International (CHI), Toronto, Canada.

**DHI, 2006:** Mike 21 & Mike 3 Flow Model FM – *Hydrodynamic Module – Short Description*, 36p.

**DHI, 2012:** website of the MIKE software by DHI consulting and research organization, consulted on May 2012. <http://www.dhisoftware.com/Products/WaterResources.aspx>

**EC, 2004:** E. Barrow, B. Maxwell, P. Gachon (Eds), *Climate Variability and change in Canada – Past, Present and Future*, ACS D Science Assessment Series No. 2, Meteorological Service of Canada, Environment Canada, Toronto, 114p.

**EC, 2012:** IDF curves downloaded from Environment Canada website in May 2012. [http://climate.weatheroffice.gc.ca/prods\\_servs/index\\_e.html](http://climate.weatheroffice.gc.ca/prods_servs/index_e.html)

**Gachon P., 2005:** *A first Evaluation of the strength and weakness of statistical downscaling methods for simulating extremes over various regions of eastern Canada*, Climate Change Action Fund, Environment Canada, Final Report, Montreal.

**GeoBase, 2012:** website of GeoBase, consulted on May 2012. <http://www.geobase.ca/geobase/en/data/index.html;jsessionid=8D96EB2EFEC259F841821BB10211E9D5>

**Haestad Methods et al, 2003:** Haestad Methods, G. Dyhouse, J. Hatchett, J. Benn, *Floodplain Modeling using Hec-RAS – First Edition*, Haestad Press, 695p.

**Hingray et al, 2009:** B. Hingray, C. Picouet, A. Musy, *Hydrologie – 2: Une science pour l'ingénieur*, Presses Polytechniques et universitaires romandes, 619p.

**Horritt M.S.& Bates P.D., 2002:** *Evaluation of 1D and 2D numerical models for predicting flood inundation*, Journal of Hydrology (268, 87-99)

**Hwang N. & Houghtalen R., 1996:** *Fundamentals of Hydraulic Engineering Systems – Third edition*, Prentice Hall.

**IPPC, 2001:** *Climate change 2001: the scientific basis - Contribution of Working Group I to the third assessment report of the Intergovernmental Panel on Climate Change*, Cambridge University Press, 881p.

**IPPC, 2007:** *Climate change 2007: the scientific basis - Contribution of Working Group I to the fourth assessment report of the Intergovernmental Panel on Climate Change*, Cambridge University Press, 966p.

**Mailhot et al, 2007:** A. Mailhot, S. Duchesne, D. Caya, G. Talbot, *Assessment of future change in intensity-duration-frequency (IDF) curves for Southern Quebec using the Canadian Regional Climate Model (CRCM)*, published in Journal of Hydrology, vol. 347, p.197-210.

**Marant L., 2009:** *Comparaison entre la modélisation de rivière unidimensionnelle (1D) et bidimensionnelle (2D) en vue d'une modélisation de la Basse Vallée de la Doller*, thesis for the obtention of the Diplôme d'Ingénieur, ENGEES, Strasbourg, France.

**MDDEP, 2011** : Ministère du Développement durable, de l'Environnement et des Parcs, *Guide de gestion des eaux pluviales – chap6: Evaluation quantitative du ruissellement – aspects hydrologiques*, downloaded on May 2012 at <http://www.mddep.gouv.qc.ca/eau/pluviales/guide.htm>

**Mearns et al, 2003**: L. O. Mearns, F. Giorgi, P. Whetton, D. Pabon, M. Hulme, M. Lal, *Guidelines for Use of Climate Scenarios Developed from Regional Model Experiments*, 38p., downloaded from the IPCC website in May 2012.

**MetOffice, 2012**: website of the UK Meteorological Office, page related on the Hadle Centre, consulted on April 2012. <http://www.metoffice.gov.uk/research/modelling-systems/unified-model/climate-models/hadcm3>.

**MPI, 2003**: Roeckner E. et al., Report No. 349, *the atmospheric general circulation model ECHAM5 – part I: model description*, 140p., downloaded from the Max-Planck-Institute for Meteorology on April 2012. <http://www.mpimet.mpg.de/en/science/models/echam.html>

**NRCS, 2012**: United State Department of Agriculture - Natural Resources Conservation Service (previously Soil Conservation Service)

**Osman Akan A., 1993**: *Urban Stormwater Hydrology – A guide to engineering calculations*, CRC Press.

**Ouranos, 2010**: C. DesJarlais, A. Blondlot, et al, *Savoir s'adapter aux changements climatiques*, 128p.

**Robitaille J., 1999**: *Regional Assessment – Lake of Two Mountains Sector – Priority Intervention Zone 24*, St. Lawrence Centre, 74p.

**Sanfilippo U. and Paoletti A., 2011**: *Rainfall modelling*, Notes of Hydrology for Flood Risk Evaluation, 2011, Politecnico di Milano.

**Steffler P., 2002a**: *R2D\_Bed – Bed Topography File Editor – User's Manual*, (September 2002, 32p.), downloaded on the River2D website on May 2012. <http://www.river2d.ualberta.ca/>

**Steffler P. et al., 2002b**: P. Steffler and T.Waddle, *R2D\_Mesh – Mesh Generation Program for River2D Two Dimensional Depth Averaged Finite Element – Introduction to Mesh Generation and User's Manual*, 32p., downloaded on the River2D website on May 2012. <http://www.river2d.ualberta.ca/>

**Steffler P. et al., 2002c**: P. Steffler and J. Blackburn, *River2D – Two Dimensional Depth Averaged Model of River Hydrodynamics and Fish Habitat – Introduction to Depth Averaged Modeling and User's Manual*, 120p., downloaded on the River2D website on May 2012. <http://www.river2d.ualberta.ca/>

**Telemac, 2010**: *TELEMAC modelling system – User Manual*, (version 6.0 – october 2010) downloaded from Telemac website on May 2012. <http://www.opentelemac.org/>

**Theberges N., 1996**: *Calibration de bassins versants urbains et conception d'un logiciel de drainage urbain*, Master thesis in Civil Engineering, University of Sherbrooke, Canada.

**USACE, 2000:** A. Feldman, *Hydrologic Modeling System Hec-HMS – Technical Reference Manual*, 146p., downloaded on the USACE software’s website on May 2012.

<http://www.hec.usace.army.mil/software/>

**USACE, 2010a:** W. Scharffenberg and M. Fleming, *Hydrologic Modeling System Hec-HMS – User’s Manual*, (version3.5 – August 2010, 316p.), downloaded on the USACE software’s website on May 2012. <http://www.hec.usace.army.mil/software/>

**USACE, 2010b:** J. Doan and M. Fleming, *HEC-GeoHMS – Geospatial Hydrologic Modeling Extension – User’s Manual*, (version5.0 – October 2010, 197p), downloaded on the USACE software’s website on May 2012. <http://www.hec.usace.army.mil/software/>

**USACE, 2010c:** G. Brunner, *HEC-RAS – River Analysis System– User’s Manual*, version 4.1, 766p., downloaded on the USACE software’s website on May 2012.

<http://www.hec.usace.army.mil/software/>

**USACE, 2010d:** G. Brunner, *HEC-RAS – River Analysis System– Hydraulic Reference Manual*, version 4.1, 411p, downloaded on the USACE software’s website on May 2012. <http://www.hec.usace.army.mil/software/>

**USACE, 2011:** C. Ackerman, *HEC-GeoRAS – GIS Tools for Support of Hec-RAS using ArcGIS – User’s Manual*, version 4.3.93, 241p., downloaded on the USACE software’s website on May 2012. <http://www.hec.usace.army.mil/software/>

**USGS, 2012:** website of the United States Geological Survey, page on the determination of the Manning coefficient for natural reaches, consulted on May 2012.

<http://wwwrcamnl.wr.usgs.gov/sws/fieldmethods/Indirects/nvalues/index.htm>

**VenTe Chow et al., 1988:** Ven Te Chow, D. Maidment, L. Mays, *Applied Hydrology*, Mc Graw-Hill International Editions, Civil Engineering Series, 573p.

**VICAIRE, 2012:** website of the VirtualCampus In hydrology and water REsources management, consulted on June 2012. [http://echo2.epfl.ch/VICAIRE/mod\\_1b/chapt\\_4/main.htm](http://echo2.epfl.ch/VICAIRE/mod_1b/chapt_4/main.htm)

**Wikipedia, 2012:** picture downloaded from the Wikipedia page of “Ottawa River”, consulted on May 2012. [http://en.wikipedia.org/wiki/Ottawa\\_River](http://en.wikipedia.org/wiki/Ottawa_River)

**Wilby et al., 2004:** RL Wilby, SP Charles, E Zorita, B Timbal, P Whetton, LO Mearns, *Guidelines for Use of Climate Scenarios Developed form Regional Model Experiments*, 27p., downloaded from the IPCC website in May 2012.



# Appendix

---

**Appendix 1:** Table of value and graphs of the IDF curves for the Ste-Agathe and St-Jerome meteorological stations (*EC, 2012*).

**Appendix 2:** Table of value and graphs of the current and future Chicago hyetographs and histograms for the Ste-Agathe and St-Jerome meteorological stations

**Appendix 3:** Parameters of the models for the rainfall-runoff transformation in Hec-HMS

**Appendix 4:** Parameters of the meteorological model of Hec-HMS.

**Appendix 5:** Table of value and graphs of the hydrographs at the exit of the Du-Nord Basin and at the entrance of the Des-Prairies River and of its tributaries

**Appendix 6:** Historical measured data at the CEHQ flow station of the Carillon Dam.

**Appendix 7:** Land-Use file used for the input of the roughness coefficient in ArcGIS

**Appendix 8:** Representation of the Des-Prairies River geometry in Hec-RAS

**Appendix 9:** Extract of the construction plans used to input the bridges' geometry in Hec-RAS.



Short Duration Rainfall Intensity-Duration-Frequency Data

2012/02/09

Données sur l'intensité, la durée et la fréquence des chutes de pluie de courte durée

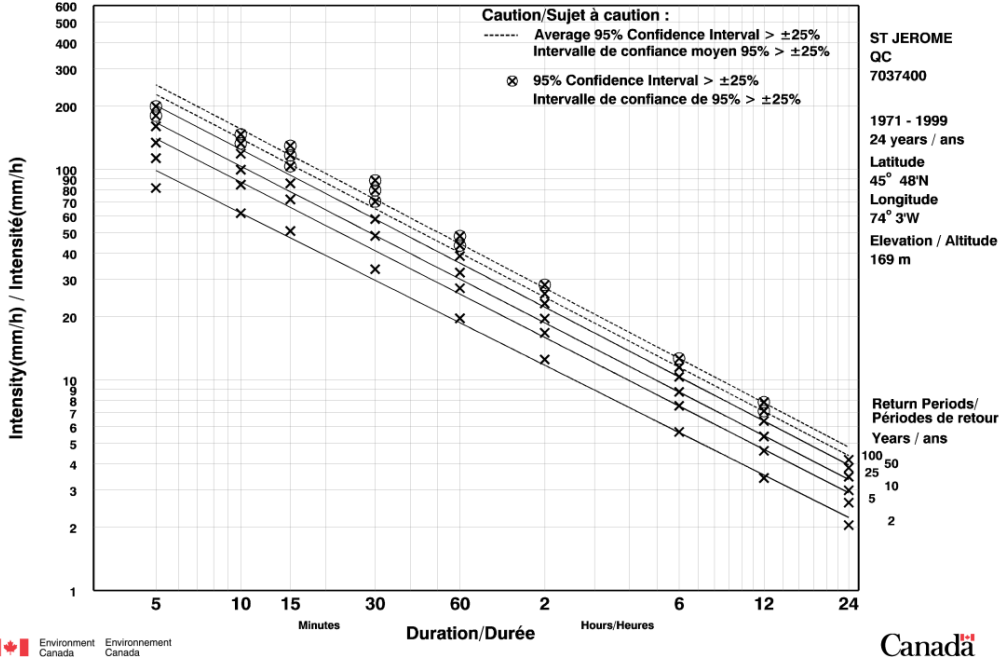


Table 2b :

Return Period Rainfall Rates (mm/h) - 95% Confidence limits  
 Intensité de la pluie (mm/h) par période de retour - Limites de confiance de 95%

\*\*\*\*\*

Duration/Durée	2	5	10	25	50	100	#Years
	yr/ans	yr/ans	yr/ans	yr/ans	yr/ans	yr/ans	Années
5 min	81.6	113.0	133.9	160.2	179.7	199.1	25
	+/- 12.8	+/- 21.6	+/- 29.1	+/- 39.3	+/- 47.0	+/- 54.8	25
10 min	61.9	84.6	99.6	118.6	132.7	146.7	25
	+/- 9.2	+/- 15.6	+/- 21.0	+/- 28.4	+/- 33.9	+/- 39.5	25
15 min	50.9	72.0	85.9	103.5	116.5	129.4	25
	+/- 8.6	+/- 14.4	+/- 19.5	+/- 26.2	+/- 31.4	+/- 36.6	25
30 min	33.6	48.3	58.0	70.3	79.5	88.5	25
	+/- 6.0	+/- 10.1	+/- 13.6	+/- 18.4	+/- 22.0	+/- 25.6	25
1 h	19.6	27.3	32.3	38.7	43.5	48.2	26
	+/- 3.1	+/- 5.1	+/- 7.0	+/- 9.4	+/- 11.2	+/- 13.1	26
2 h	12.5	16.7	19.5	23.1	25.7	28.3	26
	+/- 1.7	+/- 2.8	+/- 3.8	+/- 5.2	+/- 6.2	+/- 7.2	26
6 h	5.7	7.5	8.8	10.3	11.5	12.6	24
	+/- 0.8	+/- 1.3	+/- 1.8	+/- 2.4	+/- 2.8	+/- 3.3	24
12 h	3.4	4.6	5.4	6.4	7.1	7.8	24
	+/- 0.5	+/- 0.8	+/- 1.1	+/- 1.5	+/- 1.8	+/- 2.1	24
24 h	2.0	2.6	3.0	3.5	3.8	4.2	26
	+/- 0.2	+/- 0.4	+/- 0.5	+/- 0.7	+/- 0.8	+/- 1.0	26

\*\*\*\*\*

Table 3 : Interpolation Equation / Équation d'interpolation: R = A\*T^B

R = Interpolated Rainfall rate (mm/h)/Intensité interpolée de la pluie (mm/h)  
 RR = Rainfall rate (mm/h) / Intensité de la pluie (mm/h)  
 T = Rainfall duration (h) / durée de la pluie (h)

\*\*\*\*\*

Statistics/Statistiques	2	5	10	25	50	100
	yr/ans	yr/ans	yr/ans	yr/ans	yr/ans	yr/ans
Mean of RR/Moyenne de RR	30.1	41.8	49.6	59.4	66.7	73.9
Std. Dev. /Écart-type (RR)	28.8	40.0	47.4	56.8	63.8	70.7
Std. Error/Erreur-type	6.8	10.8	13.4	16.8	19.3	21.9
Coefficient (A)	18.7	25.6	30.1	35.9	40.1	44.3
Exponent/Exposant (B)	-0.670	-0.684	-0.689	-0.694	-0.697	-0.700
Mean % Error/% erreur moyenne	7.1	8.2	8.7	9.2	9.5	9.8

\*\*\*\*\*

**Appendix2:** Table of value and graphs of the current and future Chicago hyetographs and histograms for the Ste-Agathe and St-Jerome meteorological stations.

**Current Chicago hyetograph for Ste Agathe**

r =	0.488	
$\theta =$	24	h
tp =	11.712	h

T =	50	
a =	39.2	mm/h
b =	0	h
c =	0.686	

t [h]	i [mm/h]	P [mm]	P cumul [mm]
0	1.3912	0.0000	0.0000
0.25	1.4119	0.3504	0.3504
0.5	1.4335	0.3557	0.7061
0.75	1.4558	0.3612	1.0672
1	1.4790	0.3669	1.4341
1.25	1.5032	0.3728	1.8069
1.5	1.5283	0.3789	2.1858
1.75	1.5546	0.3854	2.5712
2	1.5819	0.3921	2.9632
2.25	1.6105	0.3990	3.3623
2.5	1.6403	0.4063	3.7686
2.75	1.6716	0.4140	4.1826
3	1.7043	0.4220	4.6046
3.25	1.7387	0.4304	5.0350
3.5	1.7748	0.4392	5.4742
3.75	1.8129	0.4485	5.9226
4	1.8530	0.4582	6.3809
4.25	1.8954	0.4685	6.8494
4.5	1.9402	0.4794	7.3289
4.75	1.9877	0.4910	7.8198
5	2.0382	0.5032	8.3231
5.25	2.0920	0.5163	8.8394
5.5	2.1494	0.5302	9.3695
5.75	2.2108	0.5450	9.9146
6	2.2767	0.5609	10.4755
6.25	2.3477	0.5781	11.0536
6.5	2.4244	0.5965	11.6501
6.75	2.5076	0.6165	12.2666
7	2.5981	0.6382	12.9048
7.25	2.6971	0.6619	13.5667
7.5	2.8059	0.6879	14.2546
7.75	2.9262	0.7165	14.9711
8	3.0600	0.7483	15.7193
8.25	3.2099	0.7837	16.5031
8.5	3.3793	0.8236	17.3267
8.75	3.5724	0.8690	18.1957
9	3.7952	0.9210	19.1166
9.25	4.0555	0.9813	20.0980
9.5	4.3646	1.0525	21.1505
9.75	4.7389	1.1379	22.2885
10	5.2034	1.2428	23.5312
10.25	5.7985	1.3752	24.9065
10.5	6.5946	1.5491	26.4556
10.75	7.7270	1.7902	28.2458
11	9.4988	2.1532	30.3991
11.25	12.7799	2.7848	33.1839
11.5	21.8075	4.3234	37.5073
11.75	73.2898	11.8872	49.3945
12	18.2655	11.4444	60.8389

t [h]	i [mm/h]	P [mm]	P cumul [mm]
12.25	11.8976	3.7704	64.6093
12.5	9.1571	2.6318	67.2411
12.75	7.5799	2.0921	69.3332
13	6.5369	1.7646	71.0978
13.25	5.7879	1.5406	72.6385
13.5	5.2198	1.3760	74.0144
13.75	4.7716	1.2489	75.2633
14	4.4075	1.1474	76.4107
14.25	4.1048	1.0640	77.4747
14.5	3.8486	0.9942	78.4689
14.75	3.6284	0.9346	79.4036
15	3.4368	0.8832	80.2867
15.25	3.2683	0.8381	81.1249
15.5	3.1188	0.7984	81.9232
15.75	2.9850	0.7630	82.6862
16	2.8645	0.7312	83.4174
16.25	2.7553	0.7025	84.1199
16.5	2.6558	0.6764	84.7963
16.75	2.5646	0.6525	85.4488
17	2.4808	0.6307	86.0795
17.25	2.4034	0.6105	86.6900
17.5	2.3317	0.5919	87.2819
17.75	2.2651	0.5746	87.8565
18	2.2029	0.5585	88.4150
18.25	2.1448	0.5435	88.9585
18.5	2.0903	0.5294	89.4879
18.75	2.0390	0.5162	90.0040
19	1.9908	0.5037	90.5078
19.25	1.9453	0.4920	90.9998
19.5	1.9022	0.4809	91.4807
19.75	1.8614	0.4705	91.9511
20	1.8227	0.4605	92.4117
20.25	1.7859	0.4511	92.8627
20.5	1.7509	0.4421	93.3048
20.75	1.7175	0.4336	93.7384
21	1.6857	0.4254	94.1638
21.25	1.6553	0.4176	94.5814
21.5	1.6261	0.4102	94.9916
21.75	1.5983	0.4030	95.3947
22	1.5715	0.3962	95.7909
22.25	1.5458	0.3897	96.1805
22.5	1.5212	0.3834	96.5639
22.75	1.4974	0.3773	96.9412
23	1.4746	0.3715	97.3128
23.25	1.4526	0.3659	97.6787
23.5	1.4314	0.3605	98.0392
23.75	1.4110	0.3553	98.3945
24	1.3912	0.3503	98.7447

## Futur Chicago hyetograph for Ste Agathe

Percentage of augmentation (Mailhot et al, 2007)

T [years]	duration [h]			
	2	6	12	24
2	20.6	13.9	11	11
5	18.1	14.5	10	8.8
10	15.8	13.1	8.2	6.9
25	13	10.1	5.1	3.9
50	11.2	7.3	2.5	1.5

percentage applied:  
1.5 %

t [h]	i [mm/h]	P [mm]	P cumul [mm]
0	1.4121	0.0000	0.0000
0.25	1.4331	0.3557	0.3557
0.5	1.4550	0.3610	0.7167
0.75	1.4777	0.3666	1.0832
1	1.5012	0.3724	1.4556
1.25	1.5257	0.3784	1.8340
1.5	1.5513	0.3846	2.2186
1.75	1.5779	0.3911	2.6097
2	1.6056	0.3979	3.0077
2.25	1.6346	0.4050	3.4127
2.5	1.6649	0.4124	3.8251
2.75	1.6966	0.4202	4.2453
3	1.7299	0.4283	4.6737
3.25	1.7648	0.4368	5.1105
3.5	1.8015	0.4458	5.5563
3.75	1.8401	0.4552	6.0115
4	1.8808	0.4651	6.4766
4.25	1.9238	0.4756	6.9521
4.5	1.9693	0.4866	7.4388
4.75	2.0175	0.4984	7.9371
5	2.0688	0.5108	8.4479
5.25	2.1234	0.5240	8.9720
5.5	2.1816	0.5381	9.5101
5.75	2.2440	0.5532	10.0633
6	2.3109	0.5694	10.6326
6.25	2.3829	0.5867	11.2194
6.5	2.4608	0.6055	11.8248
6.75	2.5452	0.6257	12.4506
7	2.6371	0.6478	13.0984
7.25	2.7375	0.6718	13.7702
7.5	2.8480	0.6982	14.4684
7.75	2.9701	0.7273	15.1956
8	3.1059	0.7595	15.9551
8.25	3.2581	0.7955	16.7506
8.5	3.4300	0.8360	17.5866
8.75	3.6260	0.8820	18.4686
9	3.8521	0.9348	19.4034
9.25	4.1164	0.9961	20.3995
9.5	4.4301	1.0683	21.4678
9.75	4.8100	1.1550	22.6228
10	5.2815	1.2614	23.8842
10.25	5.8855	1.3959	25.2801
10.5	6.6935	1.5724	26.8525
10.75	7.8430	1.8171	28.6695
11	9.6413	2.1855	30.8551
11.25	12.9716	2.8266	33.6817
11.5	22.1346	4.3883	38.0699
11.75	74.3891	12.0655	50.1354
12	18.5395	11.6161	61.7515

t [h]	i [mm/h]	P [mm]	P cumul [mm]
12.25	12.0760	3.8269	65.5784
12.5	9.2945	2.6713	68.2497
12.75	7.6936	2.1235	70.3732
13	6.6350	1.7911	72.1643
13.25	5.8747	1.5637	73.7280
13.5	5.2981	1.3966	75.1246
13.75	4.8431	1.2676	76.3923
14	4.4736	1.1646	77.5569
14.25	4.1664	1.0800	78.6369
14.5	3.9063	1.0091	79.6460
14.75	3.6829	0.9487	80.5946
15	3.4884	0.8964	81.4910
15.25	3.3174	0.8507	82.3417
15.5	3.1656	0.8104	83.1521
15.75	3.0298	0.7744	83.9265
16	2.9075	0.7422	84.6687
16.25	2.7966	0.7130	85.3817
16.5	2.6956	0.6865	86.0682
16.75	2.6031	0.6623	86.7305
17	2.5180	0.6401	87.3707
17.25	2.4395	0.6197	87.9904
17.5	2.3667	0.6008	88.5912
17.75	2.2990	0.5832	89.1744
18	2.2359	0.5669	89.7413
18.25	2.1769	0.5516	90.2929
18.5	2.1216	0.5373	90.8302
18.75	2.0696	0.5239	91.3541
19	2.0207	0.5113	91.8654
19.25	1.9744	0.4994	92.3648
19.5	1.9307	0.4881	92.8529
19.75	1.8893	0.4775	93.3304
20	1.8501	0.4674	93.7978
20.25	1.8127	0.4578	94.2557
20.5	1.7772	0.4487	94.7044
20.75	1.7433	0.4401	95.1445
21	1.7110	0.4318	95.5763
21.25	1.6801	0.4239	96.0002
21.5	1.6505	0.4163	96.4165
21.75	1.6222	0.4091	96.8256
22	1.5951	0.4022	97.2277
22.25	1.5690	0.3955	97.6233
22.5	1.5440	0.3891	98.0124
22.75	1.5199	0.3830	98.3954
23	1.4967	0.3771	98.7724
23.25	1.4744	0.3714	99.1438
23.5	1.4529	0.3659	99.5098
23.75	1.4321	0.3606	99.8704
24	1.4121	0.3555	100.2259



## Current Chicago hyetograph for St-Jerome

r =	0.488
$\theta$ =	24 h
tp =	11.712 h

T =	50	years
a =	40.1	mm/h
b =	0	h
c =	0.687	

t [h]	i [mm/h]	P [mm]	P cumul [mm]
0	1.4141	0.0000	0.0000
0.25	1.4352	0.3562	0.3562
0.5	1.4571	0.3615	0.7177
0.75	1.4799	0.3671	1.0848
1	1.5035	0.3729	1.4578
1.25	1.5281	0.3790	1.8367
1.5	1.5537	0.3852	2.2220
1.75	1.5804	0.3918	2.6137
2	1.6082	0.3986	3.0123
2.25	1.6373	0.4057	3.4180
2.5	1.6677	0.4131	3.8311
2.75	1.6995	0.4209	4.2520
3	1.7329	0.4291	4.6811
3.25	1.7679	0.4376	5.1187
3.5	1.8047	0.4466	5.5653
3.75	1.8434	0.4560	6.0213
4	1.8843	0.4660	6.4873
4.25	1.9274	0.4765	6.9637
4.5	1.9731	0.4876	7.4513
4.75	2.0215	0.4993	7.9506
5	2.0729	0.5118	8.4624
5.25	2.1277	0.5251	8.9875
5.5	2.1862	0.5392	9.5267
5.75	2.2487	0.5544	10.0811
6	2.3159	0.5706	10.6517
6.25	2.3882	0.5880	11.2397
6.5	2.4663	0.6068	11.8465
6.75	2.5510	0.6272	12.4737
7	2.6433	0.6493	13.1230
7.25	2.7441	0.6734	13.7964
7.5	2.8550	0.6999	14.4963
7.75	2.9776	0.7291	15.2254
8	3.1140	0.7614	15.9868
8.25	3.2667	0.7976	16.7844
8.5	3.4394	0.8383	17.6227
8.75	3.6363	0.8845	18.5071
9	3.8633	0.9374	19.4446
9.25	4.1287	0.9990	20.4436
9.5	4.4439	1.0716	21.5152
9.75	4.8256	1.1587	22.6738
10	5.2993	1.2656	23.9394
10.25	5.9063	1.4007	25.3401
10.5	6.7184	1.5781	26.9182
10.75	7.8739	1.8240	28.7423
11	9.6823	2.1945	30.9368
11.25	13.0324	2.8393	33.7761
11.5	22.2557	4.4110	38.1871
11.75	74.9283	12.1480	50.3351
12	18.6361	11.6955	62.0307

t [h]	i [mm/h]	P [mm]	P cumul [mm]
12.25	12.1314	3.8459	65.8766
12.5	9.3335	2.6831	68.5597
12.75	7.7238	2.1322	70.6919
13	6.6596	1.7979	72.4898
13.25	5.8955	1.5694	74.0592
13.5	5.3159	1.4014	75.4606
13.75	4.8589	1.2719	76.7325
14	4.4876	1.1683	77.9008
14.25	4.1790	1.0833	78.9841
14.5	3.9178	1.0121	79.9962
14.75	3.6933	0.9514	80.9476
15	3.4980	0.8989	81.8465
15.25	3.3263	0.8530	82.6995
15.5	3.1739	0.8125	83.5120
15.75	3.0375	0.7764	84.2885
16	2.9147	0.7440	85.0325
16.25	2.8034	0.7148	85.7473
16.5	2.7020	0.6882	86.4355
16.75	2.6092	0.6639	87.0994
17	2.5238	0.6416	87.7410
17.25	2.4450	0.6211	88.3621
17.5	2.3719	0.6021	88.9642
17.75	2.3040	0.5845	89.5487
18	2.2407	0.5681	90.1168
18.25	2.1815	0.5528	90.6695
18.5	2.1259	0.5384	91.2080
18.75	2.0738	0.5250	91.7329
19	2.0246	0.5123	92.2452
19.25	1.9783	0.5004	92.7456
19.5	1.9344	0.4891	93.2347
19.75	1.8929	0.4784	93.7131
20	1.8535	0.4683	94.1814
20.25	1.8160	0.4587	94.6401
20.5	1.7803	0.4495	95.0896
20.75	1.7464	0.4408	95.5304
21	1.7139	0.4325	95.9630
21.25	1.6829	0.4246	96.3876
21.5	1.6533	0.4170	96.8046
21.75	1.6249	0.4098	97.2144
22	1.5977	0.4028	97.6172
22.25	1.5715	0.3961	98.0134
22.5	1.5464	0.3897	98.4031
22.75	1.5223	0.3836	98.7867
23	1.4990	0.3777	99.1643
23.25	1.4766	0.3720	99.5363
23.5	1.4550	0.3665	99.9028
23.75	1.4342	0.3612	100.2639
24	1.4141	0.3560	100.6200

## Future Chicago hyetograph for St-Jerome

Percentage of augmentation (*Mailhot et al, 2007*)

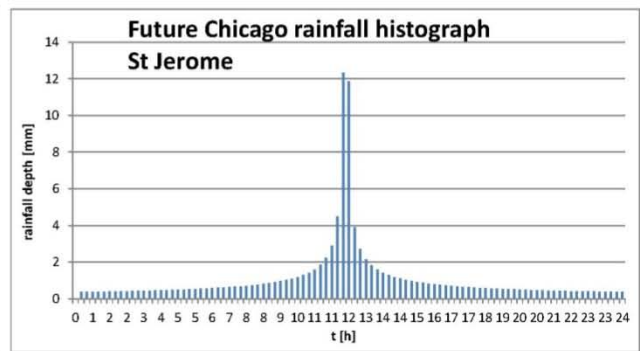
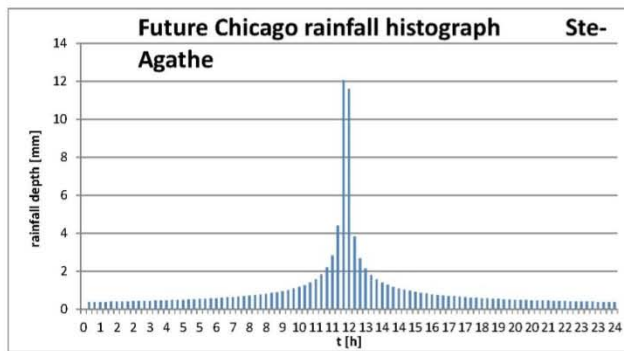
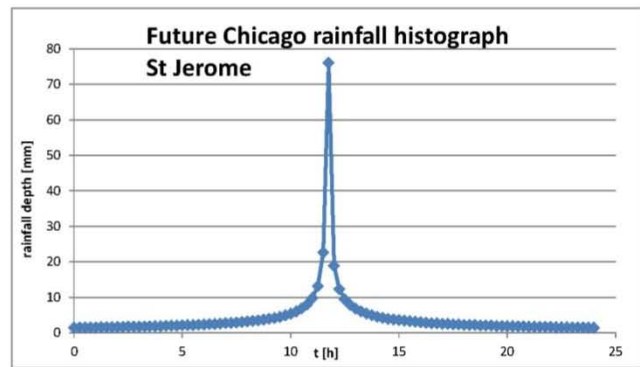
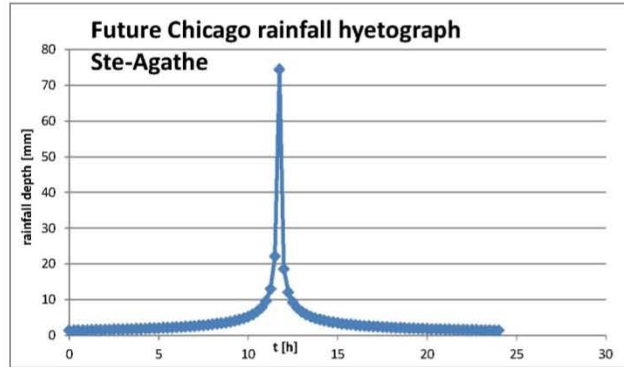
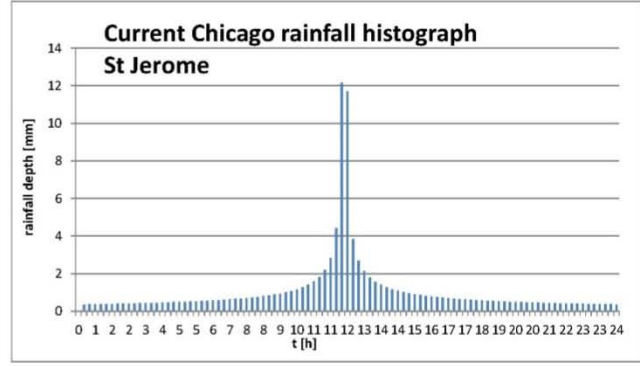
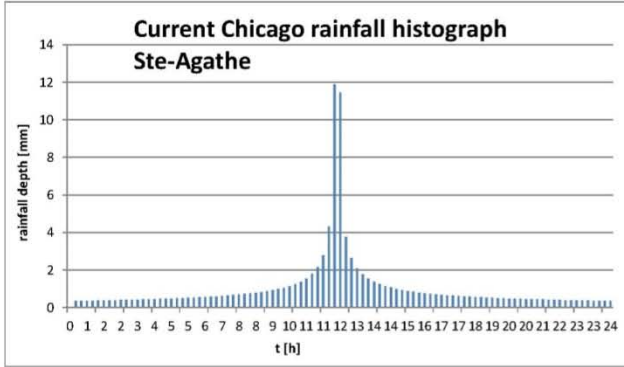
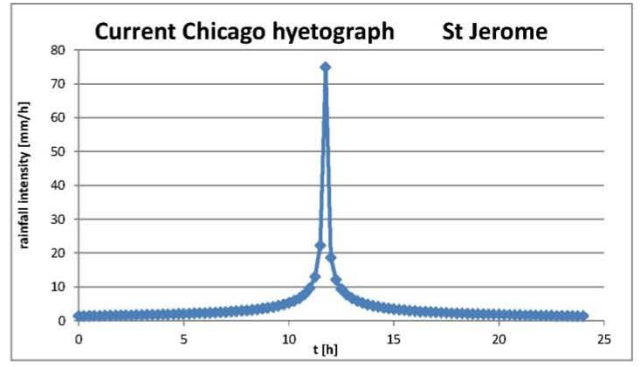
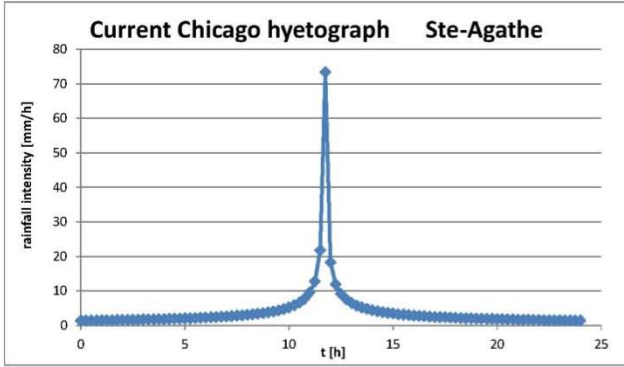
T [years]	duration [h]			
	2	6	12	24
2	20.6	13.9	11	10.6
5	18.1	14.5	10	8.8
10	15.8	13.1	8.2	6.9
25	13	10.1	5.1	3.9
50	11.2	7.3	2.5	1.5

percentage applied:  
1.5 %

t [h]	i [mm/h]	P [mm]	P cumul [mm]
0	1.4353	0.0000	0.0000
0.25	1.4568	0.3615	0.3615
0.5	1.4790	0.3670	0.7285
0.75	1.5021	0.3726	1.1011
1	1.5261	0.3785	1.4796
1.25	1.5510	0.3846	1.8643
1.5	1.5770	0.3910	2.2553
1.75	1.6041	0.3976	2.6529
2	1.6324	0.4046	3.0575
2.25	1.6619	0.4118	3.4693
2.5	1.6927	0.4193	3.8886
2.75	1.7250	0.4272	4.3158
3	1.7589	0.4355	4.7513
3.25	1.7944	0.4442	5.1955
3.5	1.8318	0.4533	5.6487
3.75	1.8711	0.4629	6.1116
4	1.9126	0.4730	6.5846
4.25	1.9564	0.4836	7.0682
4.5	2.0027	0.4949	7.5631
4.75	2.0518	0.5068	8.0699
5	2.1040	0.5195	8.5894
5.25	2.1596	0.5330	9.1223
5.5	2.2190	0.5473	9.6696
5.75	2.2825	0.5627	10.2323
6	2.3506	0.5791	10.8115
6.25	2.4240	0.5968	11.4083
6.5	2.5033	0.6159	12.0242
6.75	2.5893	0.6366	12.6608
7	2.6829	0.6590	13.3198
7.25	2.7853	0.6835	14.0033
7.5	2.8978	0.7104	14.7137
7.75	3.0223	0.7400	15.4537
8	3.1607	0.7729	16.2266
8.25	3.3157	0.8096	17.0362
8.5	3.4910	0.8508	17.8870
8.75	3.6908	0.8977	18.7847
9	3.9213	0.9515	19.7362
9.25	4.1907	1.0140	20.7502
9.5	4.5106	1.0877	21.8379
9.75	4.8980	1.1761	23.0139
10	5.3788	1.2846	24.2985
10.25	5.9949	1.4217	25.7202
10.5	6.8192	1.6018	27.3220
10.75	7.9920	1.8514	29.1734
11	9.8276	2.2274	31.4009
11.25	13.2279	2.8819	34.2828
11.5	22.5895	4.4772	38.7600
11.75	76.0522	12.3302	51.0902
12	18.9156	11.8710	62.9611

t [h]	i [mm/h]	P [mm]	P cumul [mm]
12.25	12.3133	3.9036	66.8648
12.5	9.4735	2.7234	69.5881
12.75	7.8396	2.1641	71.7523
13	6.7594	1.8249	73.5771
13.25	5.9839	1.5929	75.1701
13.5	5.3957	1.4224	76.5925
13.75	4.9317	1.2909	77.8834
14	4.5549	1.1858	79.0693
14.25	4.2417	1.0996	80.1688
14.5	3.9766	1.0273	81.1961
14.75	3.7487	0.9657	82.1618
15	3.5505	0.9124	83.0742
15.25	3.3762	0.8658	83.9400
15.5	3.2215	0.8247	84.7647
15.75	3.0831	0.7881	85.5528
16	2.9584	0.7552	86.3080
16.25	2.8455	0.7255	87.0335
16.5	2.7426	0.6985	87.7320
16.75	2.6483	0.6739	88.4059
17	2.5617	0.6512	89.0571
17.25	2.4816	0.6304	89.6875
17.5	2.4075	0.6111	90.2987
17.75	2.3386	0.5933	90.8919
18	2.2743	0.5766	91.4685
18.25	2.2142	0.5611	92.0296
18.5	2.1578	0.5465	92.5761
18.75	2.1049	0.5328	93.1089
19	2.0550	0.5200	93.6289
19.25	2.0079	0.5079	94.1368
19.5	1.9634	0.4964	94.6332
19.75	1.9213	0.4856	95.1188
20	1.8813	0.4753	95.5941
20.25	1.8432	0.4656	96.0597
20.5	1.8071	0.4563	96.5159
20.75	1.7726	0.4475	96.9634
21	1.7396	0.4390	97.4024
21.25	1.7082	0.4310	97.8334
21.5	1.6781	0.4233	98.2567
21.75	1.6493	0.4159	98.6726
22	1.6216	0.4089	99.0815
22.25	1.5951	0.4021	99.4836
22.5	1.5696	0.3956	99.8791
22.75	1.5451	0.3893	100.2685
23	1.5215	0.3833	100.6518
23.25	1.4988	0.3775	101.0294
23.5	1.4769	0.3720	101.4013
23.75	1.4557	0.3666	101.7679
24	1.4353	0.3614	102.1293





### Appendix 3: Parameters of the models for the rainfall-runoff transformation in Hec-HMS.

**Loss Method**

Basin	Data / Input						Results of calculation			chosen parameter		
	SCS soil category	Partial CN			land use [%]			CN	S [mm]	Ia [mm]	infiltration rate [mm/h]	IMP [%]
		agricultural	forest	urbanized	agricultural	forest	urbanized					
Noir					2	93	5	62.2	154.36	30.87	5	5
Ste-Agathe up					2	88	10	64.1	142.26	28.45	5	10
Ste-Agathe down					2	86	12	64.86	137.62	27.52	5	12
Doncaster					2	93	5	62.2	154.36	30.87	5	5
Mulet					2	91	7	62.96	149.43	29.89	5	7
Simon					2	93	5	62.2	154.36	30.87	5	5
St-Jerome					2	93	5	62.2	154.36	30.87	5	5
Bellefeuille	B	75	60	98	20	60	20	70.6	105.77	21.15	5	20
Bonniebrook					8	72	20	68.8	115.19	23.04	5	20
Williams					2	83	15	66	130.85	26.17	5	15
Lachute up					7	86	7	63.71	144.68	28.94	5	7
Ouest					15	65	20	69.85	109.64	21.93	5	20
St-Andre					10	85	5	63.4	146.63	29.33	5	5
Lachute down					85	13	2	73.51	91.53	18.31	5	2
					75	15	10	75.05	84.44	16.89	5	10

**Transformation method**

Basin	data		results of calculation	chosen parameter
	Length of longest flow path [km]	basin mean slope [%]	Tc [h]	Clark Storage coeff [h]
Noir	25.037	8.783	6.874	10
Ste-Agathe up	25.121	7.818	7.216	10
Ste-Agathe down	27.85	7.139	8.115	10
Doncaster	50.79	6.736	13.348	10
Mulet	35.515	9.288	8.863	10
Simon	36.28	8.114	9.508	10
St-Jerome	53.305	4.764	15.901	10
Bellefeuille	20	3.229	8.547	10
Bonniebrook	34.79	4.161	11.973	10
Williams	27.581	3.275	10.956	10
Lachute up	32.711	1.836	15.756	10
Ouest	52.35	5.21	15.13	10
St-Andre	30.357	0.857	20.069	10
Lachute down	22.96	1.035	14.937	10

### Baseflow Method

Basin	Transfert data			averaged minimum flowrate during the calibration period [m3/s]											
	area [km2]	reference basin for transfer	area ratio	jan	feb	mar	apr	may	jun	jul	aug	sep	oct	nov	dec
Ste-Agathe up	153.48			0.4	0.39	0.6	0.95	0.52	0.11	0.1	0.08	0.08	0.31	0.51	0.45
Doncaster	223.24			1.65	1.72	1.7	5.3	4.4	1.9	1.8	1.2	1.4	1.6	2.55	2.4
Simon	161.22			1.95	1.57	1.37	5.1	2.01	1.25	0.8	0.7	0.75	1.85	2.75	2.35
Bonniebrook	89.42			0.75	0.48	0.48	2.02	0.45	0.1	0.08	0.07	0.05	0.48	0.98	0.8
Ouest	352.65			1.9	1.55	2.025	9.245	6.7	2.2	1.2	0.75	0.68	1.305	3.548	2.35
Noir	140.28	Simon	0.87	1.745	1.405	1.226	4.563	1.798	1.118	0.716	0.626	0.671	1.655	2.460	2.102
Ste-Agathe down	139.95	Ste-Agathe up	0.91	0.372	0.362	0.557	0.882	0.483	0.102	0.093	0.074	0.074	0.288	0.474	0.418
Mulet	132.17	Simon	0.82	1.663	1.339	1.169	4.351	1.715	1.066	0.682	0.597	0.640	1.578	2.346	2.005
St-Jerome	287.83	Simon	1.78	3.100	2.496	2.178	8.109	3.196	1.987	1.272	1.113	1.192	2.941	4.372	3.736
Bellefeuille	48.653	Bonniebrook	0.54	0.461	0.295	0.295	1.241	0.277	0.061	0.049	0.043	0.031	0.295	0.602	0.492
Williams	60.362	Bonniebrook	0.68	0.548	0.351	0.351	1.475	0.329	0.073	0.058	0.051	0.037	0.351	0.716	0.584
Lachute up	169.28	Simon	1.05	2.028	1.632	1.425	5.303	2.090	1.300	0.832	0.728	0.780	1.924	2.859	2.444
St-Andre	137.75	Ouest	0.85	1.675	1.367	1.786	8.152	5.908	1.940	1.058	0.661	0.600	1.151	3.128	2.072
Lachute down	74.3	Simon	0.83	0.647	0.414	0.414	1.742	0.388	0.086	0.069	0.060	0.043	0.414	0.845	0.690

### Routing Method

Reach	location	data		result of calculation	
		river length [m]	basin mean slope [%]	Tc [h]	Tl [min]
R270	through Ste-Agathe_down Basin	27850	7.14	8.115	292.1
R320	Between Ste-Agathe and Ste-Adele	5284	9.12	1.982	71.34
R9650	Between Ste-Adele and the junction with Simon River	50790	8.5	12.177	438.4
R520	through the down part of St-Jerome Basin	35517	3.8	12.611	454
R10750	between the junction with Bellefeuille and Bonniebrook Rivers	3776	1.46	3.132	112.8
R700	between the junction with Bonniebrook and Williams Rivers	22591	1.85	11.726	422.7
R10700	Between the junction with Williams Rivers and Lachute City	7587	1.88	4.918	177
R780	Between Lachute and St-Andre Cities	18075	0.99	12.606	453.8
R800	Between St-Andre City and the Outlet	1439	2.24	1.235	44.45

## Appendix 4: Parameters of the meteorological model of Hec-HMS.

### Parameters of the Temperature Index Method

PX Temperature	0	°C
Base temperature	0	°C
wet meltrate	10	mm / °C - day
rain rate limit	2	mm / day
ATI meltrate coefficient	0.98	
Cold limit	30	mm / day
ATI coldrate coefficient	1	
water capacity	4	%
groundmelt	1	mm / day
lapse rate (all sub-basins)	-5	°C / 1000m

### ATI Meltrate function

ATI deg C / day	meltrate mm/deg C - day
0	1
5	1
10	1
50	8
300	8

	mean elevation [m]	initial SWE (calibration & validation)	initial SWE (simulation)
Noir	444.01	0	39
Ste-Agathe up	447	0	39
Ste-Agathe down	409.07	0	39
Doncaster	413.6	0	39
Mulet	433.3	0	39
Simon	383.25	0	30
St-Jerome	228	0	20
Bellefeuille	284	0	20
Bonniebrook	360	0	30
Williams	258	0	20
Lachute up	205	0	20
Ouest	284	0	25
St-Andre	129	0	10
Lachute down	56	0	10

### EVAPOTRANSPIRATION

	St-Jerome			St-Agathe			Lachute		
	mean t 1974 - 1978	i	EVP rate	mean t 1974 - 1978	i	EVP rate	mean t 1974 - 1978	i	EVP rate
	°C		mm / month	°C		mm / month	°C		mm / month
Jan	-12.58	0	0	-14.26	0	0	-12.66	0	0
Feb	-10.325	0	0	-11.68	0	0	-10.22	0	0
Mar	-5.175	0	0	-5.94	0	0	-3.96	0	0
Apr	3.84	0.231	0.813	1.96	0.242	0.840	4.34	0.807	1.970
May	12.78	5.491	7.657	10.98	3.290	5.328	13.06	4.279	6.417
Jun	17.575	7.013	9.104	15.6	5.600	7.764	17.875	6.881	8.983
Jul	19.725	9.165	11.004	17.62	6.733	8.846	19.96	8.132	10.111
Aug	18.24	7.547	9.591	16.32	5.995	8.148	18.68	7.356	9.418
Sep	12.12	4.101	6.228	10.26	2.969	4.955	12.68	4.091	6.217
Oct	5.98	1.885	3.592	4.28	0.790	1.941	6.4	1.453	2.987
Nov	0.26	0.309	0.997	-1.48	0.000	0.000	0.6	0.040	0.236
Dec	-9.24	0	0	-10.76	0	0	-8.86	0	0
	I =	35.742		I =	25.620		I =	33.040	
	a =	1.072		a =	0.910		a =	1.029	

	St-Jerome			St-Agathe			Lachute		
	mean t 2050	i	EVP rate	mean t 2050	i	EVP rate	mean t 2050	i	EVP rate
	°C		mm / month	°C		mm / month	°C		mm / month
Jan	-9.58	0	0	-11.26	0	0	-9.66	0	0
Feb	-7.325	0	0	-8.68	0	0	-7.22	0	0
Mar	-2.175	0	0	-2.94	0	0	-0.96	0	0
Apr	6.84	1.607	3.208	4.96	0.988	2.273	7.34	1.788	3.460
May	15.78	5.698	7.860	13.98	4.743	6.903	16.06	5.851	8.009
Jun	20.575	8.514	10.445	18.6	7.308	9.374	20.875	8.703	10.608
Jul	22.725	9.897	11.619	20.62	8.543	10.470	22.96	10.052	11.748
Aug	21.24	8.935	10.807	19.32	7.741	9.764	21.68	9.216	11.048
Sep	15.12	5.341	7.508	13.26	4.378	6.522	15.68	5.643	7.806
Oct	8.98	2.427	4.295	7.28	1.766	3.430	9.4	2.601	4.511
Nov	3.26	0.523	1.450	1.52	0.165	0.640	3.6	0.608	1.612
Dec	-6.24	0	0	-7.76	0	0	-5.86	0	0
	I =	42.941		I =	35.631		I =	44.463	
	a =	1.187		a =	1.070		a =	1.211	



## Appendix5: Table of value and graphs of the hydrographs at the exit of the Du-Nord Basin and at the entrance of the Des-Prairies River and of its tributaries.

Mean Flow of Ottawa River at Carillon dam in April	3510	m <sup>3</sup> /s
% of the Lake going into the Des-Prairies River	35	%
% of the Lake going into the Mille-les River	12	%
% of the Lake going into the first tributary	8	%

Recorded mean flow of Mille-les River in April	486	m <sup>3</sup> /s
% of mean flow of Mille-les River coming from Mille-les Basin	6	%
Calculated mean flow at the outlet of Mille-les Basin in April	29.2	m <sup>3</sup> /s
Recorded mean flow at the outlet of Du-Nord Basin in April	158	m <sup>3</sup> /s
% of Du-Nord Basin corresponding to the Mille-les Basin	18.5	%

Outlet of Du-Nord River		
max flow [m <sup>3</sup> /s] = 719.8		
date	time	outflow [m <sup>3</sup> /s]
15-Apr	0:00	58.3
15-Apr	1:00	58.3
15-Apr	2:00	58.3
15-Apr	3:00	58.4
15-Apr	4:00	58.4
15-Apr	5:00	58.4
15-Apr	6:00	58.4
15-Apr	7:00	58.5
15-Apr	8:00	58.7
15-Apr	9:00	58.9
15-Apr	10:00	59.1
15-Apr	11:00	59.4
15-Apr	12:00	59.9
15-Apr	13:00	61.2
15-Apr	14:00	63.8
15-Apr	15:00	67.3
15-Apr	16:00	71.5
15-Apr	17:00	76.5
15-Apr	18:00	82.5
15-Apr	19:00	89.6
15-Apr	20:00	97.7
15-Apr	21:00	108.9
15-Apr	22:00	124
15-Apr	23:00	141.2
16-Apr	0:00	160.3
16-Apr	1:00	180.8
16-Apr	2:00	201.8
16-Apr	3:00	222.9
16-Apr	4:00	243.5
16-Apr	5:00	262.3
16-Apr	6:00	278.6
16-Apr	7:00	291.8
16-Apr	8:00	301.6
16-Apr	9:00	307.8
16-Apr	10:00	310.9
16-Apr	11:00	310.6
16-Apr	12:00	306.7
16-Apr	13:00	301.1
16-Apr	14:00	296.1
16-Apr	15:00	292.1
16-Apr	16:00	289.9
16-Apr	17:00	289.8
16-Apr	18:00	293.4
16-Apr	19:00	300.1
16-Apr	20:00	308.9
16-Apr	21:00	319.1
16-Apr	22:00	329.8
16-Apr	23:00	340
17-Apr	0:00	349.7
17-Apr	1:00	359.7
17-Apr	2:00	371
17-Apr	3:00	382.3
17-Apr	4:00	393.2
17-Apr	5:00	404
17-Apr	6:00	413.7
17-Apr	7:00	421.4
17-Apr	8:00	427.5
17-Apr	9:00	434
17-Apr	10:00	443
17-Apr	11:00	455.8
17-Apr	12:00	473.4
17-Apr	13:00	495.3
17-Apr	14:00	520.4
17-Apr	15:00	550.1
17-Apr	16:00	582.3
17-Apr	17:00	613.5
17-Apr	18:00	642.1
17-Apr	19:00	668.2
17-Apr	20:00	689.7
17-Apr	21:00	704.6
17-Apr	22:00	713.7
17-Apr	23:00	718.7
18-Apr	0:00	719.8
18-Apr	1:00	716.9

Entrance of the Des-Prairies River		
max flow [m <sup>3</sup> /s] = 1480.43		
date	time	outflow [m <sup>3</sup> /s]
15-Apr	0:00	1248.91
15-Apr	1:00	1248.91
15-Apr	2:00	1248.91
15-Apr	3:00	1248.94
15-Apr	4:00	1248.94
15-Apr	5:00	1248.94
15-Apr	6:00	1248.94
15-Apr	7:00	1248.98
15-Apr	8:00	1249.05
15-Apr	9:00	1249.12
15-Apr	10:00	1249.19
15-Apr	11:00	1249.29
15-Apr	12:00	1249.47
15-Apr	13:00	1249.92
15-Apr	14:00	1250.83
15-Apr	15:00	1252.06
15-Apr	16:00	1253.53
15-Apr	17:00	1255.28
15-Apr	18:00	1257.38
15-Apr	19:00	1259.86
15-Apr	20:00	1262.7
15-Apr	21:00	1266.62
15-Apr	22:00	1271.9
15-Apr	23:00	1277.92
16-Apr	0:00	1284.61
16-Apr	1:00	1291.78
16-Apr	2:00	1299.13
16-Apr	3:00	1306.52
16-Apr	4:00	1313.73
16-Apr	5:00	1320.31
16-Apr	6:00	1326.01
16-Apr	7:00	1330.63
16-Apr	8:00	1334.06
16-Apr	9:00	1336.23
16-Apr	10:00	1337.32
16-Apr	11:00	1337.21
16-Apr	12:00	1335.85
16-Apr	13:00	1333.89
16-Apr	14:00	1332.14
16-Apr	15:00	1330.74
16-Apr	16:00	1329.97
16-Apr	17:00	1329.93
16-Apr	18:00	1331.19
16-Apr	19:00	1333.54
16-Apr	20:00	1336.62
16-Apr	21:00	1340.19
16-Apr	22:00	1343.93
16-Apr	23:00	1347.5
17-Apr	0:00	1350.9
17-Apr	1:00	1354.4
17-Apr	2:00	1358.35
17-Apr	3:00	1362.31
17-Apr	4:00	1366.12
17-Apr	5:00	1369.9
17-Apr	6:00	1373.3
17-Apr	7:00	1375.99
17-Apr	8:00	1378.13
17-Apr	9:00	1380.4
17-Apr	10:00	1383.55
17-Apr	11:00	1388.03
17-Apr	12:00	1394.19
17-Apr	13:00	1401.86
17-Apr	14:00	1410.64
17-Apr	15:00	1421.04
17-Apr	16:00	1432.31
17-Apr	17:00	1443.23
17-Apr	18:00	1453.24
17-Apr	19:00	1462.37
17-Apr	20:00	1469.9
17-Apr	21:00	1475.11
17-Apr	22:00	1478.3
17-Apr	23:00	1480.05
18-Apr	0:00	1480.43
18-Apr	1:00	1479.42

Entrance of the tributary at Bizard Island		
max flow [m <sup>3</sup> /s] = 338.384		
date	time	outflow [m <sup>3</sup> /s]
15-Apr	0:00	285.464
15-Apr	1:00	285.464
15-Apr	2:00	285.464
15-Apr	3:00	285.472
15-Apr	4:00	285.472
15-Apr	5:00	285.472
15-Apr	6:00	285.472
15-Apr	7:00	285.48
15-Apr	8:00	285.496
15-Apr	9:00	285.512
15-Apr	10:00	285.528
15-Apr	11:00	285.552
15-Apr	12:00	285.592
15-Apr	13:00	285.696
15-Apr	14:00	285.904
15-Apr	15:00	286.184
15-Apr	16:00	286.52
15-Apr	17:00	286.92
15-Apr	18:00	287.4
15-Apr	19:00	287.968
15-Apr	20:00	288.616
15-Apr	21:00	289.512
15-Apr	22:00	290.72
15-Apr	23:00	292.096
16-Apr	0:00	293.624
16-Apr	1:00	295.264
16-Apr	2:00	296.944
16-Apr	3:00	298.632
16-Apr	4:00	300.28
16-Apr	5:00	301.784
16-Apr	6:00	303.088
16-Apr	7:00	304.144
16-Apr	8:00	304.928
16-Apr	9:00	305.424
16-Apr	10:00	305.672
16-Apr	11:00	305.648
16-Apr	12:00	305.336
16-Apr	13:00	304.888
16-Apr	14:00	304.488
16-Apr	15:00	304.168
16-Apr	16:00	303.992
16-Apr	17:00	303.984
16-Apr	18:00	304.272
16-Apr	19:00	304.808
16-Apr	20:00	305.512
16-Apr	21:00	306.328
16-Apr	22:00	307.184
16-Apr	23:00	308
17-Apr	0:00	308.776
17-Apr	1:00	309.576
17-Apr	2:00	310.48
17-Apr	3:00	311.384
17-Apr	4:00	312.256
17-Apr	5:00	313.12
17-Apr	6:00	313.896
17-Apr	7:00	314.512
17-Apr	8:00	315
17-Apr	9:00	315.52
17-Apr	10:00	316.24
17-Apr	11:00	317.264
17-Apr	12:00	318.672
17-Apr	13:00	320.424
17-Apr	14:00	322.432
17-Apr	15:00	324.808
17-Apr	16:00	327.384
17-Apr	17:00	329.88
17-Apr	18:00	332.168
17-Apr	19:00	334.256
17-Apr	20:00	335.976
17-Apr	21:00	337.168
17-Apr	22:00	337.896
17-Apr	23:00	338.296
18-Apr	0:00	338.384
18-Apr	1:00	338.152

Entrance of the Mille-les River		
max flow [m <sup>3</sup> /s] = 507.576		
date	time	outflow [m <sup>3</sup> /s]
15-Apr	0:00	428.196
15-Apr	1:00	428.196
15-Apr	2:00	428.196
15-Apr	3:00	428.208
15-Apr	4:00	428.208
15-Apr	5:00	428.208
15-Apr	6:00	428.208
15-Apr	7:00	428.22
15-Apr	8:00	428.244
15-Apr	9:00	428.268
15-Apr	10:00	428.292
15-Apr	11:00	428.328
15-Apr	12:00	428.388
15-Apr	13:00	428.544
15-Apr	14:00	428.856
15-Apr	15:00	429.276
15-Apr	16:00	429.78
15-Apr	17:00	430.38
15-Apr	18:00	431.1
15-Apr	19:00	431.952
15-Apr	20:00	432.924
15-Apr	21:00	434.268
15-Apr	22:00	436.08
15-Apr	23:00	438.144
16-Apr	0:00	440.436
16-Apr	1:00	442.896
16-Apr	2:00	445.416
16-Apr	3:00	447.948
16-Apr	4:00	450.42
16-Apr	5:00	452.676
16-Apr	6:00	454.632
16-Apr	7:00	456.216
16-Apr	8:00	457.392
16-Apr	9:00	458.136
16-Apr	10:00	458.508
16-Apr	11:00	458.472
16-Apr	12:00	458.004
16-Apr	13:00	457.332
16-Apr	14:00	456.732
16-Apr	15:00	456.252
16-Apr	16:00	455.988
16-Apr	17:00	455.976
16-Apr	18:00	456.408
16-Apr	19:00	457.212
16-Apr	20:00	458.268
16-Apr	21:00	459.492
16-Apr	22:00	460.776
16-Apr	23:00	462
17-Apr	0:00	463.164
17-Apr	1:00	464.364
17-Apr	2:00	465.72
17-Apr	3:00	467.076
17-Apr	4:00	468.384
17-Apr	5:00	469.68
17-Apr	6:00	470.844
17-Apr	7:00	471.768
17-Apr	8:00	472.5
17-Apr	9:00	473.28
17-Apr	10:00	474.36
17-Apr	11:00	475.896
17-Apr	12:00	478.008
17-Apr	13:00	480.636
17-Apr	14:00	483.648
17-Apr	15:00	487.212
17-Apr	16:00	491.076
17-Apr	17:00	494.82
17-Apr	18:00	498.252
17-Apr	19:00	501.384
17-Apr	20:00	503.964
17-Apr	21:00	505.752
17-Apr	22:00	506.844
17-Apr	23:00	507.444
18-Apr	0:00	507.576
18-Apr	1:00	507.228

Mille-les River at junction with Des-Prairies River		
max flow [m <sup>3</sup> /s] = 640.546		
date	time	outflow [m <sup>3</sup> /s]
15-Apr	0:00	438.966
15-Apr	1:00	438.966
15-Apr	2:00	438.966
15-Apr	3:00	438.996
15-Apr	4:00	438.996
15-Apr	5:00	438.996
15-Apr	6:00	438.996
15-Apr	7:00	439.027
15-Apr	8:00	439.088
15-Apr	9:00	439.149
15-Apr	10:00	439.21
15-Apr	11:00	439.301
15-Apr	12:00	439.453
15-Apr	13:00	439.85
15-Apr	14:00	440.642
15-Apr	15:00	441.708
15-Apr	16:00	442.988
15-Apr	17:00	444.512
15-Apr	18:00	446.34
15-Apr	19:00	448.504
15-Apr	20:00	450.972
15-Apr	21:00	454.385
15-Apr	22:00	458.987
15-Apr	23:00	464.228
16-Apr	0:00	470.049
16-Apr	1:00	476.296
16-Apr	2:00	482.695
16-Apr	3:00	489.125
16-Apr	4:00	495.402
16-Apr	5:00	501.131
16-Apr	6:00	



18-Apr	2:00	710.8	18-Apr	2:00	1477.28	18-Apr	2:00	337.664	18-Apr	2:00	506.496	18-Apr	2:00	637.804
18-Apr	3:00	703	18-Apr	3:00	1474.55	18-Apr	3:00	337.04	18-Apr	3:00	505.56	18-Apr	3:00	635.427
18-Apr	4:00	693.9	18-Apr	4:00	1471.37	18-Apr	4:00	336.312	18-Apr	4:00	504.468	18-Apr	4:00	632.654
18-Apr	5:00	683.6	18-Apr	5:00	1467.76	18-Apr	5:00	335.488	18-Apr	5:00	503.232	18-Apr	5:00	629.515
18-Apr	6:00	672.5	18-Apr	6:00	1463.88	18-Apr	6:00	334.6	18-Apr	6:00	501.9	18-Apr	6:00	626.132
18-Apr	7:00	660.7	18-Apr	7:00	1459.75	18-Apr	7:00	333.656	18-Apr	7:00	500.484	18-Apr	7:00	622.537
18-Apr	8:00	648.3	18-Apr	8:00	1455.41	18-Apr	8:00	332.664	18-Apr	8:00	498.996	18-Apr	8:00	618.758
18-Apr	9:00	635.5	18-Apr	9:00	1450.93	18-Apr	9:00	331.64	18-Apr	9:00	497.46	18-Apr	9:00	614.857
18-Apr	10:00	622.3	18-Apr	10:00	1446.31	18-Apr	10:00	330.584	18-Apr	10:00	495.876	18-Apr	10:00	610.835
18-Apr	11:00	609	18-Apr	11:00	1441.65	18-Apr	11:00	329.52	18-Apr	11:00	494.28	18-Apr	11:00	606.782
18-Apr	12:00	595.5	18-Apr	12:00	1436.93	18-Apr	12:00	328.44	18-Apr	12:00	492.66	18-Apr	12:00	602.668
18-Apr	13:00	581.9	18-Apr	13:00	1432.17	18-Apr	13:00	327.352	18-Apr	13:00	491.028	18-Apr	13:00	598.524
18-Apr	14:00	568	18-Apr	14:00	1427.3	18-Apr	14:00	326.24	18-Apr	14:00	489.36	18-Apr	14:00	594.288
18-Apr	15:00	553.9	18-Apr	15:00	1422.37	18-Apr	15:00	325.112	18-Apr	15:00	487.668	18-Apr	15:00	589.991
18-Apr	16:00	539.4	18-Apr	16:00	1417.29	18-Apr	16:00	323.952	18-Apr	16:00	485.928	18-Apr	16:00	585.573
18-Apr	17:00	524.5	18-Apr	17:00	1412.08	18-Apr	17:00	322.76	18-Apr	17:00	484.14	18-Apr	17:00	581.032
18-Apr	18:00	509.6	18-Apr	18:00	1406.86	18-Apr	18:00	321.568	18-Apr	18:00	482.352	18-Apr	18:00	576.492
18-Apr	19:00	495	18-Apr	19:00	1401.75	18-Apr	19:00	320.4	18-Apr	19:00	480.6	18-Apr	19:00	572.043
18-Apr	20:00	480.8	18-Apr	20:00	1396.78	18-Apr	20:00	319.264	18-Apr	20:00	478.896	18-Apr	20:00	567.715
18-Apr	21:00	467	18-Apr	21:00	1391.95	18-Apr	21:00	318.16	18-Apr	21:00	477.24	18-Apr	21:00	563.51
18-Apr	22:00	453.6	18-Apr	22:00	1387.26	18-Apr	22:00	317.088	18-Apr	22:00	475.632	18-Apr	22:00	559.427
18-Apr	23:00	440.7	18-Apr	23:00	1382.75	18-Apr	23:00	316.056	18-Apr	23:00	474.084	18-Apr	23:00	555.496
19-Apr	0:00	428.2	19-Apr	0:00	1378.37	19-Apr	0:00	315.056	19-Apr	0:00	472.584	19-Apr	0:00	551.686
19-Apr	1:00	416	19-Apr	1:00	1374.1	19-Apr	1:00	314.08	19-Apr	1:00	471.12	19-Apr	1:00	547.969
19-Apr	2:00	404.3	19-Apr	2:00	1370.01	19-Apr	2:00	313.144	19-Apr	2:00	469.716	19-Apr	2:00	544.403
19-Apr	3:00	393	19-Apr	3:00	1366.05	19-Apr	3:00	312.24	19-Apr	3:00	468.36	19-Apr	3:00	540.96
19-Apr	4:00	382	19-Apr	4:00	1362.2	19-Apr	4:00	311.36	19-Apr	4:00	467.04	19-Apr	4:00	537.608
19-Apr	5:00	371.4	19-Apr	5:00	1358.49	19-Apr	5:00	310.512	19-Apr	5:00	465.768	19-Apr	5:00	534.378
19-Apr	6:00	361.1	19-Apr	6:00	1354.89	19-Apr	6:00	309.688	19-Apr	6:00	464.532	19-Apr	6:00	531.239
19-Apr	7:00	351.2	19-Apr	7:00	1351.42	19-Apr	7:00	308.896	19-Apr	7:00	463.344	19-Apr	7:00	528.222
19-Apr	8:00	341.6	19-Apr	8:00	1348.06	19-Apr	8:00	308.128	19-Apr	8:00	462.192	19-Apr	8:00	525.297
19-Apr	9:00	332.3	19-Apr	9:00	1344.81	19-Apr	9:00	307.384	19-Apr	9:00	461.076	19-Apr	9:00	522.463
19-Apr	10:00	323.3	19-Apr	10:00	1341.66	19-Apr	10:00	306.664	19-Apr	10:00	459.996	19-Apr	10:00	519.72
19-Apr	11:00	314.7	19-Apr	11:00	1338.65	19-Apr	11:00	305.976	19-Apr	11:00	458.964	19-Apr	11:00	517.099
19-Apr	12:00	306.2	19-Apr	12:00	1335.67	19-Apr	12:00	305.296	19-Apr	12:00	457.944	19-Apr	12:00	514.509
19-Apr	13:00	298.1	19-Apr	13:00	1332.84	19-Apr	13:00	304.648	19-Apr	13:00	456.972	19-Apr	13:00	512.041
19-Apr	14:00	290.3	19-Apr	14:00	1330.11	19-Apr	14:00	304.024	19-Apr	14:00	456.036	19-Apr	14:00	509.664
19-Apr	15:00	282.7	19-Apr	15:00	1327.45	19-Apr	15:00	303.416	19-Apr	15:00	455.124	19-Apr	15:00	507.348
19-Apr	16:00	275.3	19-Apr	16:00	1324.86	19-Apr	16:00	302.824	19-Apr	16:00	454.236	19-Apr	16:00	505.093
19-Apr	17:00	268.2	19-Apr	17:00	1322.37	19-Apr	17:00	302.256	19-Apr	17:00	453.384	19-Apr	17:00	502.929
19-Apr	18:00	261.3	19-Apr	18:00	1319.96	19-Apr	18:00	301.704	19-Apr	18:00	452.556	19-Apr	18:00	500.827
19-Apr	19:00	254.7	19-Apr	19:00	1317.65	19-Apr	19:00	301.176	19-Apr	19:00	451.764	19-Apr	19:00	498.815
19-Apr	20:00	248.2	19-Apr	20:00	1315.37	19-Apr	20:00	300.656	19-Apr	20:00	450.984	19-Apr	20:00	496.835
19-Apr	21:00	242	19-Apr	21:00	1313.2	19-Apr	21:00	300.16	19-Apr	21:00	450.24	19-Apr	21:00	494.945
19-Apr	22:00	236	19-Apr	22:00	1311.1	19-Apr	22:00	299.68	19-Apr	22:00	449.52	19-Apr	22:00	493.117
19-Apr	23:00	230.2	19-Apr	23:00	1309.07	19-Apr	23:00	299.216	19-Apr	23:00	448.824	19-Apr	23:00	491.349
20-Apr	0:00	224.5	20-Apr	0:00	1307.08	20-Apr	0:00	298.76	20-Apr	0:00	448.14	20-Apr	0:00	489.612
20-Apr	1:00	219.1	20-Apr	1:00	1305.19	20-Apr	1:00	298.328	20-Apr	1:00	447.492	20-Apr	1:00	487.967
20-Apr	2:00	213.8	20-Apr	2:00	1303.33	20-Apr	2:00	297.904	20-Apr	2:00	446.856	20-Apr	2:00	486.352
20-Apr	3:00	208.7	20-Apr	3:00	1301.55	20-Apr	3:00	297.496	20-Apr	3:00	446.244	20-Apr	3:00	484.798
20-Apr	4:00	203.8	20-Apr	4:00	1299.83	20-Apr	4:00	297.104	20-Apr	4:00	445.656	20-Apr	4:00	483.304
20-Apr	5:00	199	20-Apr	5:00	1298.15	20-Apr	5:00	296.72	20-Apr	5:00	445.084	20-Apr	5:00	481.842
20-Apr	6:00	194.4	20-Apr	6:00	1296.54	20-Apr	6:00	296.352	20-Apr	6:00	444.528	20-Apr	6:00	480.44
20-Apr	7:00	189.9	20-Apr	7:00	1294.97	20-Apr	7:00	295.992	20-Apr	7:00	443.988	20-Apr	7:00	479.069
20-Apr	8:00	185.6	20-Apr	8:00	1293.46	20-Apr	8:00	295.648	20-Apr	8:00	443.472	20-Apr	8:00	477.758
20-Apr	9:00	181.4	20-Apr	9:00	1291.99	20-Apr	9:00	295.312	20-Apr	9:00	442.968	20-Apr	9:00	476.478
20-Apr	10:00	177.4	20-Apr	10:00	1290.59	20-Apr	10:00	294.992	20-Apr	10:00	442.488	20-Apr	10:00	475.26
20-Apr	11:00	173.5	20-Apr	11:00	1289.23	20-Apr	11:00	294.68	20-Apr	11:00	442.02	20-Apr	11:00	474.071
20-Apr	12:00	169.7	20-Apr	12:00	1287.9	20-Apr	12:00	294.376	20-Apr	12:00	441.564	20-Apr	12:00	472.913
20-Apr	13:00	166.1	20-Apr	13:00	1286.64	20-Apr	13:00	294.088	20-Apr	13:00	441.132	20-Apr	13:00	471.816
20-Apr	14:00	162.6	20-Apr	14:00	1285.41	20-Apr	14:00	293.808	20-Apr	14:00	440.712	20-Apr	14:00	470.749
20-Apr	15:00	159.1	20-Apr	15:00	1284.19	20-Apr	15:00	293.528	20-Apr	15:00	440.292	20-Apr	15:00	469.683
20-Apr	16:00	155.8	20-Apr	16:00	1283.03	20-Apr	16:00	293.264	20-Apr	16:00	439.896	20-Apr	16:00	468.677
20-Apr	17:00	152.6	20-Apr	17:00	1281.91	20-Apr	17:00	293.008	20-Apr	17:00	439.512	20-Apr	17:00	467.702
20-Apr	18:00	149.5	20-Apr	18:00	1280.83	20-Apr	18:00	292.76	20-Apr	18:00	439.14	20-Apr	18:00	466.757
20-Apr	19:00	146.6	20-Apr	19:00	1279.81	20-Apr	19:00	292.528	20-Apr	19:00	438.792	20-Apr	19:00	465.874
20-Apr	20:00	143.7	20-Apr	20:00	1278.8	20-Apr	20:00	292.296	20-Apr	20:00	438.444	20-Apr	20:00	464.99
20-Apr	21:00	140.9	20-Apr	21:00	1277.82	20-Apr	21:00	292.072	20-Apr	21:00	438.108	20-Apr	21:00	464.137
20-Apr	22:00	138.2	20-Apr	22:00	1276.87	20-Apr	22:00	291.856	20-Apr	22:00	437.784	20-Apr	22:00	463.314
20-Apr	23:00	135.5	20-Apr	23:00	1275.93	20-Apr	23:00	291.64	20-Apr	23:00	437.46	20-Apr	23:00	462.491
21-Apr	0:00	133	21-Apr	0:00	1275.05	21-Apr	0:00	291.44	21-Apr	0:00	437.16	21-Apr	0:00	461.729
21-Apr	1:00	130.6	21-Apr	1:00	1274.21	21-Apr	1:00	291.248	21-Apr	1:00	436.872	21-Apr	1:00	460.998
21-Apr	2:00	128.2	21-Apr	2:00	1273.37	21-Apr	2:00	291.056	21-Apr	2:00	436.584	21-Apr	2:00	460.267
21-Apr	3:00	125.9	21-Apr	3:00	1272.57	21-Apr	3:00	290.872	21-Apr	3:00	436.308	21-Apr	3:00	459.566
21-Apr	4:00	123.7	21-Apr	4:00	1271.8	21-Apr	4:00	290.696	21-Apr	4:00	436.044	21-Apr	4:00	458.895
21-Apr	5:00	121.5	21-Apr	5:00	1271.03	21-Apr	5:00	290.52	21-Apr	5:00	435.788	21-Apr	5:00	458.225
21-Apr	6:00	119.5	21-Apr	6:00	1270.33	21-Apr	6:00	290.36	21-Apr	6:00	435.54	21-Apr	6:00	457.616
21-Apr	7:00	117.5	21-Apr	7:00	1269.63	21-Apr	7:00	290.2	21-Apr	7:00	435.3	21-Apr	7:00	457.006
21-Apr	8:00	115.5	21-Apr	8:00	1268.93	21-Apr	8:00	290.04	21-Apr	8:00	435.06	21-Apr	8:00	456.397
21-Apr	9:00	113.7	21-Apr	9:00	1268.3	21-Apr	9:00	289.896	21-Apr	9:00	434.844	21-Apr	9:00	455.848
21-Apr	10:00	111.8	21-Apr	10:00	1267.63	21-Apr	10:00	289.744	21-Apr	10:00	434.616	21-Apr	10:00	455.269
21-Apr	11:00	110.1	21-Apr	11:00	1267.04	21-Apr	11:00	289.608	21-Apr	11:00	434.412	21-Apr	11:00	454.751
21-Apr	12:00	108.4	21-Apr	12:00	1266.44	21-Apr	12:00							



21-Apr	15:00	103.6
21-Apr	16:00	102.1
21-Apr	17:00	100.7
21-Apr	18:00	99.3
21-Apr	19:00	98
21-Apr	20:00	96.7
21-Apr	21:00	95.4
21-Apr	22:00	94.2
21-Apr	23:00	93
22-Apr	0:00	91.9
22-Apr	1:00	90.8
22-Apr	2:00	89.7
22-Apr	3:00	88.7
22-Apr	4:00	87.7
22-Apr	5:00	86.7
22-Apr	6:00	85.8
22-Apr	7:00	84.9
22-Apr	8:00	84
22-Apr	9:00	83.2
22-Apr	10:00	82.4
22-Apr	11:00	81.5
22-Apr	12:00	80.7
22-Apr	13:00	79.9
22-Apr	14:00	79
22-Apr	15:00	78.3
22-Apr	16:00	77.5
22-Apr	17:00	76.8
22-Apr	18:00	76.2
22-Apr	19:00	75.3
22-Apr	20:00	74.2
22-Apr	21:00	73.6
22-Apr	22:00	73
22-Apr	23:00	72.5
23-Apr	0:00	72.1

21-Apr	15:00	1264.76
21-Apr	16:00	1264.24
21-Apr	17:00	1263.75
21-Apr	18:00	1263.26
21-Apr	19:00	1262.8
21-Apr	20:00	1262.35
21-Apr	21:00	1261.89
21-Apr	22:00	1261.47
21-Apr	23:00	1261.05
22-Apr	0:00	1260.67
22-Apr	1:00	1260.28
22-Apr	2:00	1259.9
22-Apr	3:00	1259.55
22-Apr	4:00	1259.2
22-Apr	5:00	1258.85
22-Apr	6:00	1258.53
22-Apr	7:00	1258.22
22-Apr	8:00	1257.9
22-Apr	9:00	1257.62
22-Apr	10:00	1257.34
22-Apr	11:00	1257.03
22-Apr	12:00	1256.75
22-Apr	13:00	1256.47
22-Apr	14:00	1256.15
22-Apr	15:00	1255.91
22-Apr	16:00	1255.63
22-Apr	17:00	1255.38
22-Apr	18:00	1255.17
22-Apr	19:00	1254.86
22-Apr	20:00	1254.47
22-Apr	21:00	1254.26
22-Apr	22:00	1254.05
22-Apr	23:00	1253.88
23-Apr	0:00	1253.74

21-Apr	15:00	289.088
21-Apr	16:00	288.968
21-Apr	17:00	288.856
21-Apr	18:00	288.744
21-Apr	19:00	288.64
21-Apr	20:00	288.536
21-Apr	21:00	288.432
21-Apr	22:00	288.336
21-Apr	23:00	288.24
22-Apr	0:00	288.152
22-Apr	1:00	288.064
22-Apr	2:00	287.976
22-Apr	3:00	287.896
22-Apr	4:00	287.816
22-Apr	5:00	287.736
22-Apr	6:00	287.664
22-Apr	7:00	287.592
22-Apr	8:00	287.52
22-Apr	9:00	287.456
22-Apr	10:00	287.392
22-Apr	11:00	287.32
22-Apr	12:00	287.256
22-Apr	13:00	287.192
22-Apr	14:00	287.12
22-Apr	15:00	287.064
22-Apr	16:00	287
22-Apr	17:00	286.944
22-Apr	18:00	286.896
22-Apr	19:00	286.824
22-Apr	20:00	286.736
22-Apr	21:00	286.688
22-Apr	22:00	286.64
22-Apr	23:00	286.6
23-Apr	0:00	286.568

21-Apr	15:00	433.632
21-Apr	16:00	433.452
21-Apr	17:00	433.284
21-Apr	18:00	433.116
21-Apr	19:00	432.96
21-Apr	20:00	432.804
21-Apr	21:00	432.648
21-Apr	22:00	432.504
21-Apr	23:00	432.36
22-Apr	0:00	432.228
22-Apr	1:00	432.096
22-Apr	2:00	431.964
22-Apr	3:00	431.844
22-Apr	4:00	431.724
22-Apr	5:00	431.604
22-Apr	6:00	431.496
22-Apr	7:00	431.388
22-Apr	8:00	431.28
22-Apr	9:00	431.184
22-Apr	10:00	431.088
22-Apr	11:00	430.98
22-Apr	12:00	430.884
22-Apr	13:00	430.788
22-Apr	14:00	430.68
22-Apr	15:00	430.596
22-Apr	16:00	430.5
22-Apr	17:00	430.416
22-Apr	18:00	430.344
22-Apr	19:00	430.236
22-Apr	20:00	430.104
22-Apr	21:00	430.032
22-Apr	22:00	429.96
22-Apr	23:00	429.9
23-Apr	0:00	429.852

21-Apr	15:00	452.77
21-Apr	16:00	452.313
21-Apr	17:00	451.887
21-Apr	18:00	451.46
21-Apr	19:00	451.064
21-Apr	20:00	450.668
21-Apr	21:00	450.271
21-Apr	22:00	449.906
21-Apr	23:00	449.54
22-Apr	0:00	449.205
22-Apr	1:00	448.87
22-Apr	2:00	448.534
22-Apr	3:00	448.23
22-Apr	4:00	447.925
22-Apr	5:00	447.62
22-Apr	6:00	447.346
22-Apr	7:00	447.072
22-Apr	8:00	446.798
22-Apr	9:00	446.554
22-Apr	10:00	446.31
22-Apr	11:00	446.036
22-Apr	12:00	445.792
22-Apr	13:00	445.548
22-Apr	14:00	445.274
22-Apr	15:00	445.061
22-Apr	16:00	444.817
22-Apr	17:00	444.603
22-Apr	18:00	444.421
22-Apr	19:00	444.146
22-Apr	20:00	443.811
22-Apr	21:00	443.628
22-Apr	22:00	443.445
22-Apr	23:00	443.293
23-Apr	0:00	443.171





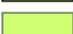

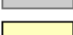
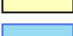
## Appendix6: Historical measured data at the CEHQ flow station of the Carillon Dam.




OUTAOUAIS (RIVIERE DES) AU BARRAGE DE CARILLON (02LB024)													
Station:	02LB024	Type de mesure:	Mensuel	Débits	pour	1994	Redessiner		Graphique				
Débit mensuel moyen (m <sup>3</sup> /s)													
Year	Janv.	Févr.	Mars	Avr.	Mai	Juin	Juil.	Août	Sept.	Oct.	Nov.	Déc.	Moy.
1962	-	-	1690	3340	3080	1680	1090	1060	1020	1070	1250	1030	-
1963	968	962	1090	3110	2390	1530	1030	851	1080	1090	1300	1470	1410
1964	1470	1440	1780	2560	2230	1750	1260	924	851	990	1030	1230	1460
1965	1260	1290	1430	2080	2850	1510	1020	1250	1790	3160	2610	2240	1880
1966	2150	1910	2650	3200	2640	2260	1340	1480	1240	1400	1920	3420	2130
1967	2220	2220	1740	4260	3920	3160	2110	1360	1310	2110	3370	2270	2500
1968	2020	1910	2340	3480	1800	1600	1660	1280	1180	1150	1220	1360	1750
1969	1450	1510	1640	3290	3500	2220	1600	1440	1100	1240	2140	1960	1920
1970	1590	1480	1540	2920	3550	2470	2260	1700	1230	1380	1610	1520	1940
1971	1400	1360	1480	3510	3540	1580	997	951	880	870	907	1170	1550
1972	1220	1160	1250	3170	4810	2380	2190	2040	1850	1940	2610	2070	2230
1973	1970	2070	3620	4140	3840	2770	2060	1560	1360	1670	1700	1900	2390
1974	1730	1680	2310	3880	6500	4350	2210	1300	1070	1240	1970	2020	2520
1975	1920	1750	2010	3210	3060	2060	1110	866	826	975	1160	1610	1710
1976	1550	1550	2340	5770	3860	1880	1550	1250	1130	1220	1230	1440	2060
1977	1350	1200	2680	3740	2330	1130	1120	930	973	1320	1570	2010	1700
1978	1970	1900	1500	3170	2920	1540	1070	949	844	1260	1230	1290	1630
1979	1450	1430	2540	4110	5020	2230	1470	1270	1300	1930	2480	2850	2350
1980	2330	1950	2180	3570	2740	1480	1430	1420	1300	2170	2290	1920	2060
1981	1600	2810	3110	4300	2990	2750	1580	1200	1700	1740	2020	1560	2270
1982	1390	1370	1550	3170	2280	1420	1100	851	852	1030	1580	2250	1570
1983	2380	2170	2570	2910	4910	3050	1230	1040	895	1080	1580	1780	2130
1984	1630	1970	2060	4440	2910	2490	1960	1430	1300	1240	1920	2050	2110
1985	2090	2010	2690	3640	3790	1530	1330	1620	1130	1110	1350	1590	1990
1986	1610	1670	1640	3350	2760	2080	1320	1340	1400	1800	1820	1740	1880
1987	1680	1560	1900	3110	1170	1200	982	816	770	924	1320	1840	1440
1988	1860	1930	1640	3700	2780	1240	914	1170	1260	2290	3450	2250	2040
1989	2060	2100	1880	2950	2980	2660	1280	918	853	932	1840	1850	1860
1990	1910	2060	2490	3220	2620	1550	1440	1020	896	1820	2170	2820	2000
1991	2260	2230	2410	4790	2540	1310	892	777	842	1170	1500	1880	1880
1992	1820	1820	1670	3150	2990	1230	1160	999	1440	1850	2680	2200	1920
1993	2160	1880	1490	3740	1780	1870	1070	879	940	1890	2410	2210	1860
1994	1710	1940	1810	2840	2570	2180	2180	1700	1130	1120	1670	1790	1880
<b>Moy.</b>	1760	1760	2020	3510	3140	2000	1420	1200	1140	1460	1850	1900	1940
<b>Max.</b>	2380	2810	3620	5770	6500	4350	2260	2040	1850	3160	3450	3420	2520
<b>Min.</b>	968	962	1090	2080	1170	1130	892	777	770	870	907	1030	1410

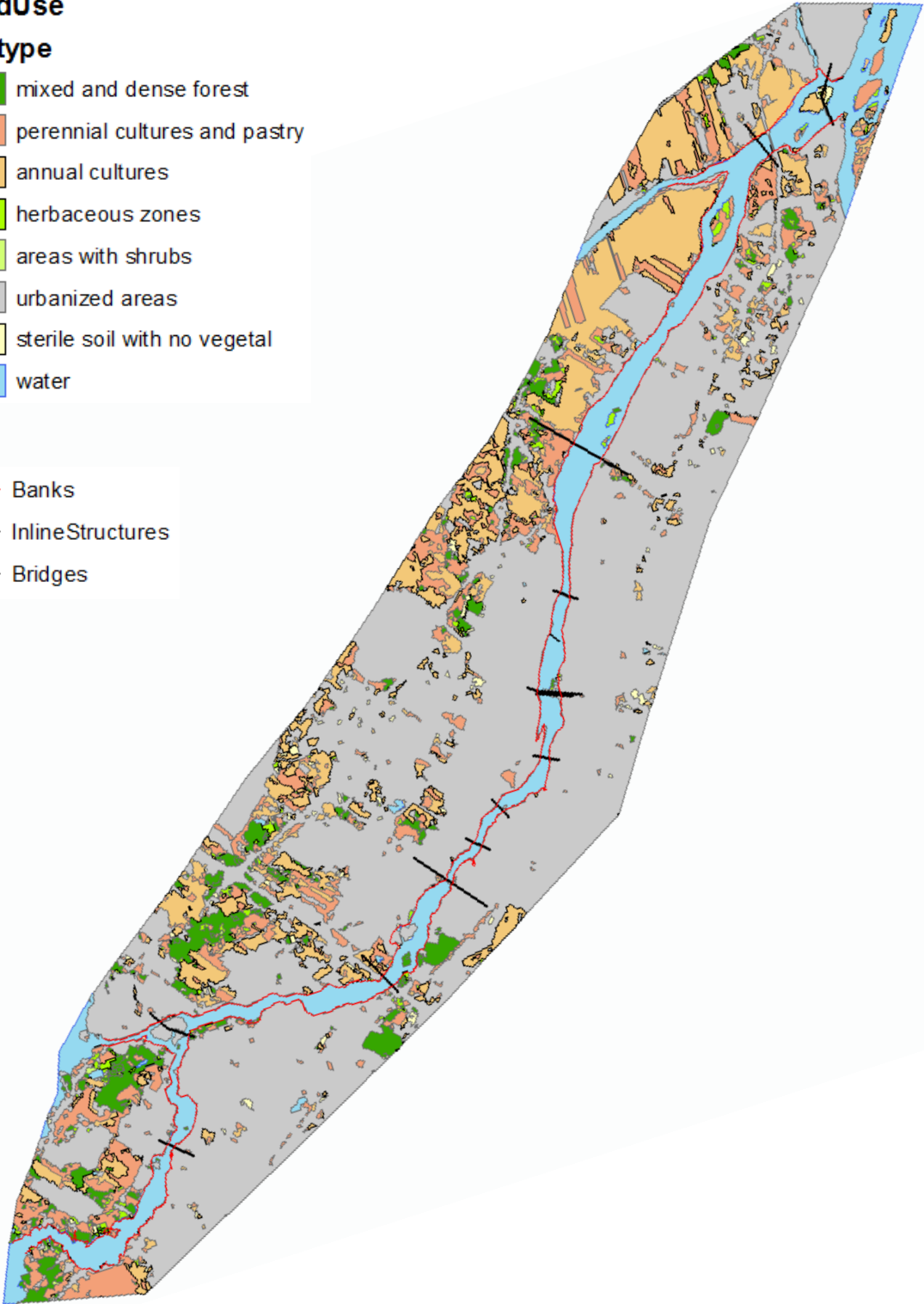
**Appendix7:** Land-Use file used for the input of the roughness coefficient in ArcGIS

**LandUse**

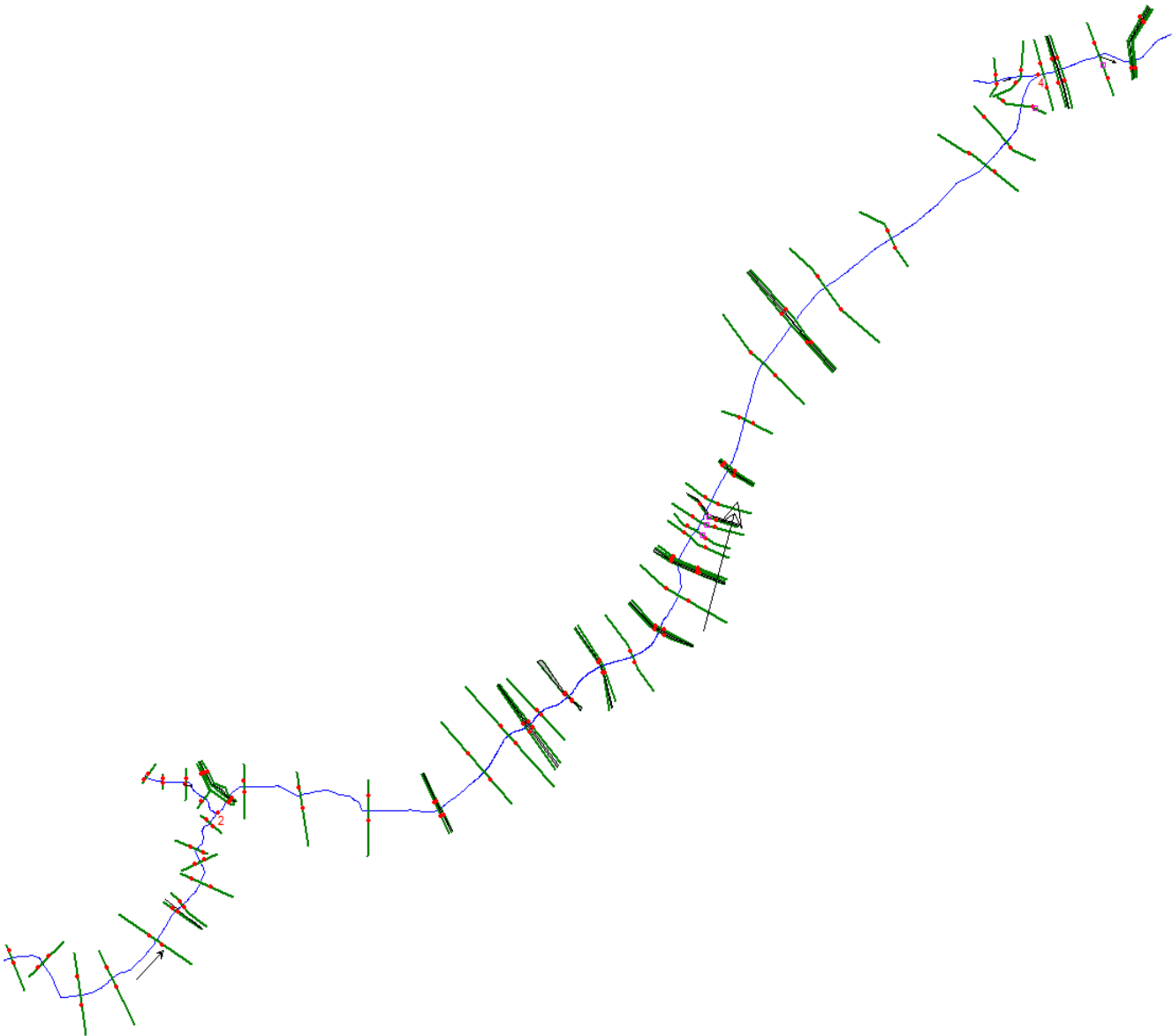
**soil type**

-  mixed and dense forest
-  perennial cultures and pastry
-  annual cultures
-  herbaceous zones
-  areas with shrubs
-  urbanized areas
-  sterile soil with no vegetal
-  water

-  Banks
-  InlineStructures
-  Bridges

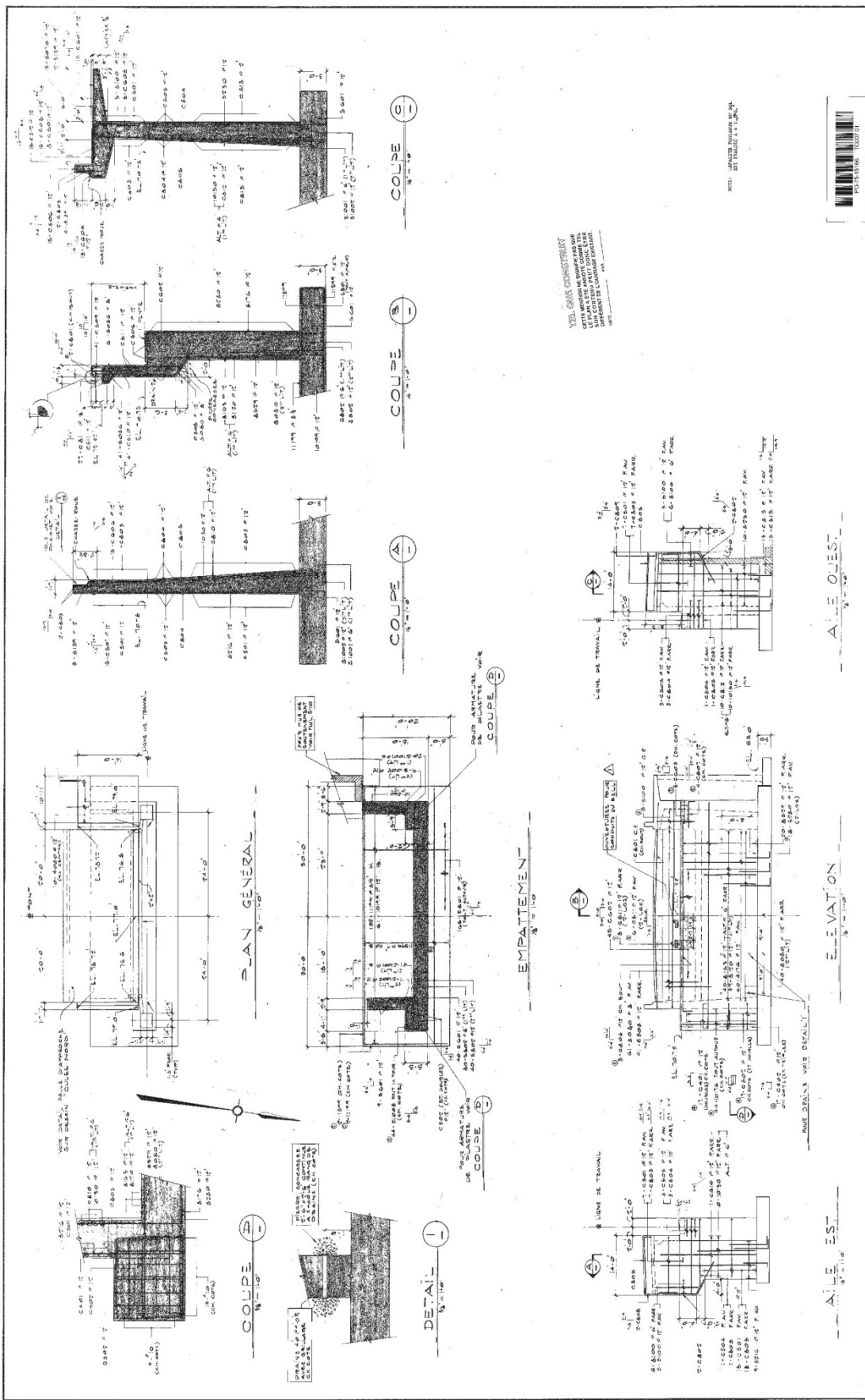


**Appendix8:** Representation of the Des-Prairies River geometry in Hec-RAS.









NO. PROJET: 100000000 VILLES DE MONTRÉAL ET DE LAMARQUE DÉPARTEMENT DES TRANSPORTS SAINT-LAMBERT ET LAMARQUE, LES DE MONTRÉAL ET DES ÎLES P-10166 ROUTE N° 117 NOUVEAU PONT LACHAPÈLLE 483-2389		S-7
DÉPARTEMENT DES TRANSPORTS SERVICE DES PONTS 3309-1 MAI 1975 TELÉPHONE: 393-1111 TÉLÉTYPE: 393-1111		
GOUVERNEMENT DU QUÉBEC SERVICE DES PONTS 3309-1 MAI 1975 TELÉPHONE: 393-1111 TÉLÉTYPE: 393-1111		CULÈE SUD
VILLE DE MONTRÉAL DÉPARTEMENT DES TRANSPORTS SERVICE DES PONTS 3309-1 MAI 1975 TELÉPHONE: 393-1111 TÉLÉTYPE: 393-1111		S-7

